THE FORM OF OPTIMAL CONTROLLERS FOR TIDAL POWER GENERATION SCHEMES

T.P. Andrews, N.K. Nichols and **Z. Xu**

Numerical Analysis Report 8/90

This work was supported in part by a research contract with National Power. The authors are grateful to Dr. John Wixcey for preliminary development of the numerical algorithms.

Table of Contents

Abstract

The report consists of two parts. In the first part the theoretical properties of an optimal controller for a tidal energy generation scheme are investigated under different assumptions on the form of the instantaneous power output function. In previous work [1] [2] [3] it is assumed that the power output and the volume flux through the turbines are non-linearly dependent on the head-difference across the tidal barrage, but directly proportional to the control function. For such 'linear' control models, the control acts as a switch, and the optimal solution is essentially 'on-off' or 'bang-bang'. Realistically, however, the power output depends non-linearly upon both the head-difference and the flux. We show here that for such 'non-linear' control systems, the optimal operating strategy is no longer bang-bang, but takes values continuously on the interval between the maximal efficiency and maximal power curves associated with the turbines. A simple flat-basin model of the tidal generation scheme is used in the analysis, but the results also apply to more sophisticated, dynamic models of the system.

In the second part of this report numerical algorithms for computing the optimal control are investigated. The theoretical results of the first part give only qualitative properties of the solutions under different assumptions on the power output function. In order to obtain precise forms of the solution it is necessary to use a computational method. Algorithms are developed and analysed in [1] [2] and [3] for the 'linear' models where the optimal control is 'bang-bang', and conditional gradient methods are proved effective in these cases. Difficulties with this type of procedure are encountered, however, for 'non-linear' models.

We show here that a projected gradient algorithm is more appropriate for these problems and for general use. Experiments with three iterative algorithms are described. The methods are applied to two simple models derived in the first part of the report, one 'linear' and one 'non-linear'. Discretized state and adjoint equations are used. The algorithms are observed to converge within a suitable tolerance for fixed choices of the discretization step, and convergence of the optimized power output is observed as the discretization step tends to zero. Different choices of the coefficients in the power output functions and different forms of constraint on the turbine flux are examined. Both two-way generation and ebb generation schemes are studied.

PART I - THEORY

1. Introduction

The research into tidal-power-generation by the Reading University Group has made use of optimal control techniques in order to maximise the power, or revenue, functional for a given estuary tidal barrage scheme, subject to the satisfaction of certain fluid-flow equations. As this research has developed, the system models used in this process have become more complex - ordinary differential fluid-flow dynamics being replaced by non-linear partial differential ones - and have incorporated additional relevant features - such as expansion losses, two-way power generation and pumping options. The more realistic models are thus capable of producing more accurate results. One area which has received relatively little attention in our work to date, however, is the control structure of the model, and, in particular, the form of an optimal controller and the important factors which determine it. The simple control structure that has been adopted, has, with the exception of singular arcs, resulted in simple bang-bang optimal controls.

In this paper we investigate analytically the form of an optimal controller. In order to achieve this aim most easily we use a simple flat basin system model, where the fluid-dynamics are governed by an ordinary differential equation. We demonstrate that by changing the cost functional - i.e. the power function - we can obtain more interesting optimal control regimes that incorporate internal control values. We also investigate the concept of a maximum efficiency operating level for a turbine, and examine its consequences for the power function, and hence, the optimal controller.

2. The Model

We take the volume flux $q(t)$ across the barrage as control (positive in the seaward direction), constrained to lie in some restraint set, and adopt simple ordinary differential fluid-flow dynamics of the form

$$\dot{\eta}(t) = -\frac{1}{A}q(t)$$

where $\eta(.)$, the basin level above some datum point, is our state variable.

The forcing function is the tidal level $f(t)$ above some datum point, and for convenience we write $h(t) \equiv \eta(t) - f(t)$ for the head difference.

This is a simple flat basin model.

The control problem associated with this model is given by

$$\left.\begin{aligned} &\text{Max } E = \int_0^T e(q(t), h(t))dt \\ &\text{subject to} \\ &\dot{\eta}(t) = -\frac{1}{A}q(t) \\ &\eta(0) = \eta(T) \\ &q(t) \in [-Q_1(h), 0] \qquad h(t) \leq 0 \\ &q(t) \in [0, Q_2(h)] \qquad h(t) > 0 \end{aligned}\right\} \qquad (1)$$

where T is the tidal period,

A is the basin surface area,

$e(q,h)$ is the instantaneous power function for flow q and head h,

$Q_1(h)$ is the maximum sluicing capacity of the turbines for head h,

$Q_2(h)$ is the maximum flow for turbine use for head h.

This is the simplest model available incorporating ebb generation only and no separate sluices. A greater degree of complexity, in the form of two-way power generation and sluicing in both directions, could, however, easily be incorporated within this model structure at a later stage.

2.1 The Transformed Model

As the bounds on the control variable q are functions of h and hence the state η, we are unable to apply the standard theory - Pontryagin's Maximum Principle - directly to this problem. We therefore make the following simple transformation:

Define

$$X(h) \equiv \begin{cases} -Q_1(h) & h \leq 0 \\ Q_2(h) & h > 0 \end{cases}.$$

Then problem (1) is equivalent to the following

$$\left.\begin{aligned} &\text{Max } E = \int_0^T e(X(h)u(t),\ h(t))dt \\ &\text{subject to} \\ &\dot{\eta}(t) = -\frac{1}{A}X(h)u(t) \\ &\eta(0) = \eta(T) \\ &u(t) \in [0,1] \end{aligned}\right\} \qquad (2)$$

With the problem written in this form we are now able to analyse the form of an optimal controller.

3. The Form of an Optimal Controller

In this section we investigate analytically the form of the optimal controller for various choices of power function $e(.,.)$. The power function is representative of characteristics of the turbines and the way they are situated. In order to achieve this end, we apply the following form of Pontryagin's Maximum Principle [5]:

Theorem

In order for the control $u^*(t)$, with corresponding state response $\eta^*(t)$, to be optimal, it is necessary that there exists a continuous function $\lambda(t)$ such that if the Hamiltonian is defined by

$$H(u(t), h(t), \lambda(t)) \equiv e(X(h)u(t), h(t)) - \lambda(t)\frac{1}{A}X(h)u(t)$$

Then

i) $\lambda(t)$ and $u^*(t)$ are solutions of the costate equations

$$\dot{\eta}^*(t) = \frac{\partial}{\partial\lambda}H(u^*(t), h^*(t), \lambda(t))$$

$$\dot{\lambda}(t) = -\frac{\partial}{\partial\eta}H(u^*(t), h^*(t), \lambda(t)) \qquad (h^*(t) = \eta^*(t)-f(t))$$

with boundary conditions

$$\eta^*(0) = \eta^*(T)$$

$$\lambda(0) = \lambda(T)$$

and

ii) $H(u(t), h^*(t), \lambda(t))$ has an absolute maximum as a function of admissible $u(t)$ at $u(t) = u^*(t)$ for each $t\in[0,T]$.

3.1 A Linear Power Function for Fixed Head

We start by assuming

$$e(Xu, h) \equiv \begin{cases} 0 & h \leq 0 \\ cQ_2uh & h > 0 , \end{cases} \tag{3}$$

a simple linear relationship between flow and instantaneous power for each fixed head h, with c some constant.

The Hamiltonian associated with this problem is then

$$H = \begin{cases} \lambda\frac{1}{A} Q_1u & h \leq 0 \\ Q_2u(ch-\lambda\frac{1}{A}) & h > 0 , \end{cases}$$

with costate equation

$$\dot{\lambda} = \begin{cases} \lambda\frac{1}{A} Q_1'u & h \leq 0 \\ -cQ_2u - Q_2'u(ch-\lambda\frac{1}{A}) & h > 0 , \end{cases}$$

having end-point constraint

$$\lambda(0) = \lambda(T) .$$

Now, using ii) of the Maximum Principle, we maximise H with respect to u for each t to give the optimal controller $u^*(t)$:

For $h(t) < 0$

$$u^*(t) = \begin{cases} 1 & \text{if } \lambda(t) > 0 \\ 0 & \text{if } \lambda(t) < 0 ; \end{cases}$$

if $\lambda(t) = 0$ on some interval of positive measure then we have a singular arc and $u^*(t)$ is not defined by the Maximum Principle.

For $h(t) = 0$

$u^*(t) = 0$ since $Q_1(0) = 0$.

For $h(t) > 0$

$$u^*(t) = \begin{cases} 0 & \text{if } \lambda(t) > cAh(t) \\ 1 & \text{if } \lambda(t) < cAh(t) \end{cases} .$$

Since it can be shown that if $\lambda(t) = cAh(t)$ on some interval of positive measure then $\dot{f}(t) = 0$ on that interval, we may deduce that this does not occur, and so define $u^*(t) = 0$, say, when $\lambda(t) = cAh(t)$.

Since we clearly require $\lambda(t) \geq 0 \ \forall \ t$ in order for the basin to be filled, we may deduce that the optimal controller $u^*(t)$ is given by:

$$u^*(t) = 1 , \quad \dot{\lambda}(t) > 0 \quad \text{when} \quad h(t) < 0$$

$$u^*(t) = 0 , \quad \dot{\lambda}(t) = 0 \quad \text{when} \quad 0 \leq h(t) \leq \frac{\lambda(t)}{cA}$$

$$u^*(t) = 1 , \quad \dot{\lambda}(t) > 0 \quad \text{when} \quad \frac{\lambda(t)}{cA} < h(t).$$

This simple bang-bang solution results from the linearity of the control u in the Hamiltonian, and replicates the previous solution obtained at Reading.

3.2 Expansion Losses

A more realistic form for the power function e(...) includes a term representing expansion losses in the head difference actually available for power generation

$$e(Xu,h) \equiv \begin{cases} 0 & h \leq 0 \\ Q_2 u(c_1 h - c_2 Q_2^2 u^2) & h > 0 \end{cases} \qquad (4)$$

with c_1 and c_2 again given constants.

The Hamiltonian now becomes

$$H = \begin{cases} \lambda \frac{1}{A} Q_1 u & h \leq 0 \\ Q_2 u(c_1 h - c_2 Q_2^2 u^2 - \lambda \frac{1}{A}) & h > 0 \end{cases}$$

with costate equation

$$\dot{\lambda} = \begin{cases} -\lambda \frac{1}{A} Q_1' u & h \leq 0 \\ -c_1 Q_2 u - Q_2' u(c_1 h - 3c_2 Q_2^2 u^2 - \lambda \frac{1}{A}) & h > 0 \end{cases}$$

$$\lambda(0) = \lambda(T).$$

Clearly for $h(t) \leq 0$ the optimal solution follows identical lines to that given for the problem of section 3.1. However, now, for $h(t) > 0$ we have

$$u^*(t) = \begin{cases} 0 & \text{if} \quad c_1 Ah(t) < \lambda(t) \\ \left[\frac{c_1 Ah(t) - \lambda(t)}{3c_2 AQ_2^2}\right]^{1/2}, & \text{if} \quad c_1 Ah(t) - 3c_2 AQ_2^2 \leq \lambda(t) \\ 1 & \text{if} \quad \lambda(t) < c_1 Ah(t) - 3c_2 AQ_2^2 . \end{cases}$$

and we can therefore deduce that the optimal controller is given by

$$u^*(t) = 1 , \qquad \dot{\lambda}(t) > 0 \quad \text{when} \quad h(t) < 0$$

$$u^*(t) = 0 , \qquad \dot{\lambda}(t) = 0 \quad \text{when} \quad 0 \leq h(t) < \frac{\lambda(t)}{c_1 A}$$

$$u^*(t) = \left[\frac{c_1 A h(t) - \lambda(t)}{3c_2 A Q_2^2}\right]^{\frac{1}{2}} , \qquad \dot{\lambda}(t) < 0 \quad \text{when} \quad \frac{\lambda(t)}{c_1 A} \leq h(t) \leq \frac{\lambda(t) + 3c_2 A Q_2^2}{c_1 A}$$

$$u^*(t) = 1 , \qquad \dot{\lambda}(t) < 0 \quad \text{when} \quad \frac{\lambda(t) + 3c_1 A Q_2^2}{c_1 A} < h(t).$$

So we see here that the non-linearity of the control $u(.)$ in the power function, and hence the Hamiltonian, results in an internal - non-extreme - optimal control as part of the solution. This form of controller has not previously been examined as an optimal solution at Reading, and represents an interesting variation from the simple bang-bang control.

4. Turbine Efficiency

It is clearly realistic to have some notion of efficiency of power generation for the turbines, and this should be reflected in our model through the power function. We can therefore derive a formula for calculating the most efficient rate of flow $u^E(.)$, for each fixed head $\bar{h}$, by solving the following problem:

$$\underset{u,T}{\text{Max}}\ E = \int_0^T e(u(t),\bar{h})dt$$

subject to

$$\int_0^T u(t)dt \leq V \qquad V \text{ a fixed volume of flow.}$$

Since $e(.,.)$ is explicitly independent of t the optimal choice of flow is constant. Thus the problem reduces to

$$\underset{u,T}{\text{Max}}\ E = Te(u,\bar{h})$$

subject to

$$u \leq \frac{V}{T}.$$

Clearly the constraint holds with equality at the maximum, so that we have

$$\underset{u}{\text{Max}}\ E = \frac{V}{u}\, e(u,\bar{h})$$

which gives

$$-\frac{V}{u^{E^2}}\, e(u^E,\bar{h}) + \frac{V}{u^E}\frac{\partial}{\partial u}\, e(u^E,\bar{h}) = 0 .$$

So the turbines are operating at their maximum efficiency when

$$\frac{e(u(t),h(t))}{u(t)} = \frac{\partial}{\partial u}\, e(u(t),\, h(t)) \qquad (5)$$

If we now apply this condition to the models of section 3, then we see from (3), where there is a linear relationship between flow and instantaneous power,

$$cQ_2h(t) = cQ_2h(t) ,$$

from which we deduce that all choices of rates of flow are equally efficient.

When the extra term representing expansion losses is added, we have, from (4)

$$Q_2(c_1h - c_2Q_2^2u^2) = Q_2(c_1h - 3c_2Q_2^2u^2)$$

which implies $u^E = 0$, and efficiency increases as u tends to zero.

So neither of the forms of power function adopted in Section 3 provide a satisfactory model in respect of turbine efficiency, indeed they do not even have a concept of a most efficient operating level for a given head. As it is clearly desirable that our power function has such a property, we consider the following

$$e(Xu,h) \equiv \begin{cases} 0 & h \leq 0 \\ Q_2u(c_1h + c_2Q_2uh - c_3Q_2^2u^2) & h > 0 \end{cases} \qquad (6)$$

For some constants c_1, c_2, c_3. From (5) we obtain

$$Q_2(c_1h + c_2Q_2u^Eh - c_3Q_2^2u^{E^2}) = Q_2(c_1h + 2c_2Q_2u^Eh - 3c_3Q_2^2u^{E^2})$$

giving

$$u^E(t) = \frac{c_2h(t)}{2c_3Q_2}$$

If the power function (6) is representative of a barrage containing k turbines, then for rates of flow $u(t) < u^E(t)$ it would clearly be more efficient in terms of energy output to operate $\frac{ku(t)}{u^E(t)}$ turbines at their maximum efficiency levels $\frac{u^E(t)}{k}$. This operating strategy gives a new power function

$$e^E(Xu,h) \equiv \begin{cases} 0 & h \leq 0 \\ \frac{u}{u^E}\, e(Xu^E, h) & h > 0\,, \quad u \leq u^E \\ e(Xu,h) & h > 0\,, \quad u > u^E \end{cases}$$

Applying the Maximum Principle to this we obtain

$$H = \begin{cases} \lambda\frac{1}{A}\, Q_1u & h \leq 0 \\ Q_2u(c_1h + \frac{c_2^2h^2}{4c_3} - \lambda\frac{1}{A}) & h > 0\,, \quad u \leq u^E \\ Q_2u(c_1h + c_2Q_2uh - c_3Q_2^2u^2 - \lambda\frac{1}{A}) & h > 0\,, \quad u > u^E \end{cases}$$

with costate equation

$$\dot{\lambda} = \begin{cases} \lambda\frac{1}{A}\, Q_1' u & h \le 0 \\ Q_2' u(c_1 h + \frac{c_2^2 h^2}{4c_3} - \lambda\frac{1}{A}) + Q_2 u(c_1 + \frac{c_2^2 h}{2c_3}) & h > 0\ ,\ u \le u^E \\ Q_2' u(c_1 h + c_2 Q_2 uh - c_3 Q_2^2 u^2 - \lambda\frac{1}{A}) + Q_2 u(c_1 + c_2 Q_2 u + c_2 Q_2' uh - 2c_3 Q_2 Q_2' u^2) & h > 0\ ,\ u > u^E \end{cases}$$

$$\lambda(0) = \lambda(T)\ .$$

For $h(t) \le 0$ the optimal solution is again the same as for the problem of section 3.1. However, for $h(t) > 0$ we now have two possibilities, when $u(t) \le u^E(t)$ the Hamiltonian is linear in the control so $u^*(t)$ will take on its extreme values

$$u^*(t) = \begin{cases} 0 & \text{if} \quad c_1 h + \frac{c_2^2 h^2}{4c_3} < \lambda\frac{1}{A} \qquad (7) \\ u^E(t) & \text{if} \quad c_1 h + \frac{c_2^2 h^2}{4c_3} > \lambda\frac{1}{A}\ . \qquad (8) \end{cases}$$

But, when $u(t) \ge u^E(t)$ the Hamiltonian is quadratic in the control which gives the possibility of an internal solution

$$u^*(t) = \begin{cases} \dfrac{c_2 h + (c_2^2 h^2 + 3c_3(c_1 h - \lambda\frac{1}{A}))^{1/2}}{3c_3 Q_2} & \text{if} \quad c_1 h + \frac{c_2^2 h^2}{4c_3} > \lambda\frac{1}{A} \\ & \text{and} \quad c_1 h + 2c_2 hQ_2 < \lambda\frac{1}{A} + 3c_3 Q_2^2 \qquad (9) \\ 1 & \text{if} \quad c_1 h + \frac{c_2^2 h^2}{4c_3} > \lambda\frac{1}{A} \\ & \text{and} \quad c_1 h + 2c_2 hQ_2 \ge \lambda\frac{1}{A} + 3c_3 Q_2^2 \qquad (10) \end{cases}$$

We note that condition (8) is made redundant by (9), with $u^*(t) = \dfrac{c_2h + (c_2^2h^2 + 3c_3(c_1h-\lambda\frac{1}{A}))^{\frac{1}{2}}}{3c_3Q_2} = u^E(t)$ when $c_1h + \dfrac{c_2^2h^2}{4c_3} = \lambda\frac{1}{A}$, so that the optimal control strategy is given by (7), (9), (10), and the double condition of (10) is required in case $c_1h + \dfrac{c_2^2h^2}{4c_3} > \lambda\frac{1}{A}$ implies $u^E \geq 1$ when (9) also becomes redundant.

We conclude from this analysis that the optimal strategy, when the turbines are modelled adequately in terms of efficiency, is to operate them only between their total maximum efficiency, $u^* = u^E$, and their maximum power, $u^* = 1$, levels.

5. Conclusion

In this paper we investigate the form of an optimal controller for a tidal-power-generation scheme using a simple ordinary differential flat-basin model. By using the volume flux across the barrage as control variable, and having the power function explicitly dependent on both this and the head difference, we are able in Section 3, despite the simplicity of the model's fluid dynamics, to obtain interesting forms for the optimal controller by varying our choice of power function. Most notably, for all but the most simple case where the control occurs linearly in the power function (and hence, since we have linear dynamics, the Hamiltonian), the solution contains internal values as part of the optimal controller, rather than being a purely "bang-bang" control. Further work is clearly required here to investigate the significance of the internal part of the solution, as we have given no indication as to how long is spent there,

or, more importantly, how much extra power is generated by this as opposed to a simple "bang-bang" solution. A numerical approach to this aspect of the problem is required.

In section 4 we examine the concept of efficient operation of the turbines and demonstrate that the power functions of section 3 - frequently used in early work at Reading - are not sufficient in this regard. After suggesting a more appropriate form for the power function, we show that the optimal controller should only take on values between its maximum efficiency and maximum power levels, again with an internal solution in part. Further work is necessary here in determining an accurate form for the power function probably through the use of manufacturers' data. It should be noted that this data produces a model of the turbines' power generating capabilities, with an associated maximum efficiency and maximum power level, but that factors arising from the particular use made of the turbines, such as expansion losses, needs to be added in. The resulting power function also has a maximum efficiency and maximum power level, slightly different to that implied by the manufacturer's data, and it is these new levels that we are interested in for operating purposes.

In conclusion we point to the importance of the power function in determining the form of the optimal controller, as illustrated in this paper, and suggest that consequently great care should be given to its modelling in future work. The likely presence of internal values as part of the optimal controller for any realistic model is also an important insight, and has implications for the choice of numerical optimization algorithm. The model developed in this paper provides a good tool for investigating the relative merits of such algorithms.

PART II - NUMERICAL ALGORITHMS

1. Introduction

In Part I of this paper we investigate the theoretical properties of the optimal control of a tidal energy generation scheme for different forms of the power output functional. In earlier work, [1] [2] [3], we assume that the power output is non-linearly dependent upon the head difference across the tidal barrage, but directly proportional to the control function. The flux across the barrage is similarly assumed to be a non-linear function of head, but linearly dependent on the control. The control thus acts as a switch, and the optimal solution (apart from singular arcs) is "on-off" or "bang-bang".

In practice, the power output from the turbines is non-linearly dependent upon both the head-difference and the flow through the turbines - and is usually characterized by a Hill-chart. In order to investigate the form of the optimal control in the case where the instantaneous energy generated by the turbines is a general function of both head-difference and flux, we develop a simple flat-basin model in which the system equations are represented by an ordinary differential equation (for mass conservation). It is shown that, for realistic forms of the energy functional, the optimal control is no longer bang-bang, but internal operating states, between the maximal efficiency and maximal power states, may be optimal. These results also apply in the case of more sophisticated, dynamic models of the system.

The analysis of Part I gives qualitative properties of the optimal control under different assumptions. In order to obtain the precise forms of the solution for various power output functionals, it is necessary to

use a numerical procedure. For 'linear' models, where the optimal operating strategy is 'bang-bang', computational algorithms are developed and analysed in previous reports [1] [2] [3]. A conditional gradient type of algorithm proves efficient and accurate in these cases. Difficulties with this procedure are encountered, however, for 'non-linear' models, and some other types of method, including projected gradient algorithms, are expected to be more appropriate for general use.

The aim of this part of the paper (Part II) is to investigate the application of various numerical techniques to the models derived in Part I. The two simplest models are selected for the tests, with modifications for two-way generation. The system equations are given by

$$\dot{\eta}(t) = \begin{cases} Q_1(h)\ u/A & h \leq 0 \\ -\ Q_2(h)\ u/A & h > 0 \end{cases} \tag{1}$$

$$\eta(0) = \eta(T) \ . \tag{2}$$

and the control function $u(t)$ is constrained such that

$$u(t) \in [0,1] \ . \tag{3}$$

The model problems are then written:

$$\max_u E(u) \equiv \int_0^T e(u,h)dt$$

subject to (1) (2) and (3), where

Model 1 - Linear

$$e(u,h) \equiv \begin{cases} -Q_1(h)uh & h \leq 0 \\ Q_2(h)uh & h > 0 \end{cases} \tag{4}$$

and

Model 2 - Non-linear

$$e(u,h) = \begin{cases} -Q_1(h)u(h + cQ_1(h)^2u^2) & h \leq 0 \\ Q_2(h)u(h - cQ_2(h)^2u^2) & h > 0 . \end{cases} \tag{5}$$

The notation used here is essentially the same in Part I with a few obvious minor changes. For these problems the gradient $\nabla E(u)$ of the power output functional is defined in terms of the Hamiltonian of the system and is given by

$$\nabla E(u) = \frac{\partial}{\partial u}\Big[e(u,h) + \lambda X(h)\, u/A\Big],$$

where $X(h) = -Q_1(h)$ for $h \leq 0$ and $X(h) = Q_2(h)$ for $h > 0$. Here h is defined by $h = f - \eta$.

We remark that in the non-linear model (Model 2), the line of maximal efficiency is $u^E = 0$. Although this is less realistic than the model proposed in Section 4 of Part I, the optimal must nevertheless lie between $u = u^E$ and $u = 1$, and this model retains the properties in which we are interested.

Three numerical methods are investigated, and the effects of different choices of the constraint functions $Q_1(h)$, $Q_2(h)$ and different choices of the constants are studied. Results for ebb flow models are also obtained. In the next section the methods are described and in Section 3, computational results for the two-way generation schemes are

presented and discussed. In Section 4, the ebb generation models are examined and the conclusions are summarized in Section 5.

2. Numerical Solution Procedures

The problems as formulated in the preceeding sections are state-constrained optimal control problems. In order to solve these problems, a numerical solution procedure is used which determines an optimal admissible control $u(t)$ with corresponding response $\eta(t)$ and adjoint $\lambda(t)$ satisfying the state and adjoint equations. The procedure consists of a constrained optimisation algorithm for iteratively determining the optimal control function, together with a numerical approximation scheme for solving the state and adjoint equations.

The numerical solution to the state and adjoint equations is achieved by the use of a finite difference scheme, with the state equation being integrated forward in time from the initial condition $\eta(0)$ and the adjoint equation then being integrated backward in time from the final condition $\lambda(T)$. A similar scheme is adopted by [1] [2] [3] in the previous tidal power generation optimisation studies and is proved absolutely stable for the type of ordinary differential equation under consideration. Details of the scheme are given in [1].

In what follows two optimization algorithms for the current control problems are presented. These are modifications of those found in [1] and are known respectively as the conditional gradient and the projected gradient method. The main reason for employing gradient based optimisation algorithms is that the functional gradient can be evaluated analytically for the type of problems under consideration. The gradient algorithm, as a class, generally has a fast rate of convergence as opposed

to the other classes of optimisation algorithms. In addition to these two optimisation algorithms, a third which is a revised conditional gradient algorithm proposed in [3], is also included in the investigation. This algorithm differs form the first conditional gradient algorithm in that a quadratic step length rule is utilised at each iteration for step length determination.

2.1. Conditional Gradient Algorithm (Algorithm 1 - CG)

The structure of this algorithm is illustrated in the flow chart given in Fig. 1. As shown in the diagram, the algorithm generates a sequence of admissible controls $\{u^k\}$ for which the values of the functional $E^k = E(u^k)$ are monotonically non-decreasing. To be more specific, if an approximation u^k to the optimal control with a response η^k and an adjoint λ^k satisfying the state and adjoint equations exists, then a new approximation can be made as follows:

$$u^{k+1} = (1 - S)u^k + S\,\tilde{u}^{k+1}$$

where S is step size and $\tilde{u}^{k+1}$ is obtained according to the following

$$\begin{aligned} \tilde{u}^{k+1} &:= 1.0 \quad \text{if} \quad \nabla E(u^k) > 0 \\ &:= 0 \quad \text{otherwise,} \end{aligned}$$

where $\nabla E(u)$ is the functional gradient. This selection maximises the first variation $\langle \nabla E(u^k), \tilde{u}^{k+1} - u^k \rangle$ of the functional over all possible choices for $\tilde{u}^{k+1}$. Since the response η of the system (1) is continuously dependent on the control u and is uniformly bounded for all

(non-trivial) $u \in U_{ad}$, it can be shown [1] that the sequence $\{E^k\}$ is bounded and convergent.

2.2. Projected Gradient Algorithm (Algorithm 2 - PG)

The flow chart of the projected gradient algorithm is given in Fig. 2. In this method the new approximation to the optimal control is chosen as

$$u^{k+1} = P(u^k + S\nabla E(u^k)) ,$$

where P is the L_2 projection operator onto U_{ad}. As the operator P has the following property

$$\langle \hat{P}v - v, \hat{P}v - v \rangle = \min_{u \in U_{ad}} \langle u - v, u - v \rangle$$

it follows, therefore, that for the selected control u^{k+1}, the inequality

$$\langle \nabla E(u^k), u^{k+1} - u^k \rangle \geq \frac{1}{S} \| u^{k+1} - u^k \|_2^2$$

holds, and it can be shown that for some choice of S, $E(u^{k+1}) \geq E(u^k)$ [4]. If the initial approximation $u^o(t)$ is continuous, on $[0,T]$, then the algorithm generates a sequence of continuous controls u^k for which the functionals $E^k = E(u^k)$ are monotonically non-decreasing, and, provided that an optimal solution exists amongst the admissible controls, the process converges and the limiting control satisfies the necessary conditions.

2.3. Revised Conditional Gradient Algorithm (Algorithm 3 - NCG)

The flow chart of this revised conditional gradient algorithm is illustrated in Fig. 3. The algorithm generates a sequence of admissible controls $\{u^k\}$ in much the same way as Algorithm 1, i.e., if an approximation u^k to the optimal control with a response η^k and an adjoint λ^k satisfying the state and adjoint equations exists, then a new approximation can be made as follows:

$$u^{k+1} = (1 - S)u^k + S\,\tilde{u}^{k+1}$$

where S is the step size and $\tilde{u}^{k+1}$ is obtained according to

$$\begin{aligned} \tilde{u}^{k+1} &:= 1.0 \qquad \text{if } \nabla E(u^k) > 0 \\ &:= 0 \qquad \text{otherwise .} \end{aligned}$$

It has been mentioned briefly that the main difference between the two conditional gradient algorithms lies in the choice of step size at each iteration. Here the step size S at each iteration is computed based on a Taylor series expansion of the Lagrangian, which is

$$L(u^k + S(\tilde{u}^{k+1} - u^k)) = L(u^k) + SD_1 + S^2D_2/2 + O(S^3\|\tilde{u}^{k+1} - u^k\|^3)$$

where D_1 and D_2 are the first and second derivatives of L in the direction of $\tilde{u}^{k+1} - u^k$ respectively. To a second order approximation, it is desirable that the following quadratic expression be maximised

$$L(u^k) + SD_1 + S^2D_2/2 \ .$$

subject to the constraint that $S \in [0,1]$. Hence we have

$$S = \begin{cases} 1 & \text{if } D_2 > 0 \\ 1 & \text{if } D_2 < 0 \text{ and } -D_1/D_2 > 1 \\ -D_1/D_2 & \text{if } D_2 < 0 \text{ and } -D_1/D_2 \in [0,1] \end{cases},$$

where the first derivative D_1 is calculated as

$$D_1 = \langle \nabla E(u^k), \tilde{u}^{k+1} - u^k \rangle$$

and the second derivative D_2 is approximated by

$$D_2 \approx \frac{\langle \nabla E(u^k + \Delta(\tilde{u}^{k+1} - u^k)), \tilde{u}^{k+1} - u^k \rangle - D_1}{\Delta}$$

for small Δ.

3. Results and Discussion

The numerical procedures are tested with both linear and non-linear models of the power functional (Model 1 and 2 of Section 1). The model data used in the current study to define the tidal period and estuary geometry are typical of those from the Severn estuary and are given by

$$T = 4.32 \times 10^4 \text{ s}$$

$$A = 3.\dot{3}\dot{3} \times 10^3 \text{ m}^2$$

It is assumed that the forcing function imposed on the seaward side of the barrage is given by $f(t) = \cos 2\pi t$ over a complete tidal period $[0,T]$. Throughout the computation, the initial approximation for the control function is taken as $u(t) = 1.0$ on $[0,T]$, and the whole tidal period is divided into N computational steps.

To begin with the algorithms are applied to the linear power functional model (Model 1). It is known from the analytical work that the optimal control for this problem is bang-bang in nature. For the sake of simplicity and clarity it is postulated that the flow functions $Q_1(h)$ and $Q_2(h)$ take the simple form $-Q_1(h) = Q_2(h) = h$. The computational results corresponding to $N = 200$ and $N = 25$ are illustrated in Figs. 4-9, while the detailed comparison of their optimised power outputs and number of iterations for various choices of N are given in Table 1. It should be noted that the results are based on the convergence criterion that the first order correction is within 1% of the functional value. It can be seen that both conditional and projected gradient algorithms have predicted the optimal control reasonably well even at large computational steps, with their calculated power outputs in agreement to within 1.0 percent. The revised conditional gradient algorithm has produced good output but its control fucntion is relatively poor. In terms of rate of convergence the conditional gradient algorithm appears to be most efficient, requiring only a few iterations. We remark that the results obtained by this method are comparable to the results given in [1] for the same model problem.

For illustrative purposes the results with more accuracy (first order correction to within 0.1% of the functional value as indicated in the flow chart) are obtained and listed in Table 2. The computed solutions for

Table 1 Computational Result for Linear Model (1.0% Tolerance)

No. of Steps	No. of Iterations			Power Output		
	CG	PG	NCG	CG	PG	NCG
200	4	8	5	0.2273	0.2267	0.2255
100	3	7	9	0.2269	0.2262	0.2259
50	4	7	29	0.2278	0.2268	0.2255
25	4	7	50	0.2292	0.2287	0.2271

Table 2 Computational Result for Linear Model (0.1% Tolerance)

No. of Steps	No. of Iterations			Power Output		
	CG	PG	NCG	CG	PG	NCG
200	5	16	10	0.2277	0.2275	0.2275
100	4	16	17	0.2278	0.2277	0.2276
50	4	15	81	0.2278	0.2276	0.2275
25	5	9	167	0.2294	0.2293	0.2291

$N = 200$ and $N = 25$ are shown in Figs. 10-15. Some observations can be made on these results. Firstly much better agreement in the predicted power outputs and in the optimal controls has been achieved with all three algorithms. Secondly there is some small amount of gain in the power output, indicating that the iteration converges for each fixed choice of computational step size. However, this is achieved at the expense of more iterations, i.e. more computational cost. It is doubtful whether this gain in power output is worthwhile as opposed to the corresponding rise in computational cost by opting for more accuracy.

Next the algorithms are applied to the non-linear power functional model (Model 2) in which an internal optimal control is expected as part of the solution. As in the linear model, the flow functions $Q_1(h)$, $Q_2(h)$ and the constant c are assumed to take the following simple forms:

$$-Q_1(h) = Q_2(h) = h$$
$$c = 1.0 .$$

Again, computational steps between $N = 200$ and $N = 25$ are selected and the results are presented in Figs. 16-27 and Tables 3 and 4 for tolerances of 1.0% and 0.1% respectively. As shown in the diagrams, all three algorithms predict the internal control reasonably well with a generally smooth control function. The projected gradient algorithm is the most efficient both in terms of rate of convergence and smoothness of the control function obtained. By contrast the conditional gradient algorithm is the least efficient. One point which must be made regarding the convergence rate in the Tables is that the figures inside the brackets are the total number of times the state equation is solved. Therefore it

Table 3 Computational Result for Non-Linear Model (1.0% Tolerance)

No. of Steps	No. of Iterations			Power Output		
	CG	PG	NCG	CG	PG	NCG
200	76(440)	23(33)	130	0.1535	0.1535	0.1530
100	84(516)	23(33)	129	0.1534	0.1536	0.1531
50	94(590)	24(35)	121	0.1532	0.1539	0.1531
25	62(759)	27(41)	122	0.1539	0.1547	0.1538

Table 4 Computational Result for Non-Linear Model (0.1% Tolerance)

No. of Steps	No. of Iterations			Power Output		
	CG	PG	NCG	CG	PG	NCG
200	462(4070)	118(192)	>1000	0.1537	0.1538	0.1537
100	>600	48(76)	>1000	0.1538	0.1539	0.1537
50	>600	32(50)	>1000	0.1537	0.1539	0.1538
25	>600	35(57)	>1000	0.1545	0.1547	0.1546

appears more reasonable to cite this figure when the convergence rate is considered. A comparison with the results in Tables 1 and 2 shows that by accounting for a large expansion loss in the power functional the power output has fallen by 32.6%.

It should be noticed at this point that with the revised conditional gradient algorithm (NCG) it can no longer be guaranteed that the power function is monotonically non-decreasing. As is evidenced from the power output versus iteration number diagram in Fig. 18, the power output obtained in iteration 2 actually drops below that obtained in the previous iteration. This is also encountered in the more general problems which are to be discussed shortly (see Fig. 44), and casts further doubt on the use of this algorithm in more complex situations.

It should also be remarked that all three of the discretized algorithms are only guaranteed to converge to within some region near the optimal solution of the continuous problem. Therefore, if too strict a convergence tolerance is imposed, relative to the size of the discretization step, the iteration may never satisfy the stopping criterion. In practice it can be observed from the Figures that after a relatively small number of iterations there is little improvement in the computed power output, though more accurate controls are obtained when a higher convergence tolerance is imposed.

After testing all three algorithms for the linear and simple non-linear problems, we next extend the computation to more general practical control problems where the constant c takes values other than unity and the flow functions $Q_1(h)$ and $Q_2(h)$ are allowed to vary. For convenience of description the additional experiments can be further broken down into two groups: group A in which the constant c is

varied in the range 0.0 to 1.0 while the flow functions remain unchanged from the previous two models; group B in which the flow functions $Q_1(h)$, $Q_2(h)$ are assumed to be restricted at a prescribed head difference. The main purpose of the second group is to simulate the choking effect which is invariably experienced in sluices and turbines when the head difference exceeds a certain limit. In other words the flow function is expressed as

$$\begin{aligned} -Q_1(h) &= Q_2(h) = h \quad \text{for} \quad |h| \leq h_0 , \\ Q_1(h) &= Q_2(h) = h_0 \quad \text{for} \quad |h| > h_0 , \end{aligned}$$

where h_0 is selected in the range (0, 1). The computed results for the two groups are presented in Tables 5 and 6 respectively. The optimal solutions are shown in Figs. 28-33 and Figs. 34-57, respectively. It is found that convergence is achieved in all cases tested, although the convergence rate varies considerably from one algorithm to another. Upon examination of these results the following remarks can be made:

(1) For large values of c, the projected gradient algorithm performs better, whereas for smaller c, the two conditional gradient algorithms fare relatively well. This is quite obvious from the point of view that the degree of non-linearity of the power functional is directly associated with c. In fact, if the value is set to zero, i.e. c = 0, then the problem is simply reduced to the linear model problem. Generally as the value of c decreases the power output increases.

(2) For the linear problem, the restriction of the flow through the barrage leads to a reduction in the optimised power output. The lower the maximum flow rate, the lower the power output. The same phenomenon is not

Table 5 Computational Results for Group A

C = 0.25 (1.0% Tolerance)

No. of Steps	No. of Iterations			Power Output		
	CG	PG	NCG	CG	PG	NCG
200	21(68)	10(10)	25	0.1950	0.1942	0.1944
100	21(67)	10(10)	24	0.1952	0.1943	0.1945
50	20(63)	10(10)	21	0.1954	0.1947	0.1948
25	20(55)	10(10)	21	0.1968	0.1957	0.1959

C = 0.1 (1.0% Tolerance)

No. of Steps	No. of Iterations			Power Output		
	CG	PG	NCG	CG	PG	NCG
200	12(29)	10(10)	10	0.2105	0.2099	0.2102
100	11(25)	10(10)	10	0.2105	0.2100	0.2103
50	8(15)	11(11)	9	0.2110	0.2105	0.2105
25	11(24)	12(12)	10	0.2126	0.2122	0.2120

C = 0.25 (0.1% Tolerance)

No. of Steps	No. of Iterations			Power Output		
	CG	PG	NCG	CG	PG	NCG
200	132(900)	23(23)	305	0.1953	0.1953	0.1953
100	131(929)	20(20)	295	0.1954	0.1953	0.1954
50	165(1148)	18(18)	274	0.1958	0.1959	0.1957
25	74(481)	23(23)	224	0.1969	0.1969	0.1968

C = 0.1 (0.1% Tolerance)

No. of Steps	No. of Iterations			Power Output		
	CG	PG	NCG	CG	PG	NCG
200	36(166)	19(19)	91	0.2108	0.2108	0.2108
100	37(172)	24(24)	88	0.2110	0.2109	0.2109
50	39(205)	14(14)	82	0.2113	0.2113	0.2113
25	23(98)	17(17)	76	0.2128	0.2129	0.2128

TABLE 6 Computational Result for Group B (N = 200)

Linear Problem

h_o	No. of Iterations			Power Output		
	CG	PG	NCG	CG	PG	NCG
1.0	6(6)	10(10)	4	0.2245	0.2243	0.2256
0.5	14(19)	9(9)	27	0.2002	0.1983	0.1998
0.25	5(8)	12(12)	6	0.1366	0.1359	0.1357
0.1	2(2)	33(33)	2	0.0617	0.0613	0.0617

Non-Linear Problem

h_o	No. of Iterations			Power Output		
	CG	PG	NCG	CG	PG	NCG
1.0	77(456)	32(56)	125	0.1534	0.1536	0.1529
0.5	29(107)	13(13)	31	0.1534	0.1529	0.1531
0.25	15(31)	11(11)	4	0.1257	0.1254	0.1259
0.1	2(2)	34(34)	2	0.0608	0.0605	0.0608

observed in the non-linear problem in which there is little fall in the power output due to this restriction until h_0 is dropped below 0.5. The reason for this is that both linear and non-linear terms in the power functional are affected simultaneously by the flow. As a result, any reduction in the power output due to the restriction is compensated by the corresponding reduction in the expansion loss. However, when h_0 is below 0.5, the linear term seems to be dominant and any further drop in h_0 leads to a cut in power output.

In view of the results presented here for a wide range of problems, the following conclusions can be drawn:

The conditional gradient algroithm is the most efficient for the linear 'bang-bang' problem, whereas the projected gradient algorithm is the most efficient for the non-linear problem. As a majority of practical problems is non-linear in nature, the projected gradient algorithm is recommended. As regards the revised conditional gradient algorithm, some modification is necessary before it can be used effectively.

4. Ebb Generation Results

In this section we extend our numerical investigation of the optimal control problem in tidal power generation to the ebb generation only scheme. Only two cases are examined here. These include the linear power function model where the instantaneous energy output is given by

Linear Model

$$e(u,h) = \begin{cases} 0 & h \leq 0 \\ hQ_2(h)u & h > 0 \end{cases},$$

and the non-linear model, where the power output function is given by

Non-linear Model

$$e(u,h) = \begin{cases} 0 & h \leq 0 \\ Q_2(h)u(h-cQ_2(h)^2u^2) & h > 0 \end{cases},$$

with $c = 0.25$. As in the case of the two-way generation scheme, the flow functions $Q_1(h)$ and $Q_2(h)$ are assumed to be linearly proportional to the head difference across the tidal barrier. Numerical results are presented for four choices of the computational step number N ($N = 200$, 100, 50 and 25), and two tolerances (1.0% and 0.1%). The iteration counts and optimized power output are given in Tables 7-10, and the optimal solutions obtained with a tolerance of 0.1% and $N = 200$ are shown in Figs. 58-64.

An inspection of these results indicates that in general they support the findings made for the two-way generation scheme. Quantitatively the two-way schemes produce about 40% more power than the ebb scheme with the current data. However, since only a very simple model is used here, it is unreasonable to draw conclusions from the comparison between the results from these two modes of generation with this data.

This fact is further underlined by observing the forms of the optimal control given in the figures. It can be seen that when the head difference crosses from positive to negative, the turbines switch instantaneously from generation mode to sluicing mode, with no switching time. This is an artefact due to the choice of the flow functions $Q_1(h)$ and $Q_2(h)$ and due to the fact that the model admits only one control. In practice the sluices and turbines can be controlled separately and a

Table 7 Ebb Generation Computational Result for Linear Model

(1.0% Tolerance)

No. of Steps	No. of Iterations			Power Output		
	CG	PG	NCG	CG	PG	NCG
200	2	13	2	0.1315	0.1307	0.1315
100	2	13	2	0.1317	0.1308	0.1317
50	2	13	2	0.1322	0.1309	0.1322
25	2	13	2	0.1323	0.1308	0.1323

Table 8 Ebb Generation Computational Result for Linear Model

(0.1% Tolerance)

No. of Steps	No. of Iterations			Power Output		
	CG	PG	NCG	CG	PG	NCG
200	3	30	3	0.1319	0.1319	0.1319
100	3	28	3	0.1320	0.1319	0.1320
50	2	34	2	0.1322	0.1321	0.1322
25	2	46	2	0.1323	0.1321	0.1323

Table 9 Ebb Generation Computational Result for Non-Linear Model

C = 0.25

(1.0% Tolerance)

No. of Steps	No. of Iterations			Power Output		
	CG	PG	NCG	CG	PG	NCG
200	22(73)	14(14)	29	0.1169	0.1165	0.1165
100	20(62)	14(14)	27	0.1169	0.1165	0.1165
50	19(61)	14(14)	31	0.1170	0.1167	0.1167
25	17(51)	14(14)	21	0.1174	0.1165	0.1169

Table 10 Ebb Generation Computational Result for Non-Linear Model

C = 0.25

(0.1% Tolerance)

No. of Steps	No. of Iterations			Power Output		
	CG	PG	NCG	CG	PG	NCG
200	152(1071)	28(28)	364	0.1170	0.1170	0.1170
100	146(1087)	28(28)	364	0.1170	0.1170	0.1170
50	172(1253)	31(31)	299	0.1172	0.1172	0.1172
25	134(937)	34(34)	292	0.1176	0.1176	0.1175

more sophisticated model can be developed. The aim of this study, however, is to obtain qualitative results concerning the nature of the optimal control under different assumptions, and the behaviour of various computational algorithms for determining the optimal.

One valuable observation that can be made from the ebb generation results concerns the behaviour of the algorithms when the functional gradient $\nabla E(u)$ is close to zero. For the non-linear model the conditional gradient algorithms predict a very brief switch at time $t = 0.625$, where the head difference crosses the zero axis (see Figs. 62 and 64). At this point the function gradient is very nearly zero, and small computational errors can introduce sign changes leading to switches of this kind. For the linear model the same situation arises, but in this case, no switch is predicted by the conditional gradient algorithms (see Figs. 58 and 61). By contrast, with the projected gradient algorithm, at points where the gradient $\nabla E(u)$ is near zero, the control is essentially maintained at its initial value. This can be observed in Fig. 59 and 60, where different initial values for u^o are selected. In the first of these, (Fig. 59), the initial value is $u^o = 1$, and no switches are predicted at the critical point. In the second (Fig. 60), the initial value is set to an intermediate position in the range (0,1) at the critical time, and since this position is maintained by the algorithm at each iteration, a switch appears to be predicted here. For the non-linear model, where the initial value is taken to be $u^o = 1$, the initial value is also maintained at the critical time, and no switch is predicted (see Fig. 63).

In practice, with realistic data, cases where $\nabla E(u)$ is essentially zero may not arise; however, it is important to consider in detail the

required form of the controls at points where the gradient vanishes and to modify the numerical methods to ensure the correct behaviour of the optimal.

5. Conclusions

In this part of the paper we examine three numerical methods for solving optimal tidal power generation control problems - a conditional gradient, a projected gradient and a revised conditional gradient method. The methods are applied to two simple models - Model 1 and Model 2, with linear and non-linear power output functions, respectively. It is observed that for the linear problem, the computed optimal control is bang-bang in nature, as predicted, and for the non-linear problem the turbine control increases continuously from its minimum to its maximum value when switched on. For the linear model the conditional gradient method is most effective - giving precise bang-bang controls with least computational effort. The other methods are also quite efficient, although the revised conditional gradient method does not appear as effective for large discretization steps. For the non-linear model the projected gradient method is most efficient and also produces the smoothest controls. The revised conditional gradient method is generally much more efficient than the original, but both algorithms suffer when a high tolerance is demanded. For low tolerances, however, the optimal solutions can be very rough. These effects vary with the degree of non-linearity, as is shown by varying the data in the energy output functions.

The algorithms are all observed to converge, although theoretically the tolerance that can be achieved is limited by the size of the discretization step used. The optimized solutions are also observed to converge as the discretization step tends to zero, although for $N \geq 50$, the results are all probably accurate to within computational error.

It is observed that in the revised conditional gradient method, the values of the energy functional do not increase monotonically with the iteration, and a further modification to the algorithm is advisable to avoid this behaviour. It is also observed that at points where the gradient of the energy functional is close to zero, the optimal control is not well-defined by the first order necessary conditions and the choice of the control at these points is somewhat arbitrary. The conditional gradient and projected gradient algorithms behave differently at such points, and further modifications to all the methods are needed to ensure the correct behaviour of the optimal control.

Results for both two-way generation and ebb only generation are given here. Reasonable conclusions and comparisons between these cases cannot be made however, since the simplicity of the control model constrains the flow in an unrealistic way. More sophisticated models can be derived which allow the sluices and turbines to be controlled independently and which take into account the estuarine flow dynamics. It is expected that the results of the studies presented here concerning the qualitative nature of the optimal controls and the behaviour of the numerical algorithms also hold for the more sophisticated models.

Summary

The form of an optimal controller for a tidal power generation scheme is investigated here under different assumptions on the instantaneous power output function. In the first part, theoretical properties of the controller are examined analytically using a simple flat-basin model of the system dynamics. Power output functions which are linearly dependent on the control are contrasted qualitatively with power functions which depend non-linearly on flux and head-difference across the tidal barrage. It is shown that whereas the optimal controller in the 'linear' case is essentially bang-bang, in the 'non-linear' case the controller can take interior values lying between the maximal efficiency and maximal power curves of the turbines. In the second part of the report, the form of the optimal controllers is examined numerically for various choices of the power output function, and various constraints on the turbine flux. Three computational algorithms are investigated - two conditional gradient type methods and one projected gradient method. It is shown that whereas the conditional gradient methods are effective in the 'linear' cases, provided the numerical discretization steps are sufficiently small, the projected gradient method is more efficient in the 'non-linear' cases. Moreover, the projected gradient method provides a qualitatively 'smoother' approximation to the optimal control in both cases. It is therefore concluded that for general use, the projected gradient method is the preferred algorithm.

The results of these studies can be extended to more sophisticated models of the estuarine dynamics. The same conclusions regarding the qualitative forms of the optimal controller apply. The projected gradient method is also expected to be preferable to the conditional gradient

techniques, but difficulties with parameter choices are likely to be more serious in the sophisticated models. The revised conditional algorithm offers a reasonable, intermediate solution, but other algorithms, such as trust region methods, may prove to be more reliable and efficient in these cases. For problems where singular arcs arise, the optimal forms of the solutions need to be ascertained, and adjustments to the algorithms must be made to ensure the proper behaviour of the computed results. Further investigations are currently being carried out.

REFERENCES

[1] Birkett, N.R.C. and Nichols, N.K., *Optimal control problems in tidal power generation*, Tech. Rpt. NA 8/83, Department of Mathematics, University of Reading, 1983.

[2] Birkett, N.R.C., *Nonlinear optimal control problems in tidal power calculations*, Tech. Rpt. NA 2/85, Department of Mathematics, University of Reading, 1985.

[3] Birkett, N.R.C., *Nonlinear optimal control of tidal power schemes in long estuaries*, Tech. Rpt. NA 9/86, Department of Mathematics, University of Reading, 1986.

[4] Gruver, W.A. and Sachs, E., *Algorithmic Methods in Optimal Control*. Pitman, 1980.

[5] Pontryagin, L.S., Boltyanskii, V.G. and Gamkrelidze, R.V., *The Mathematical Theory of Optimal Processes*. Interscience, 1962.

LIST OF FIGURES

53	"	"		"	"		$h_o = 1.0$
54	Non-linear	NCGA		"	"		$h_o = 0.1$
55	"	"		"	"		$h_o = 0.25$
56	"	"		"	"		$h_o = 0.5$
57	"	"		"	"		$h_o = 1.0$
58	Ebb Generation		Linear	CGA	Tol = 0.1%	N = 200	
59	"	"	"	PGA	"	"	$u^o = 1$
60	"	"	"	PGA	"	"	$u^o \neq 1$
61	"	"	"	NCGA	"	"	
62	Ebb Generation		Non-linear	CGA	Tol = 0.1%	N = 200	c = 0.25
63	"	"	"	PGA	"	"	"
64	"	"	"	NCGA	"	"	"

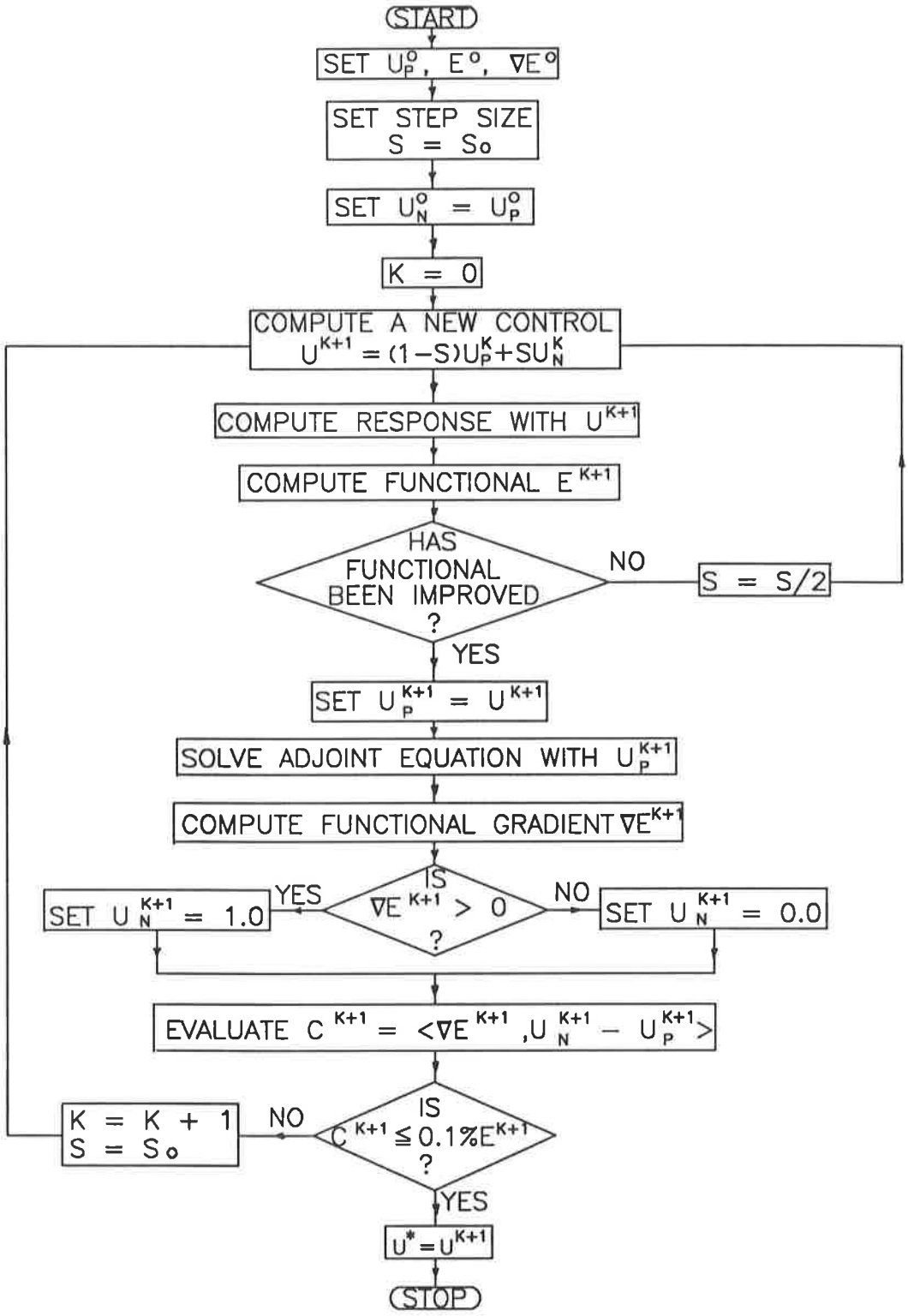

FIG.1 FLOW CHART – CONDITIONAL GRADIENT ALGORITHM (CGA)

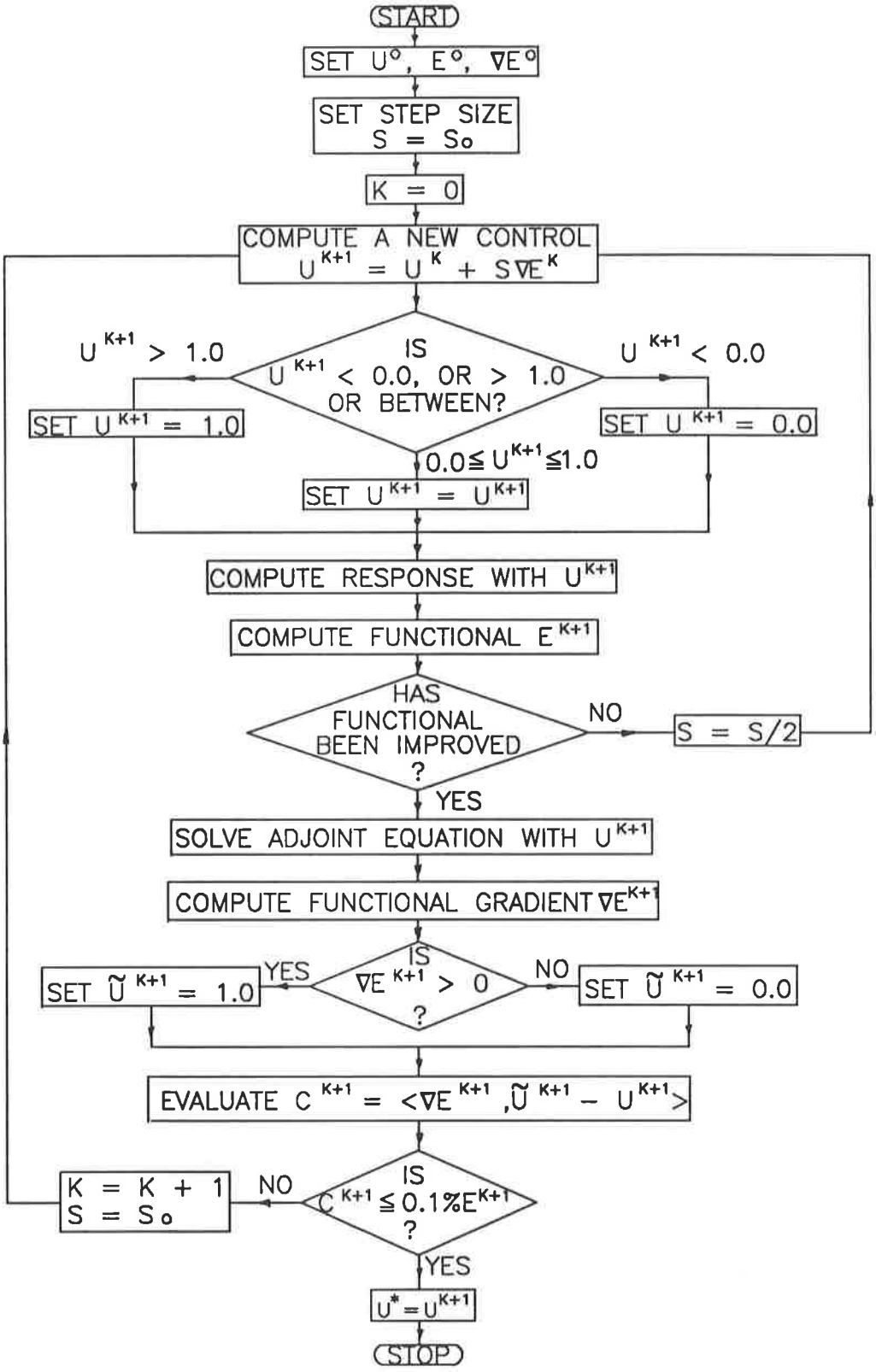

FIG.2 FLOW CHART — PROJECTED GRADIENT ALGORITHM (PGA)

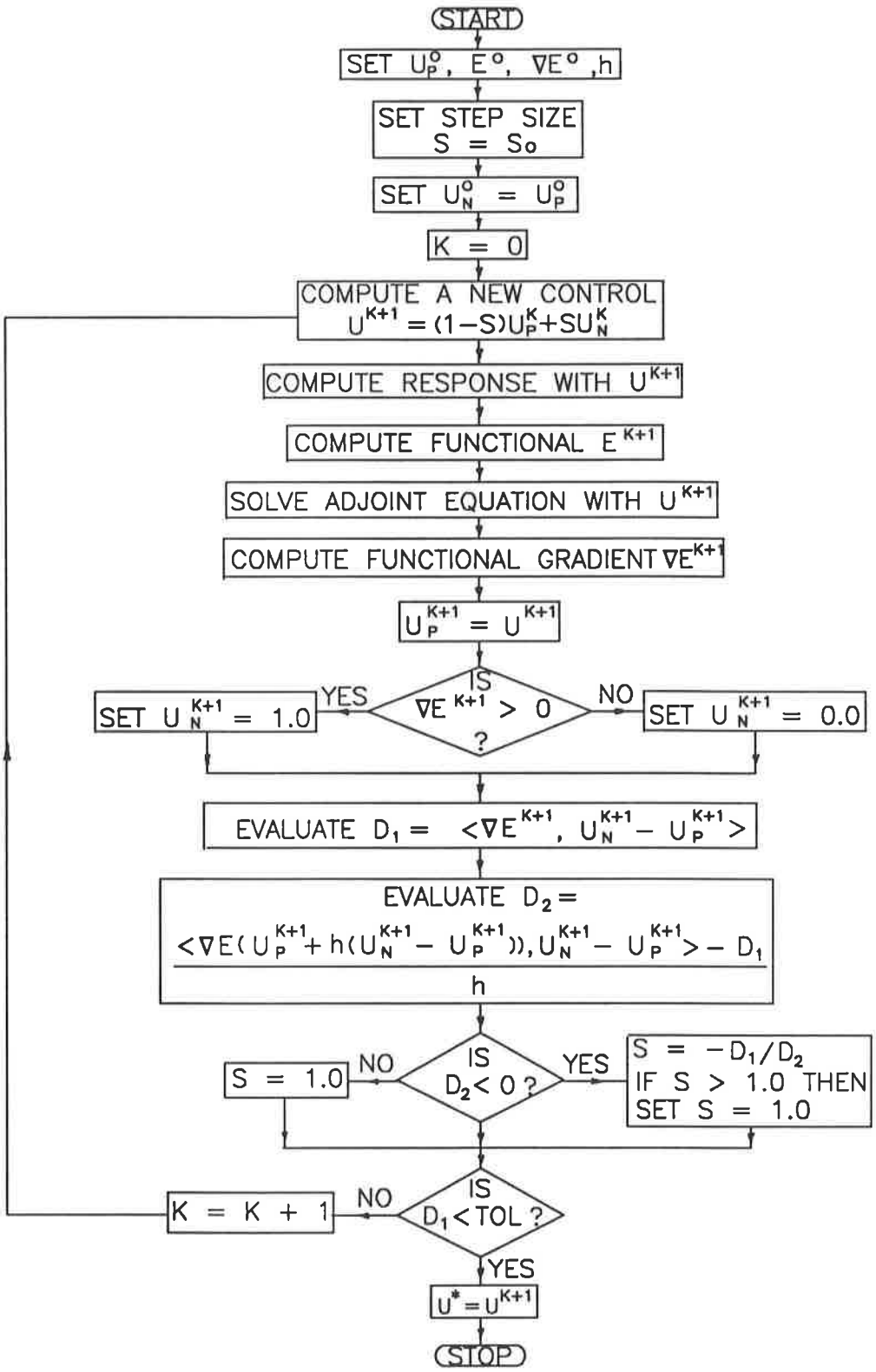

FIG.3 FLOW CHART – REVISED CONDITIONAL GRADIENT ALGORITHM (NCGA)

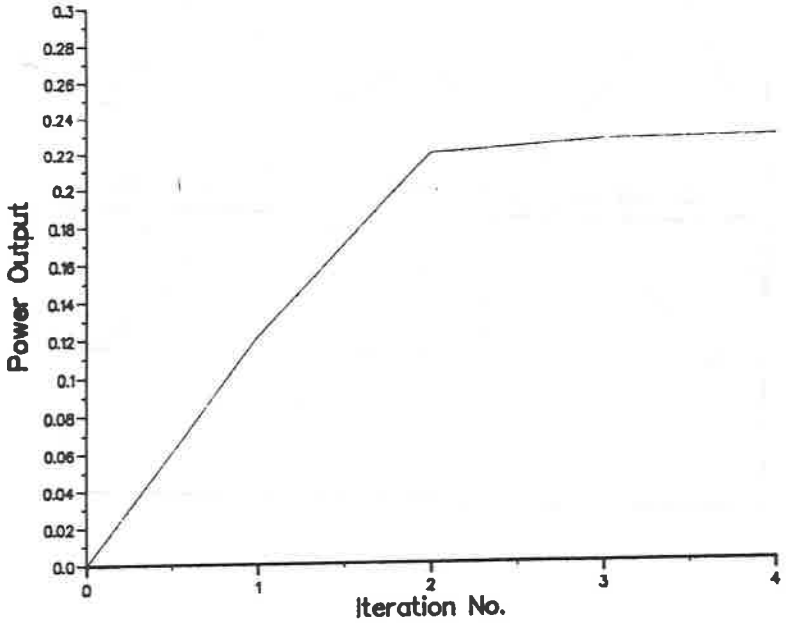

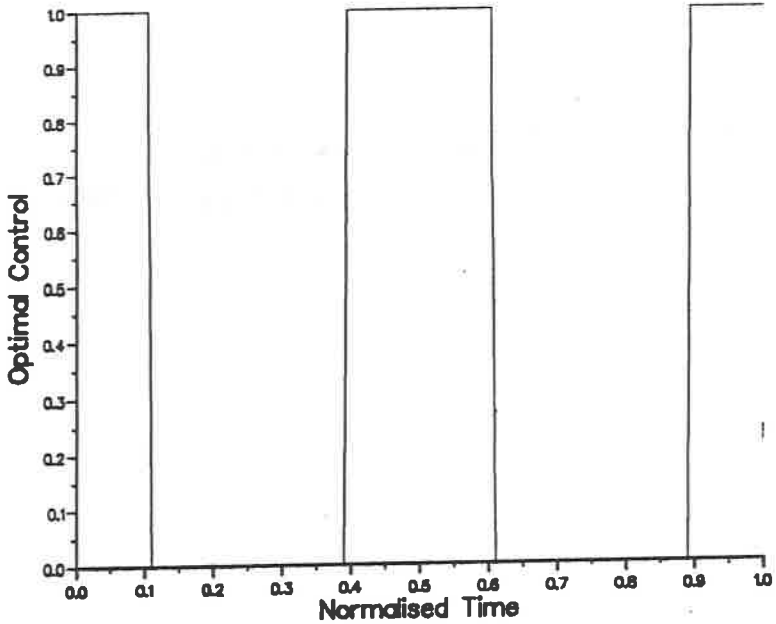

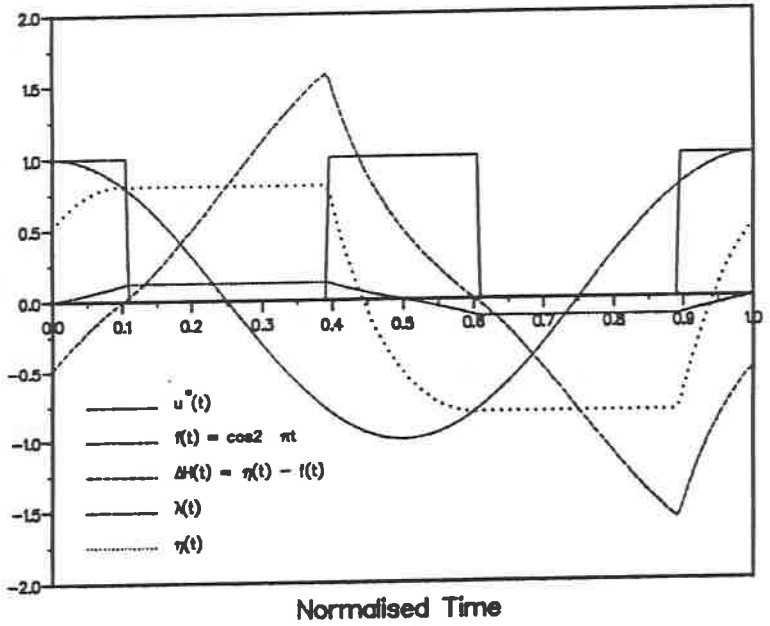

FIG. 4 Linear - CGA

Tol = 1%, N = 200

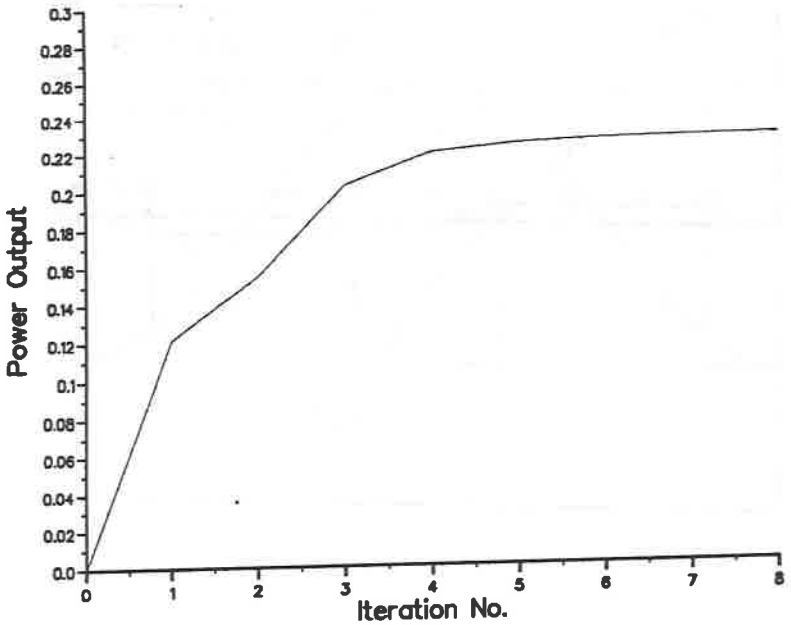

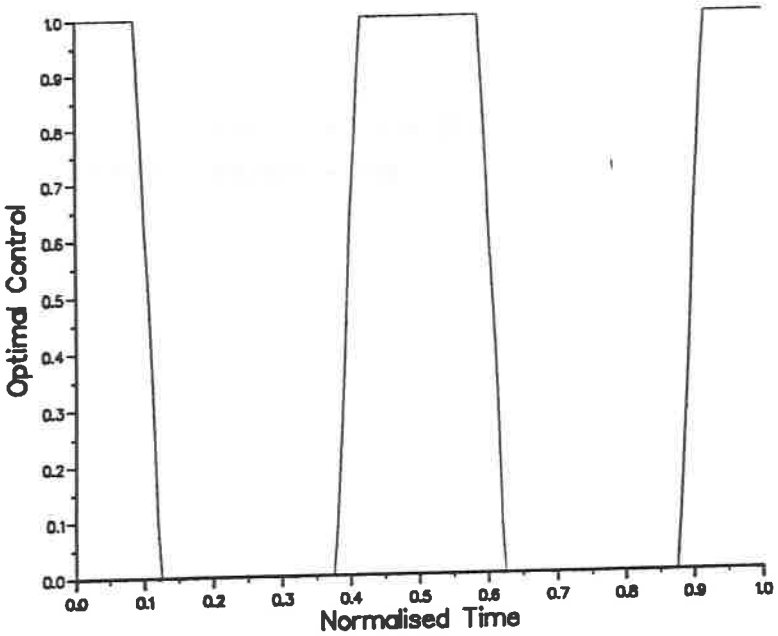

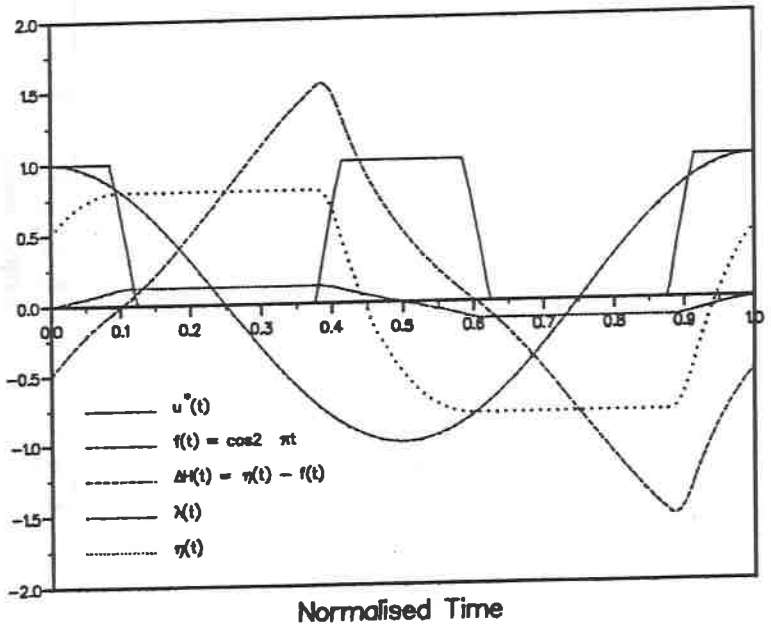

FIG. 5 Linear - PGA

Tol = 1%, N = 200

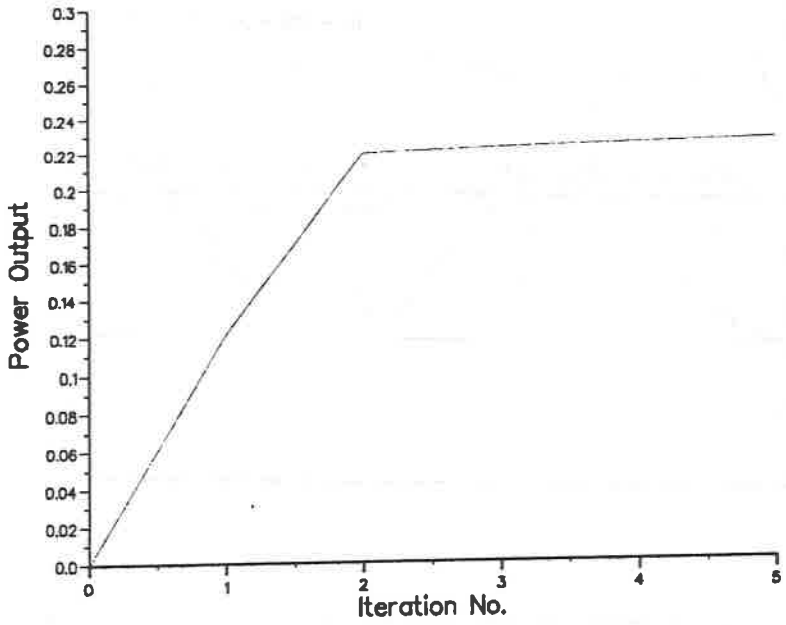

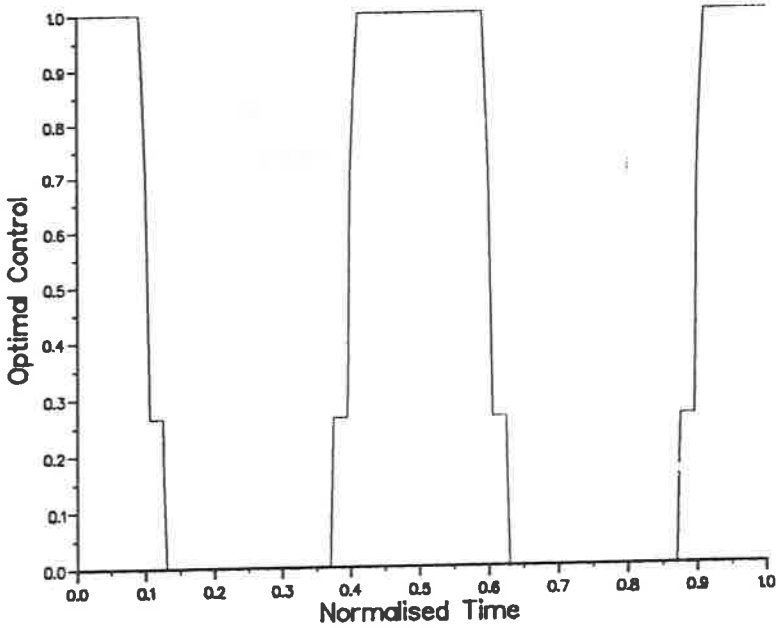

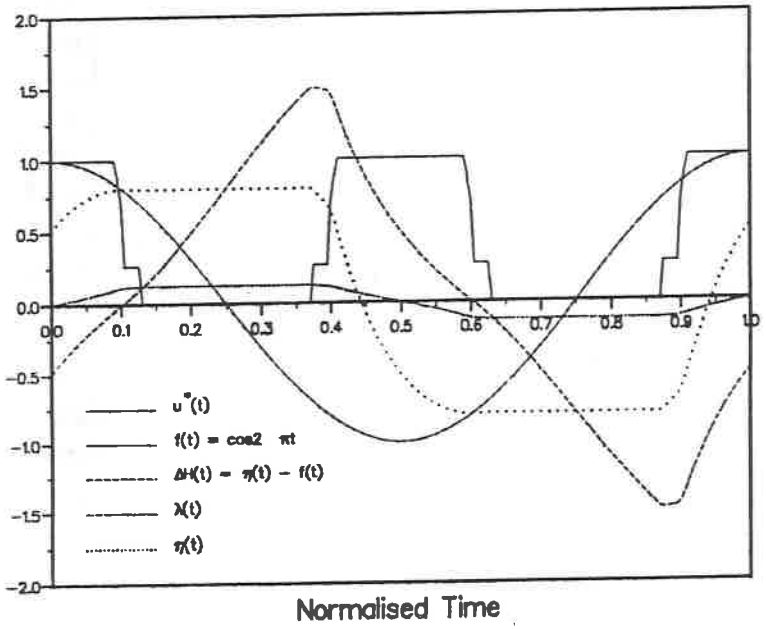

FIG. 6 Linear - NCGA
Tol = 1%, N = 200

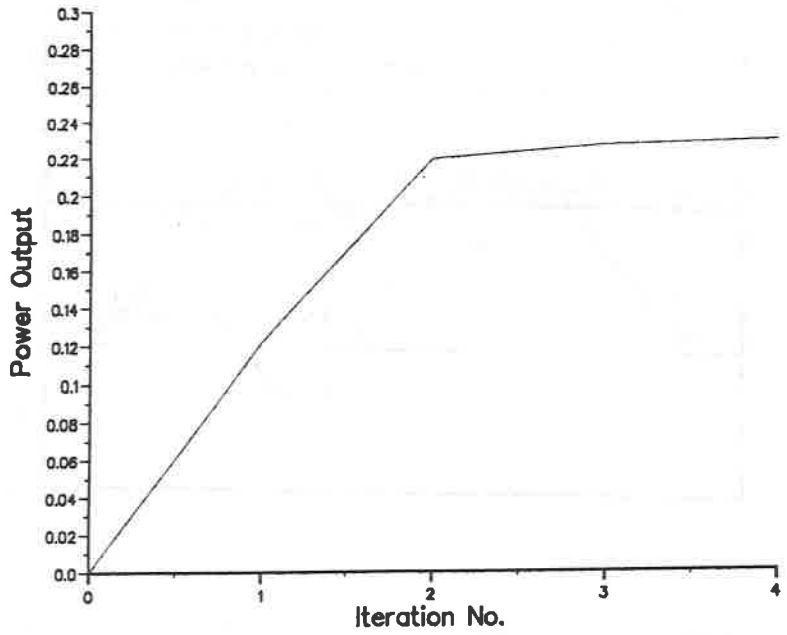

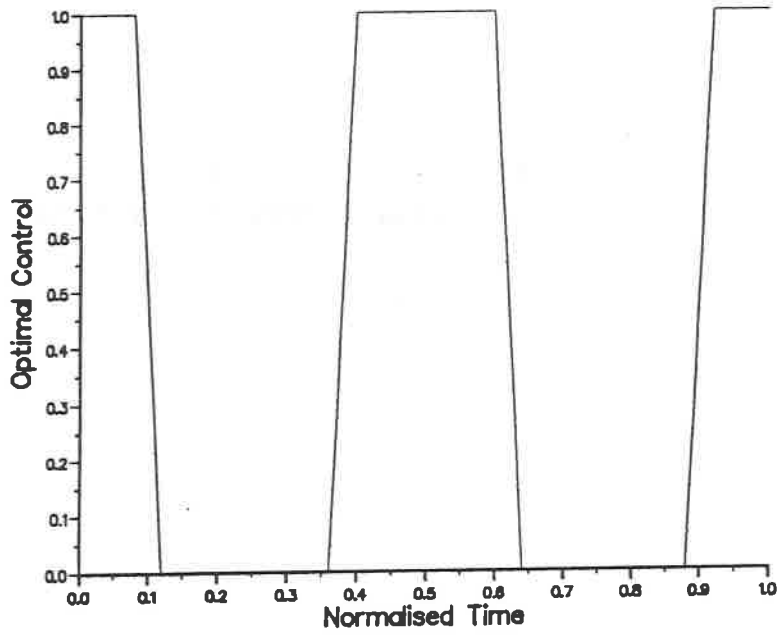

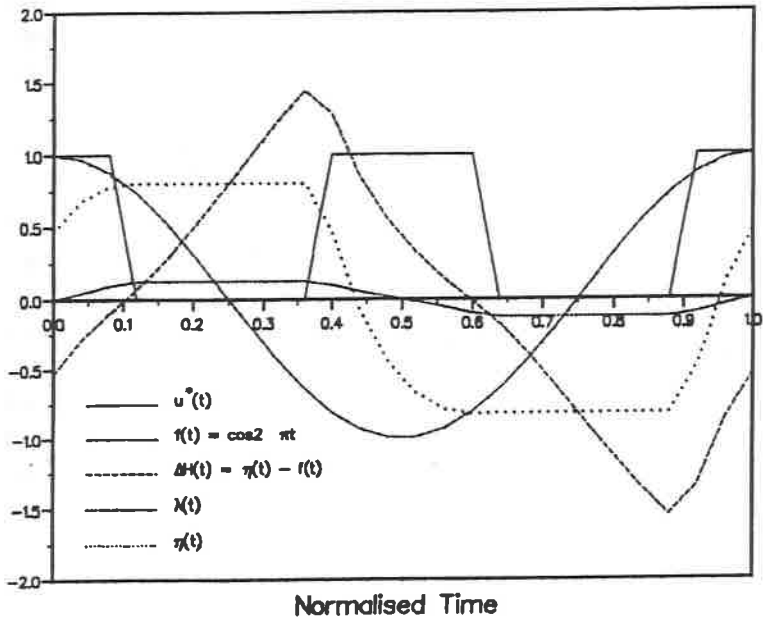

FIG. 7 Linear - CGA
Tol = 1%, N = 25

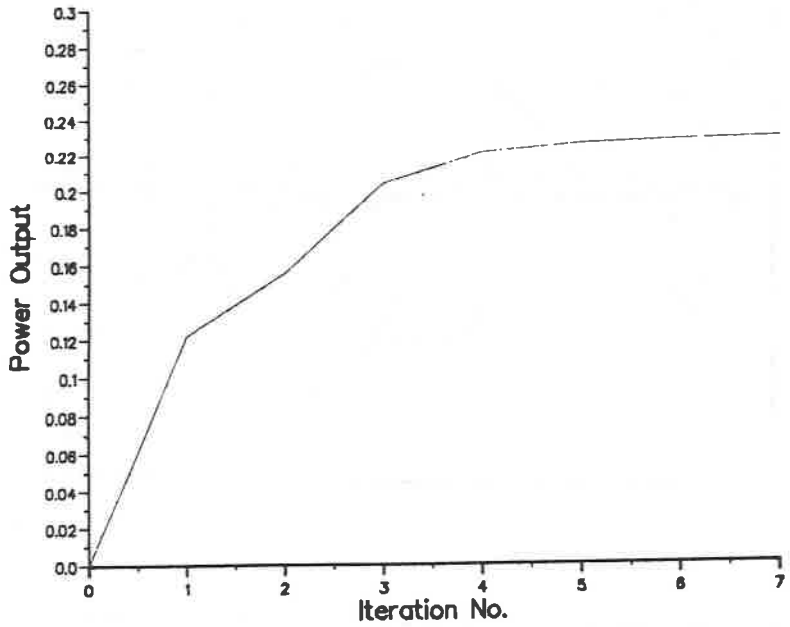

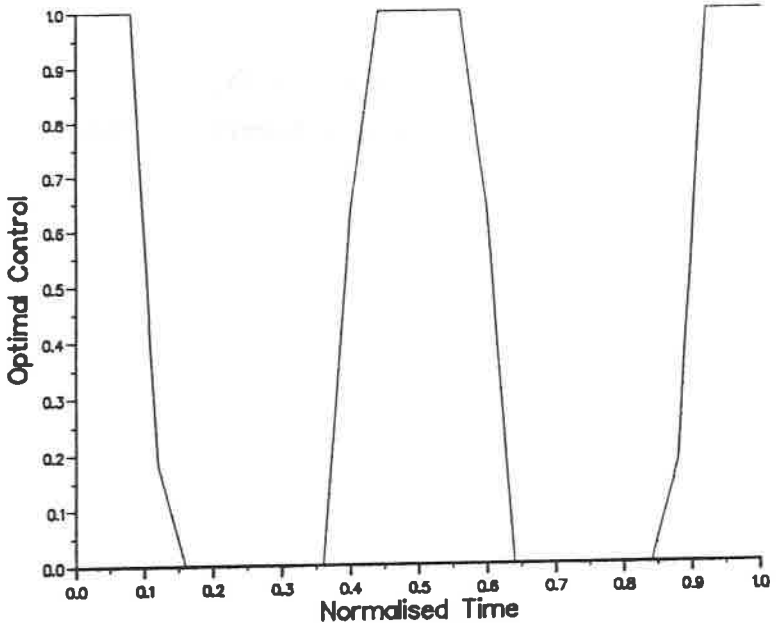

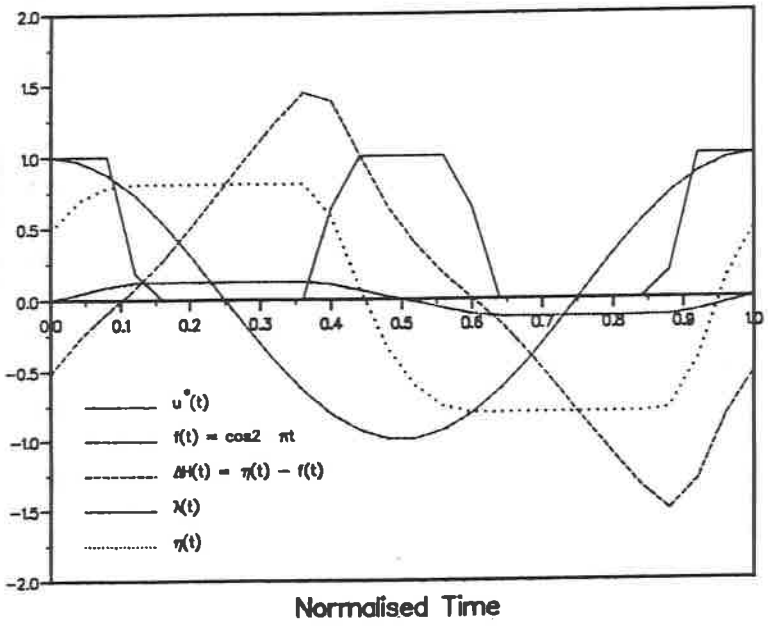

FIG. 8 Linear - PGA

Tol = 1%, N = 25

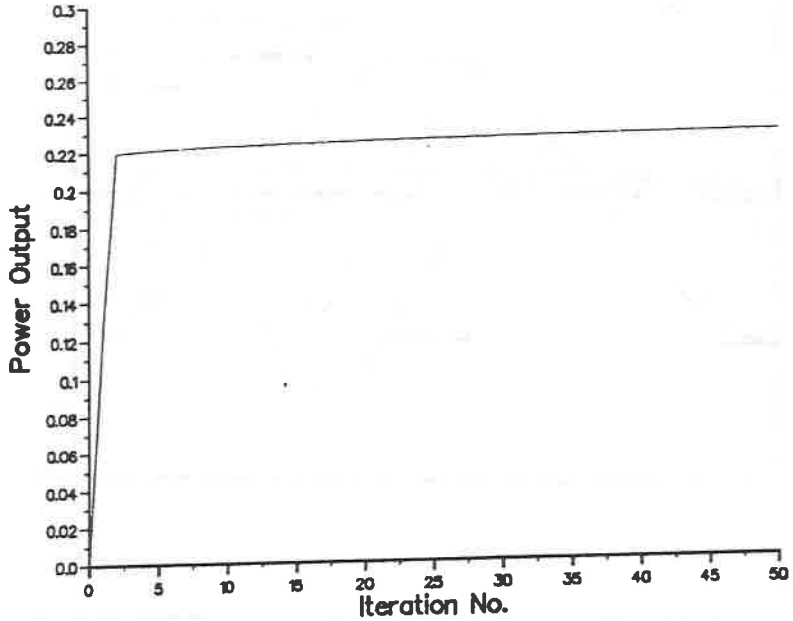

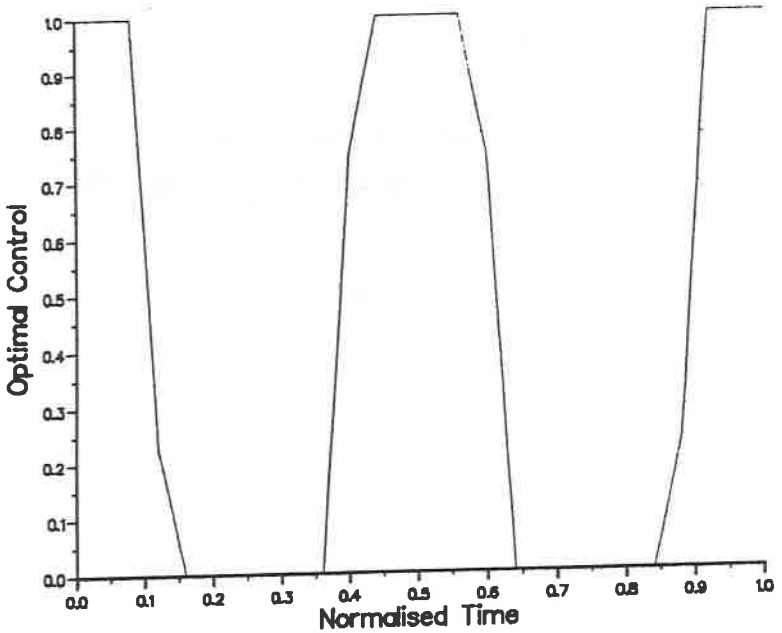

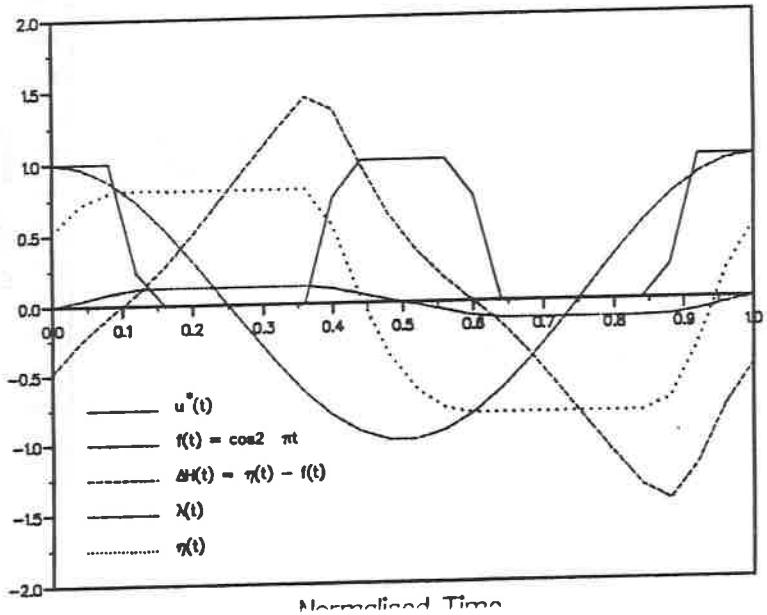

FIG. 9 Linear - NCGA
Tol = 1%, N = 25

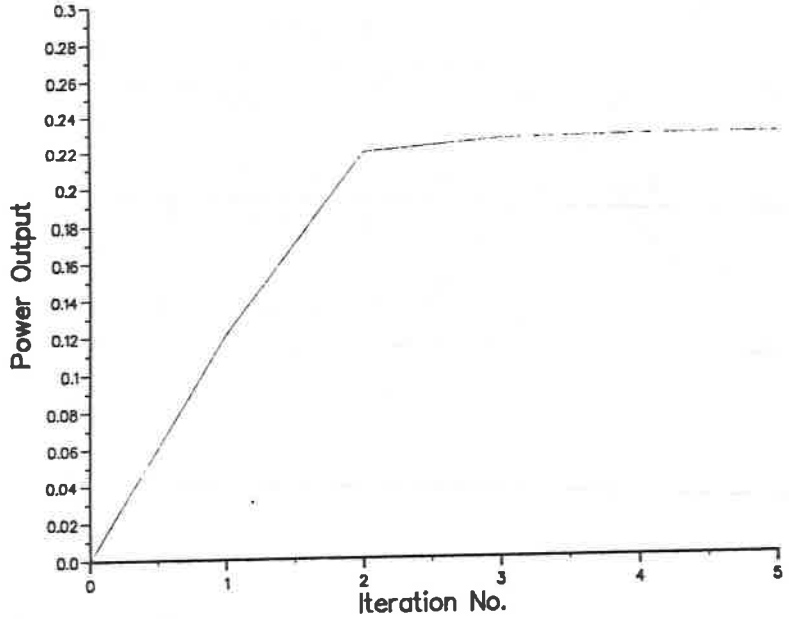

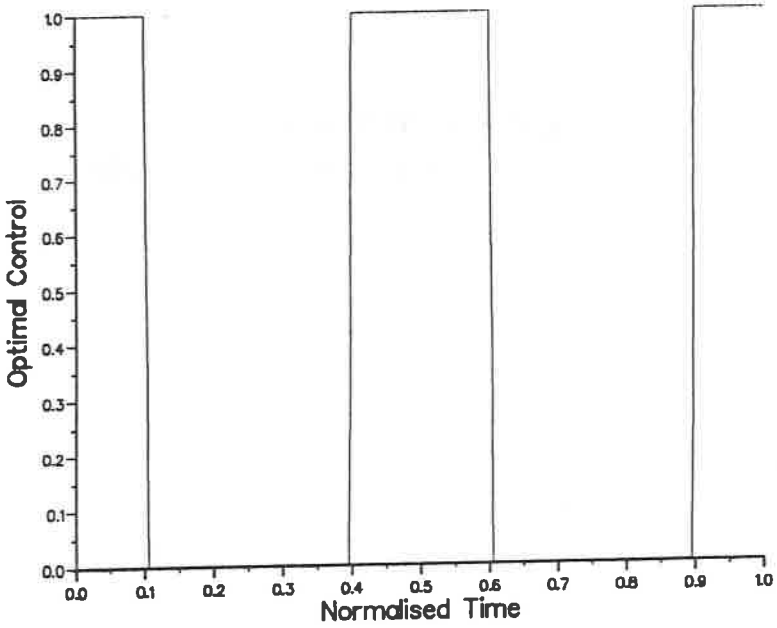

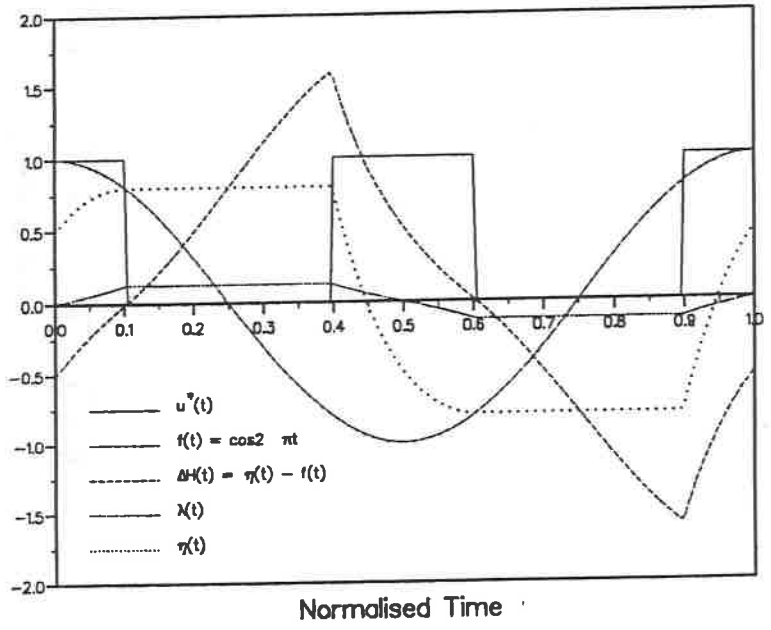

FIG. 10 Linear - CGA

Tol = 0.1%, N = 200

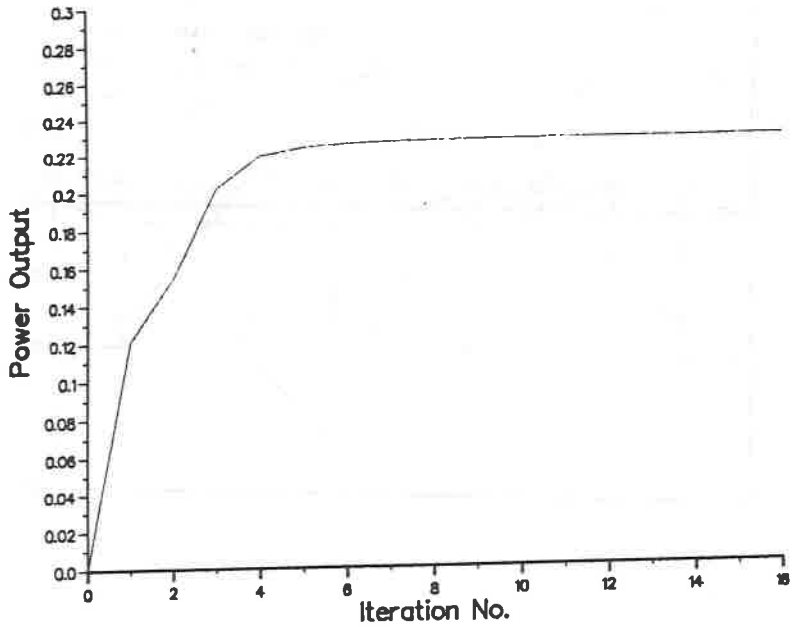

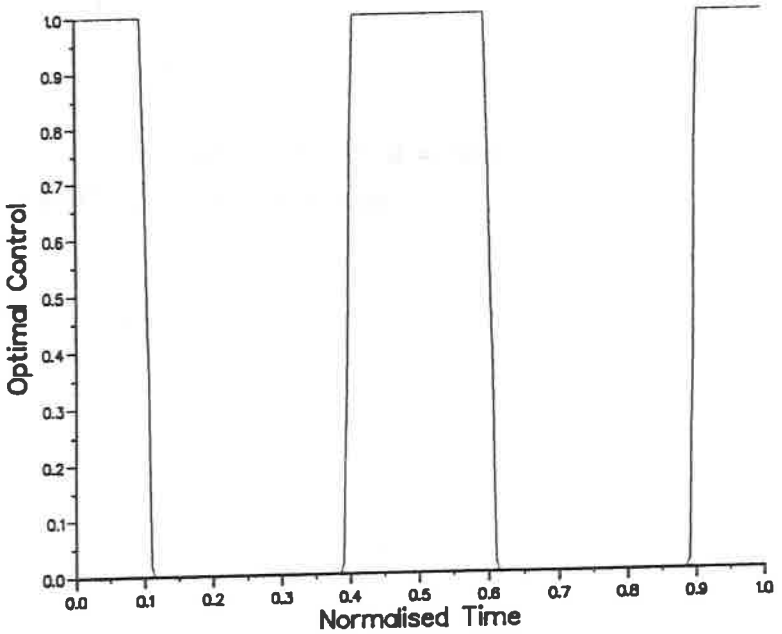

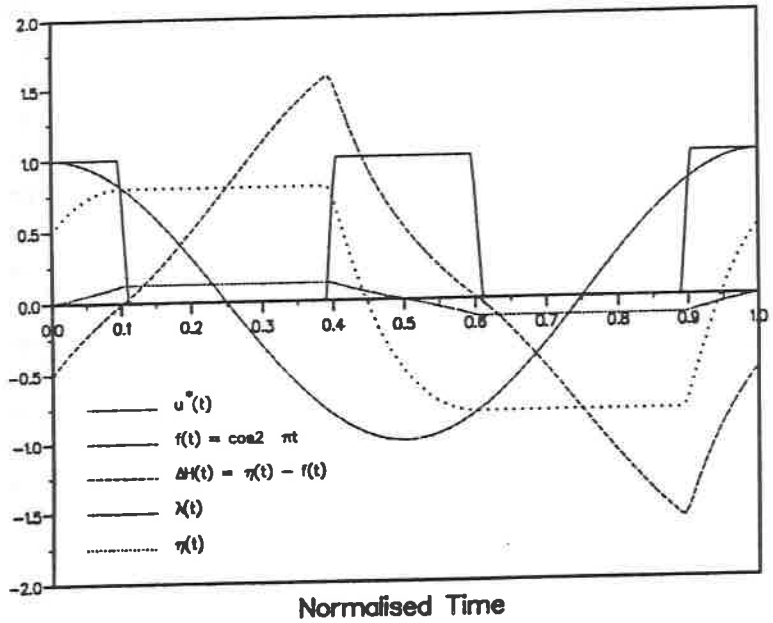

FIG. 11 Linear - PGA

Tol = 0.1%, N = 200

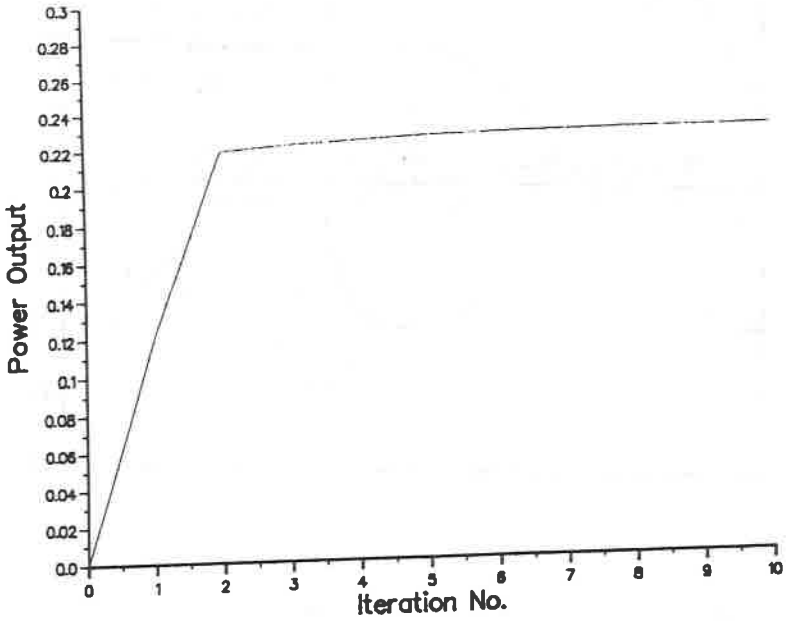

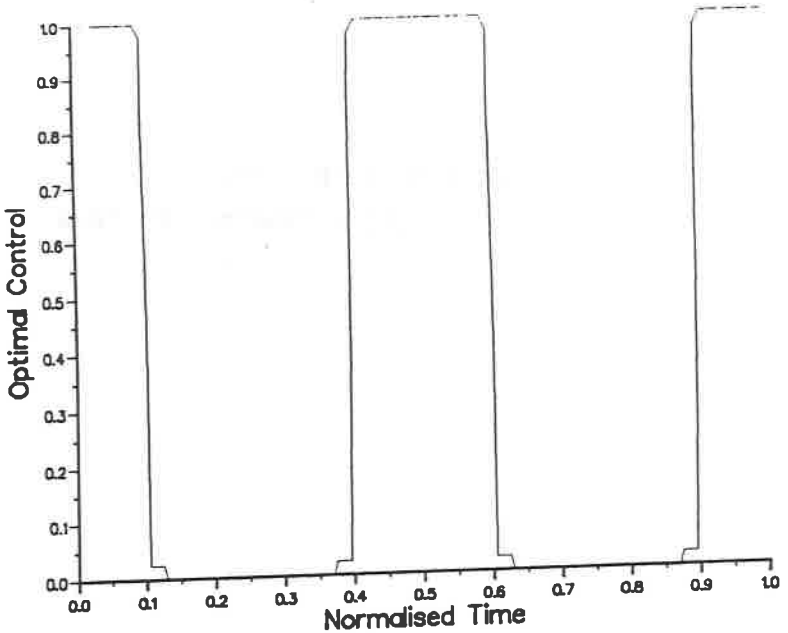

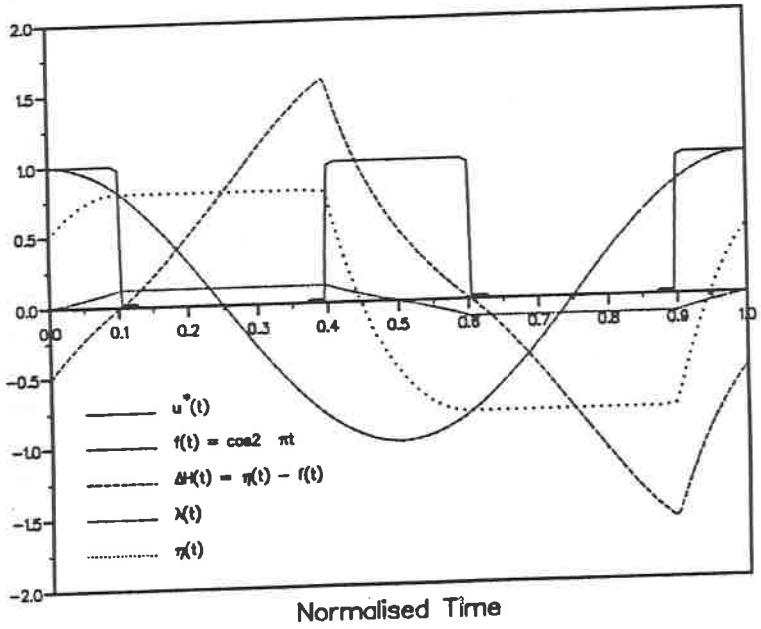

FIG. 12 Linear - NCGA
Tol = 0.1%, N = 200

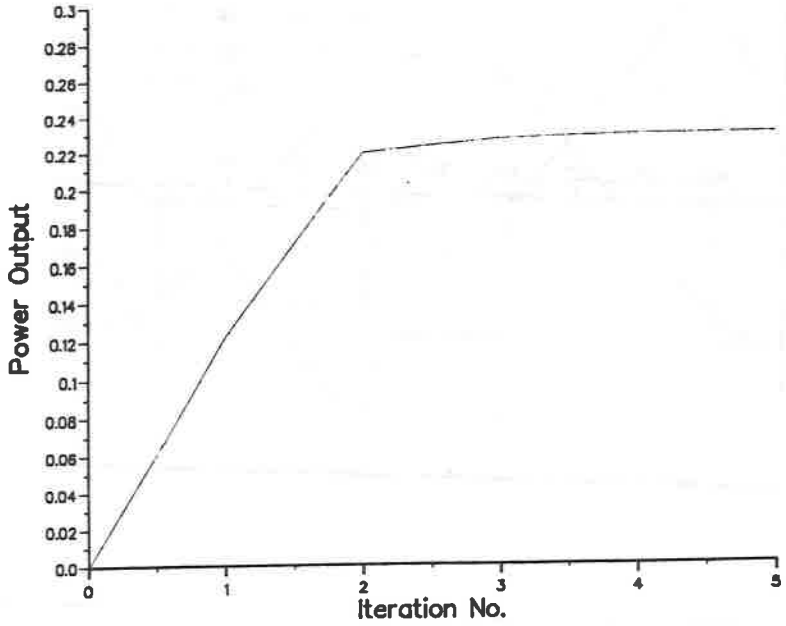

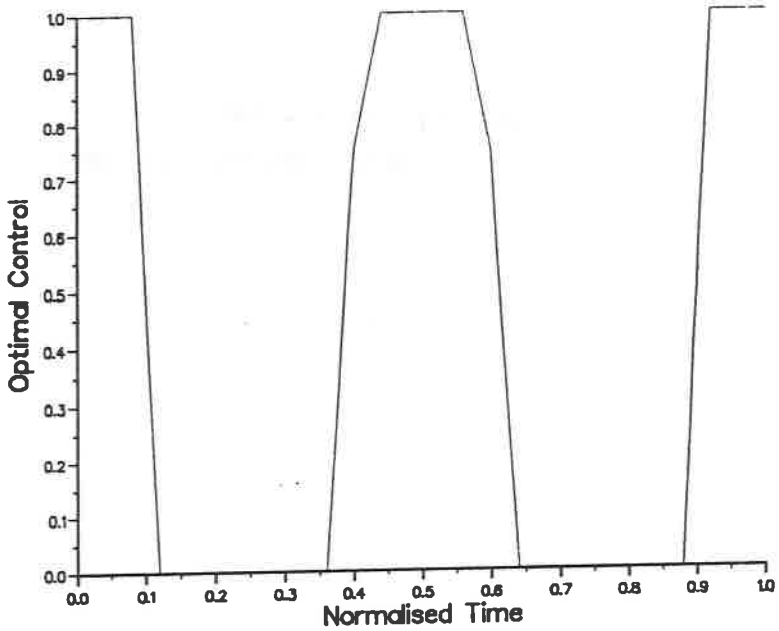

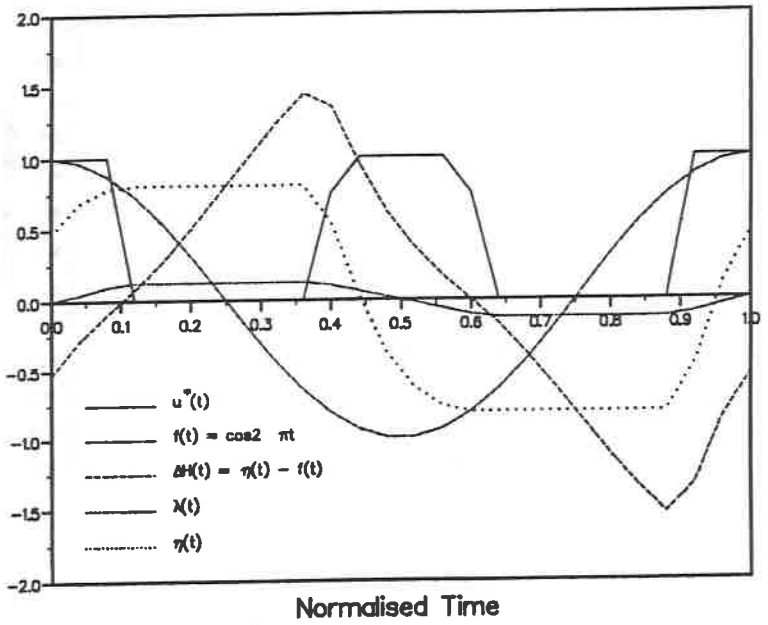

FIG. 13 Linear - CGA
Tol = 0.1%, N = 25

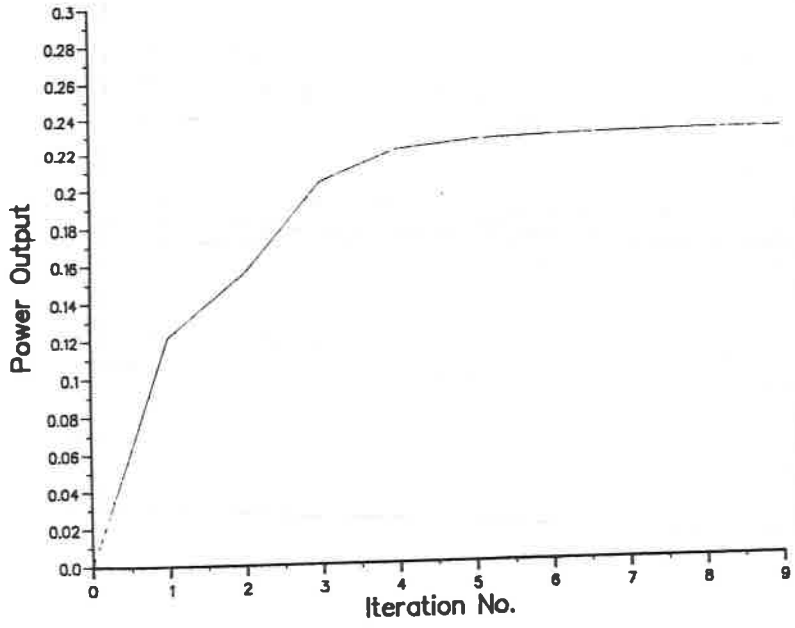

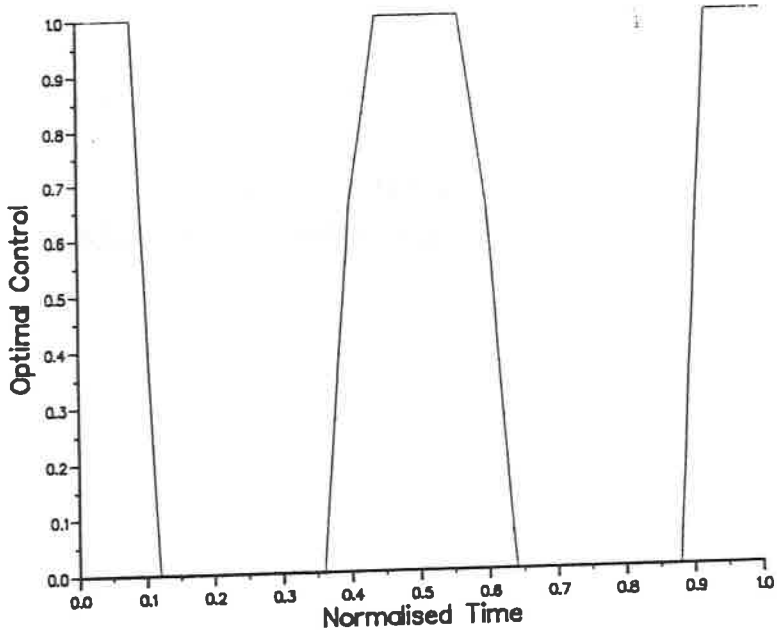

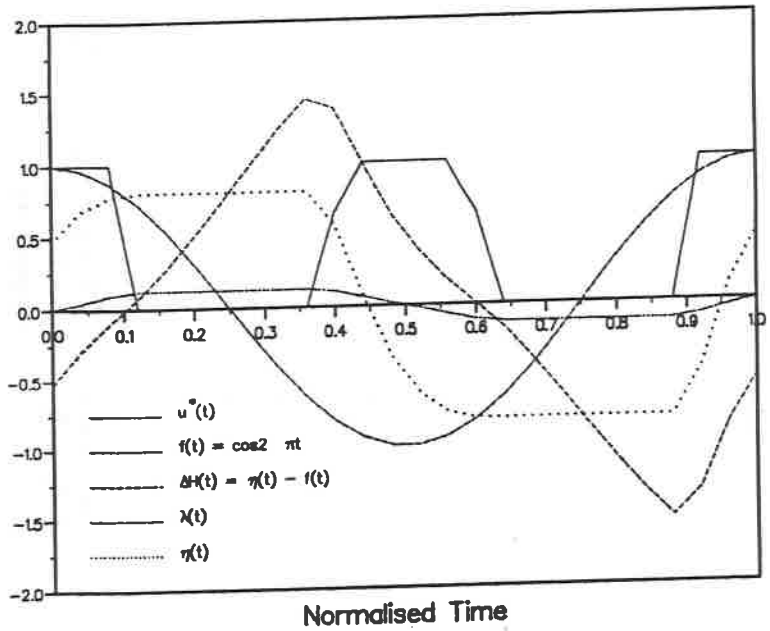

FIG. 14 Linear - PGA

Tol = 0.1%, N = 25

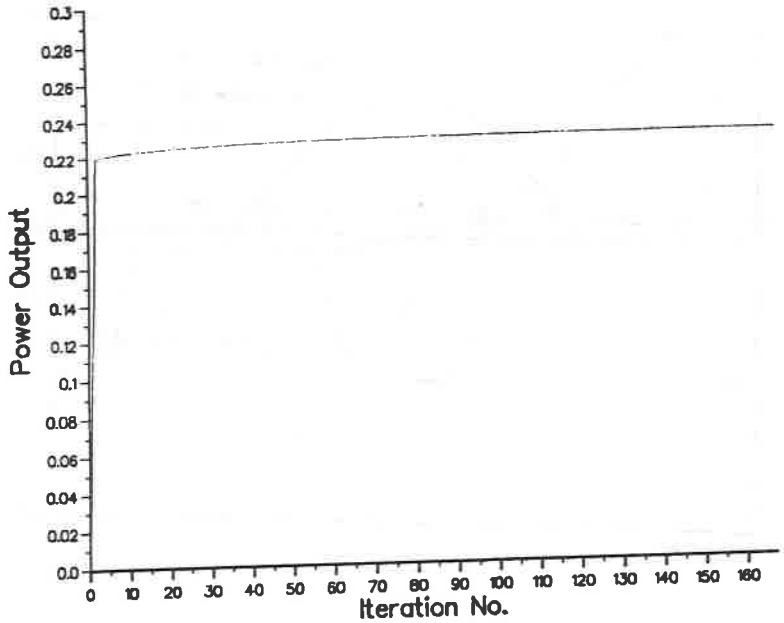

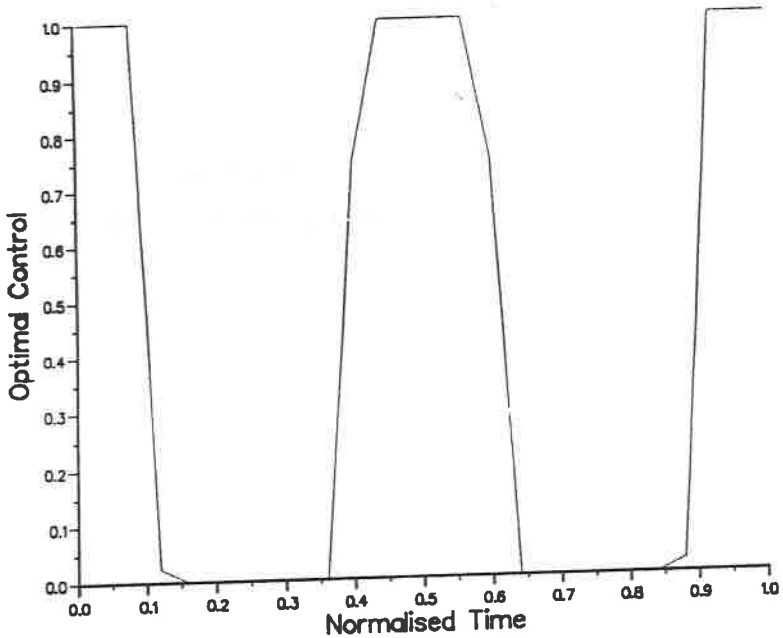

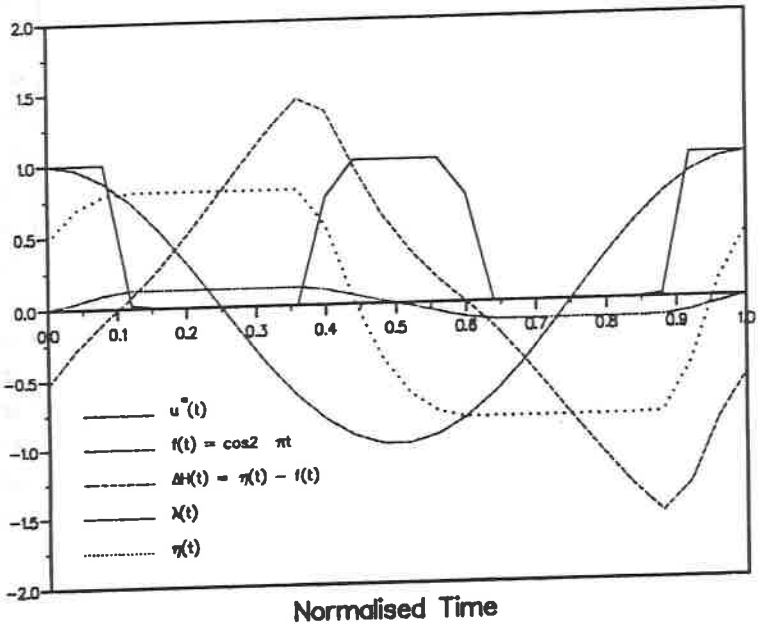

FIG. 15 Linear - NCGA

Tol = 0.1%, N = 25

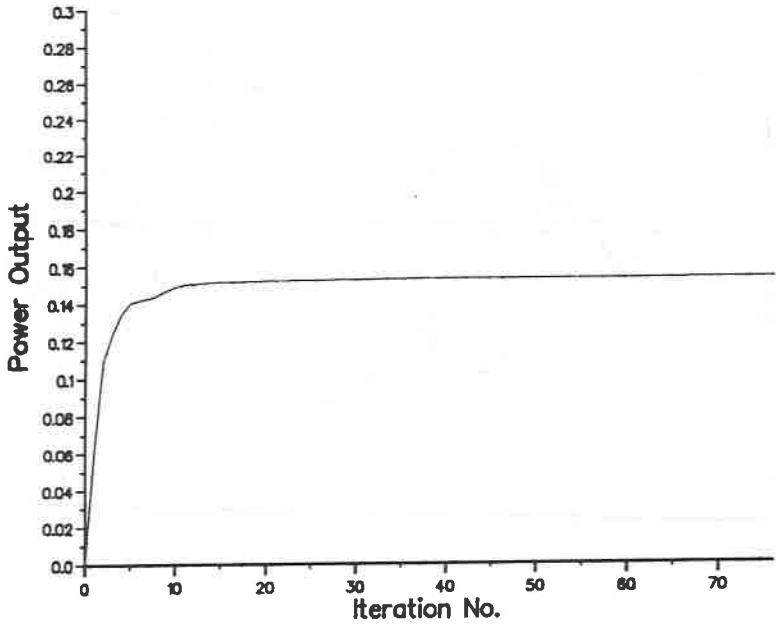

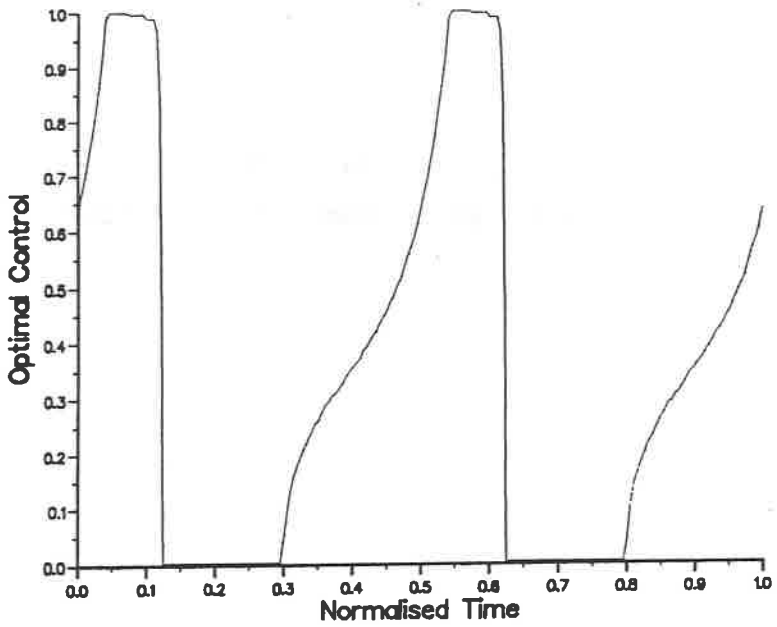

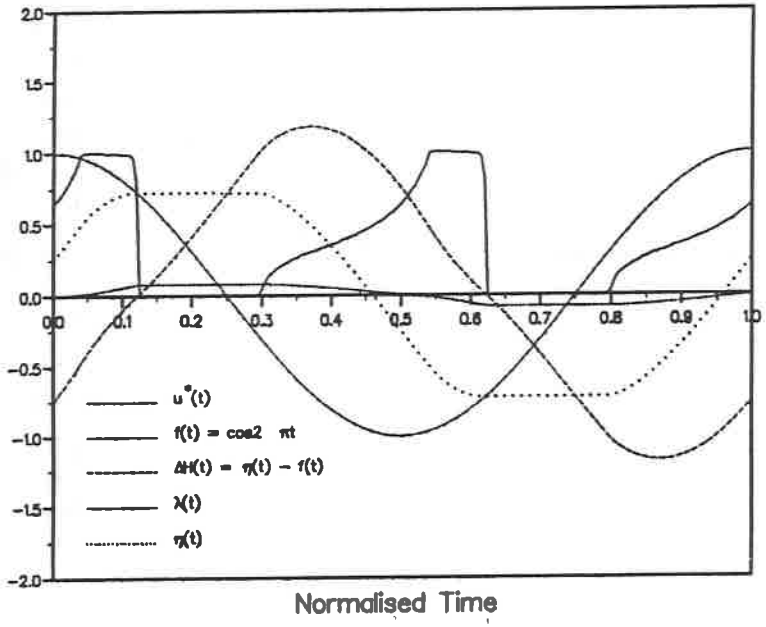

FIG. 16 Non-Linear - CGA c = 1

Tol = 1%, N = 200

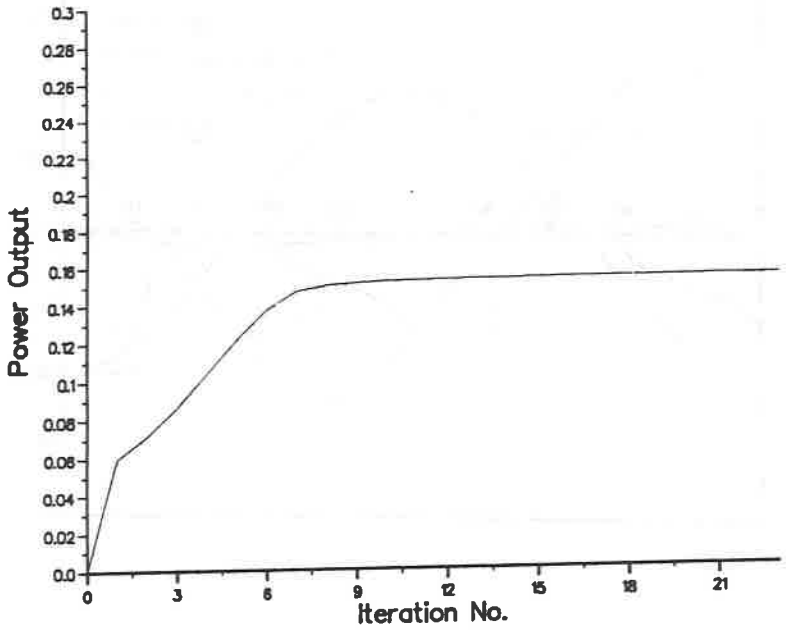

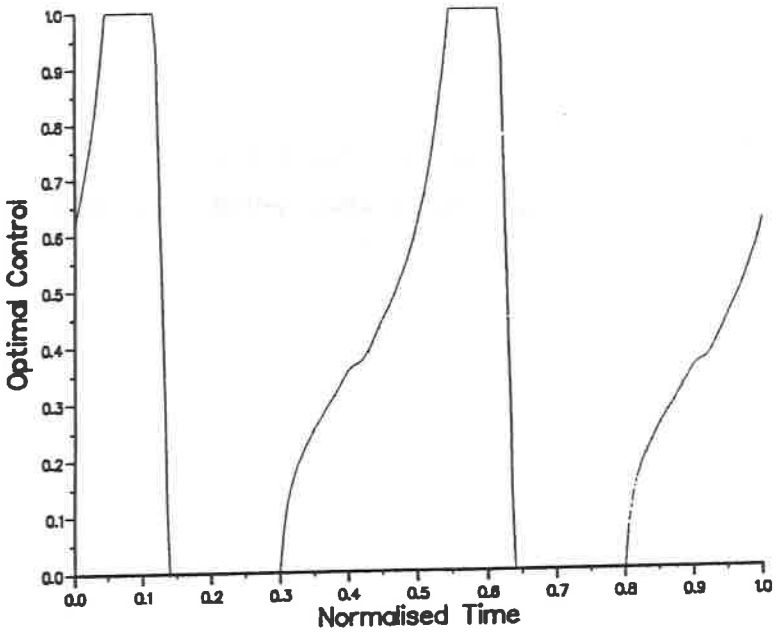

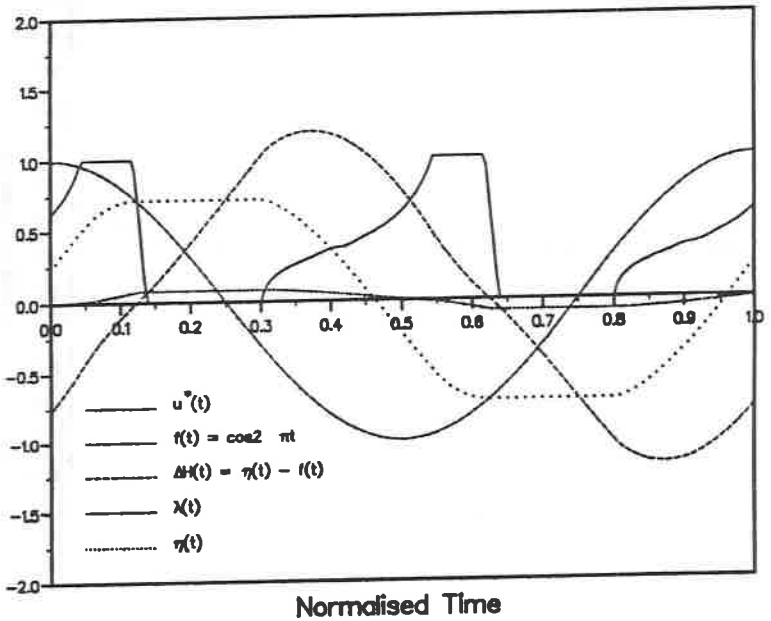

FIG. 17 Non-linear - PGA c = 1
Tol = 1%, N = 200

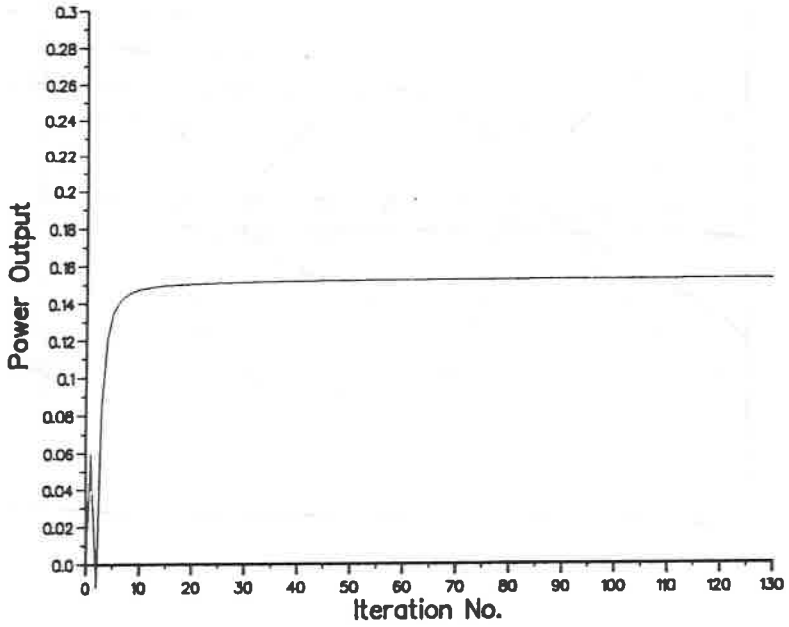

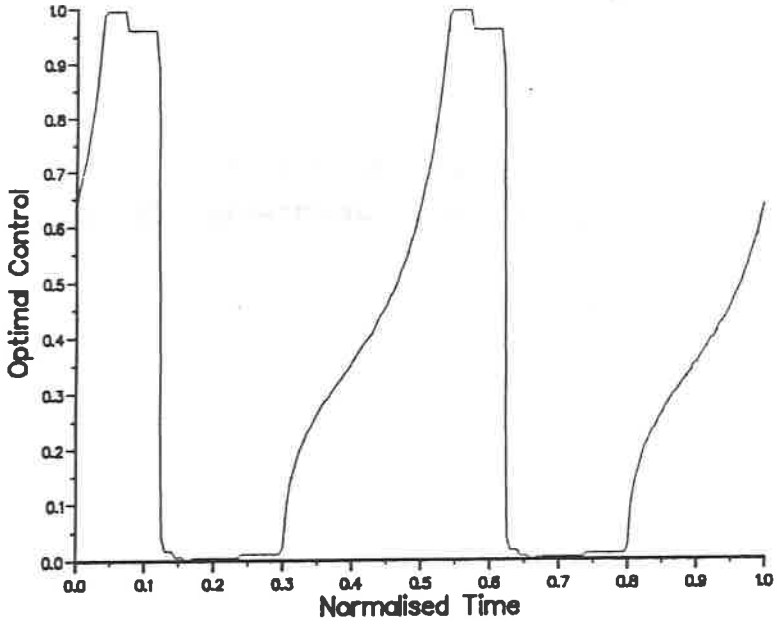

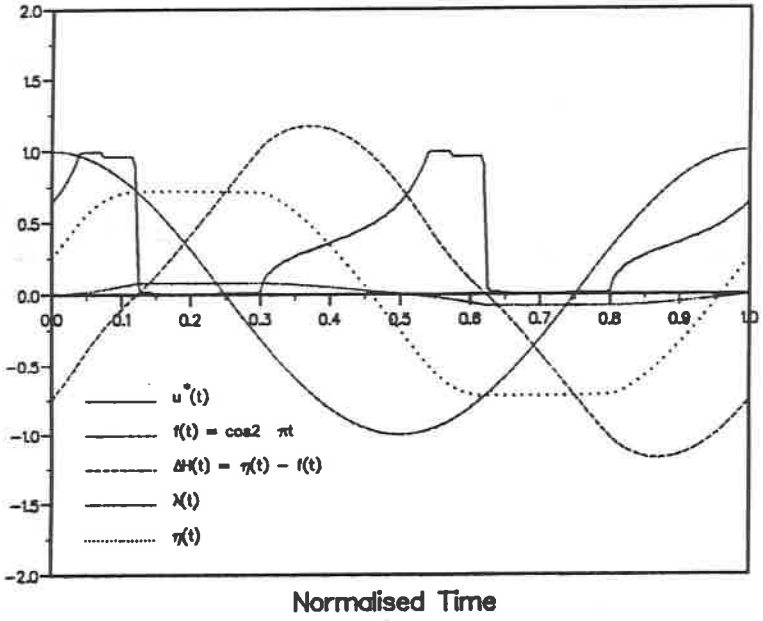

FIG. 18 Non-linear - NCGA c = 1

Tol = 1%, N = 200

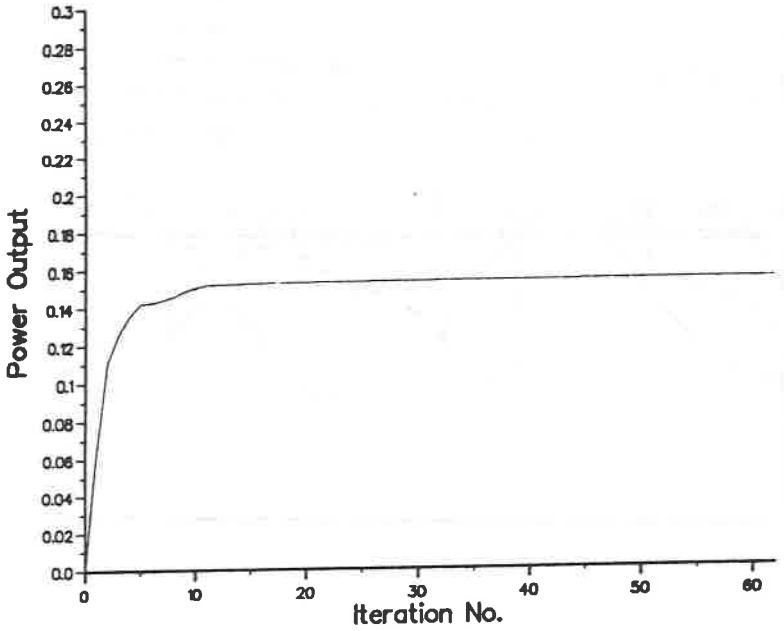

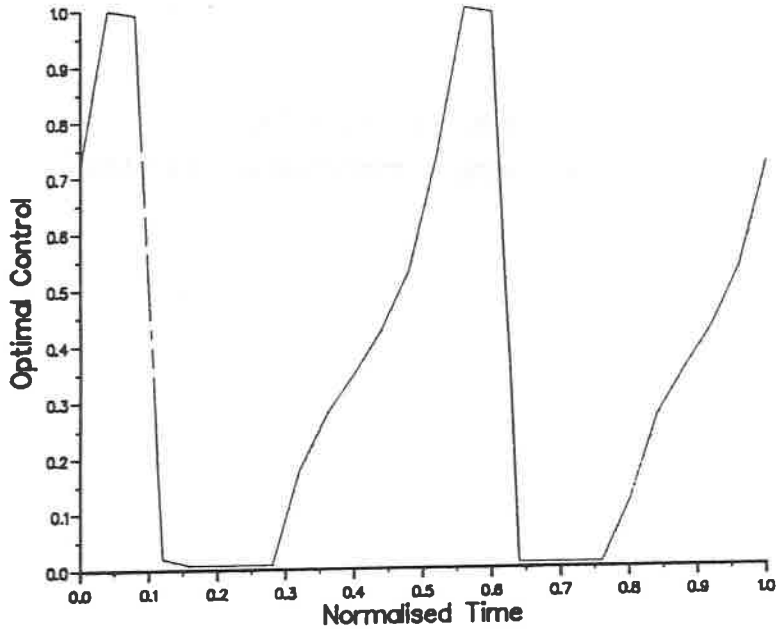

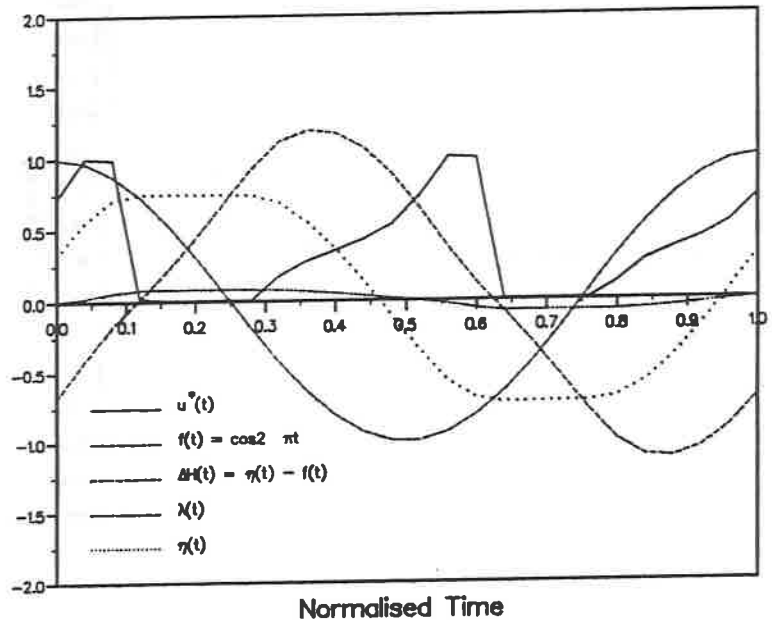

FIG. 19 Non-linear - CGA c = 1
Tol = 1%, N = 25

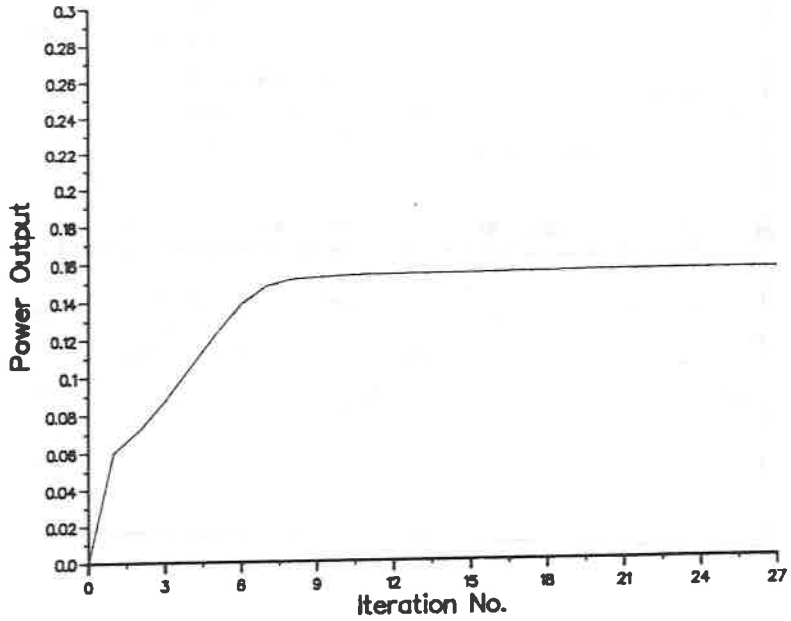

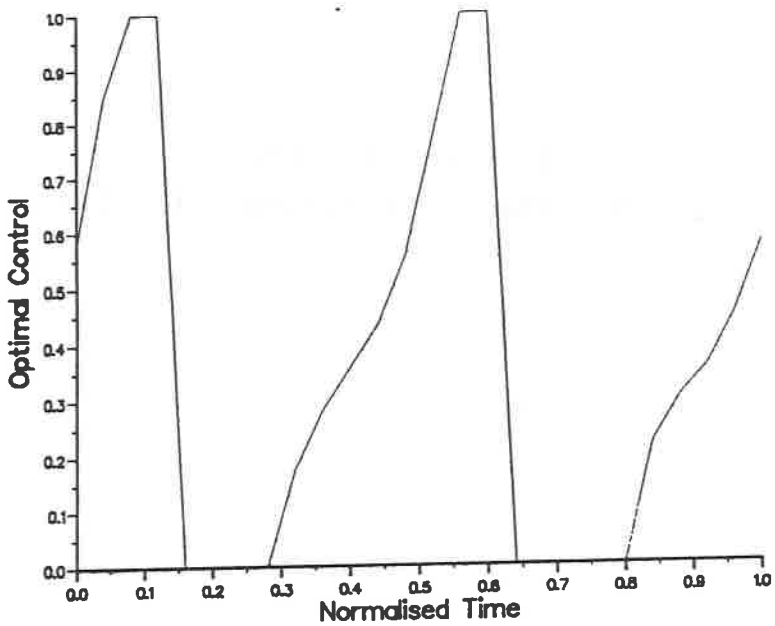

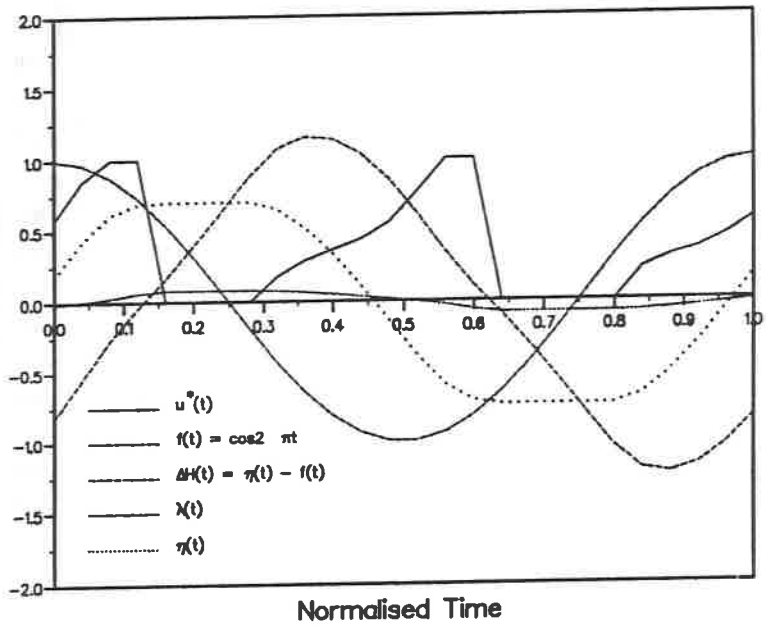

FIG. 20 Non-linear - PGA c = 1

Tol = 1%, N = 25

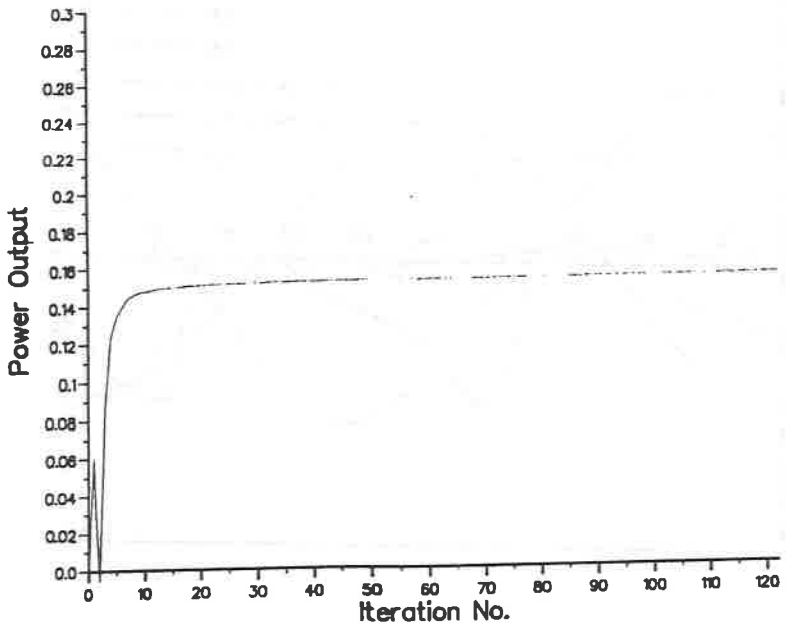

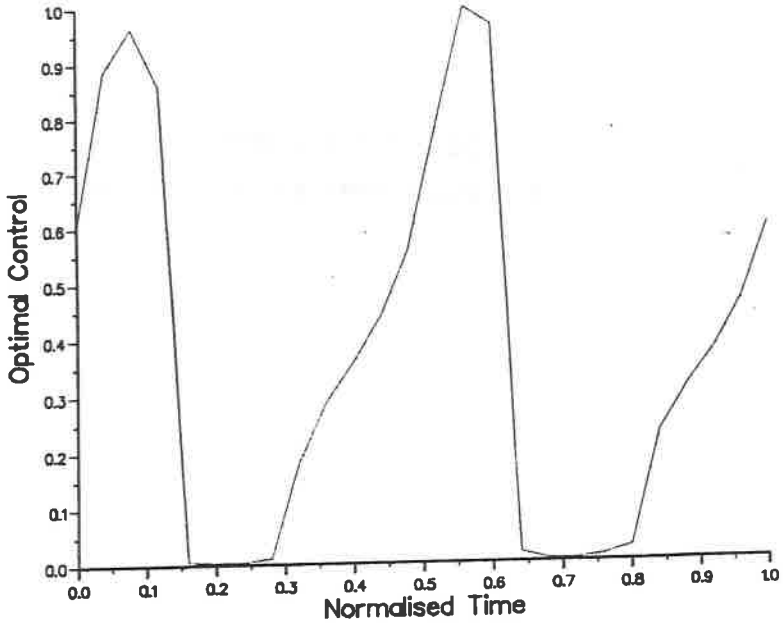

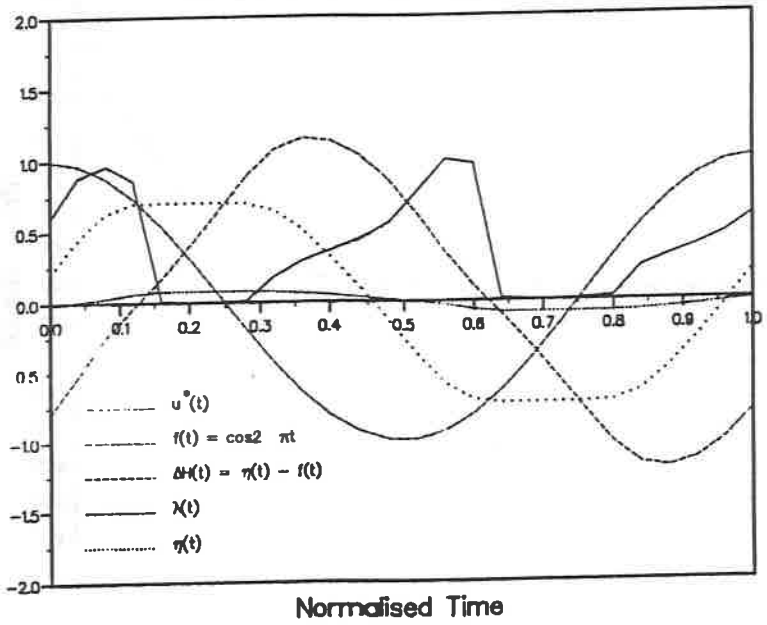

FIG. 21 Non-linear - CGA c = 1
Tol = 1%, N = 25

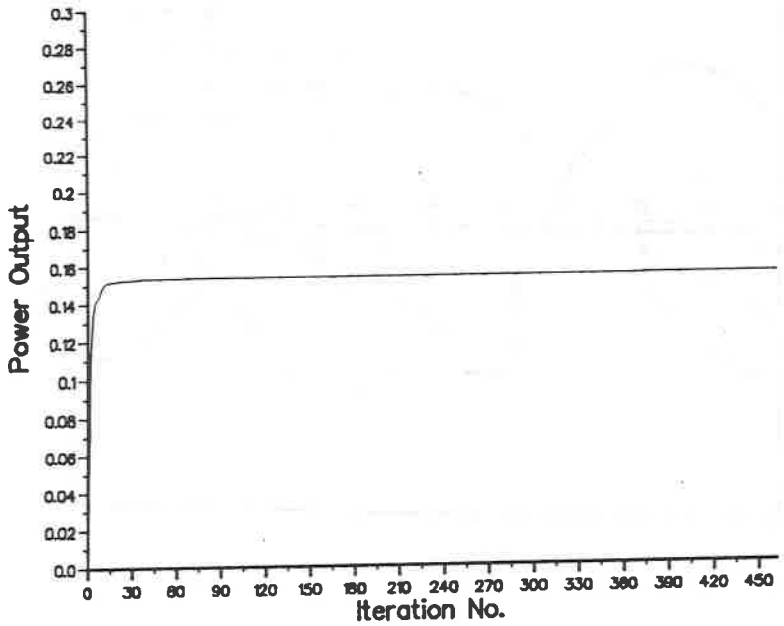

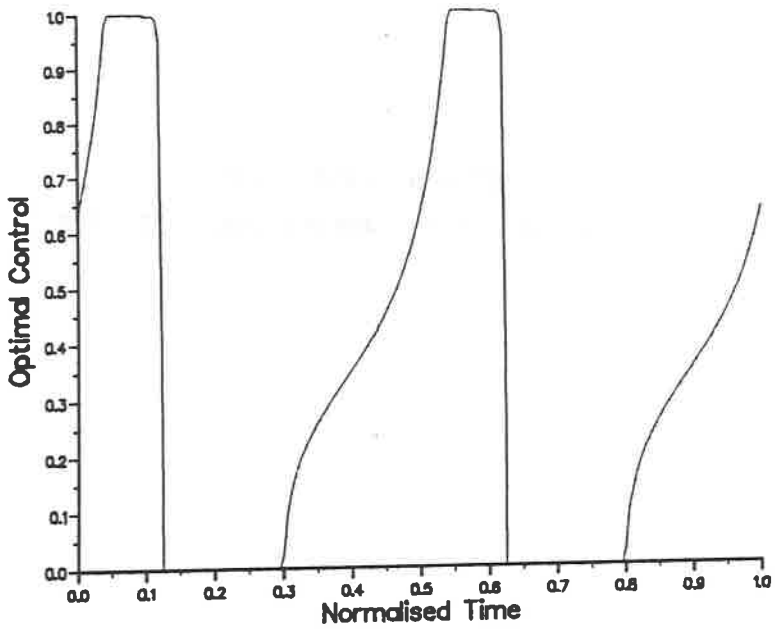

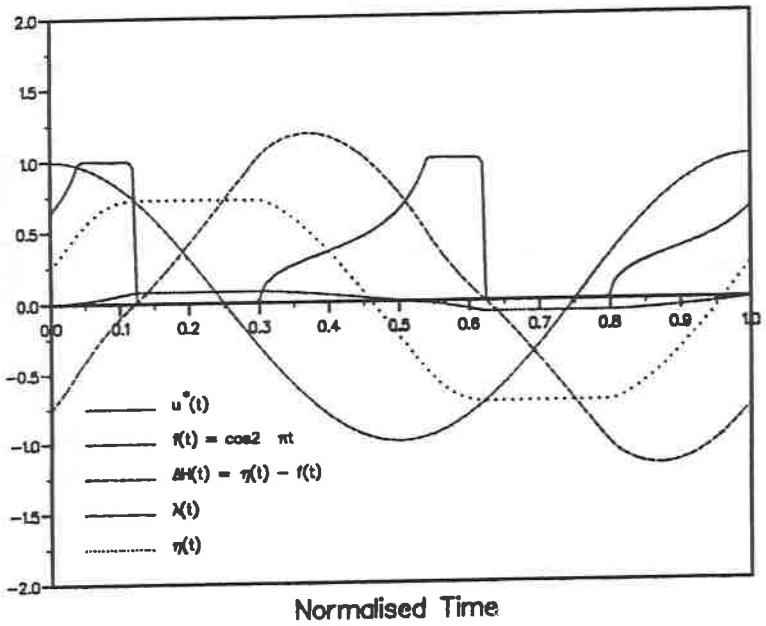

FIG. 22 Non-linear - CGA c = 1
Tol = 0.1%, N = 200

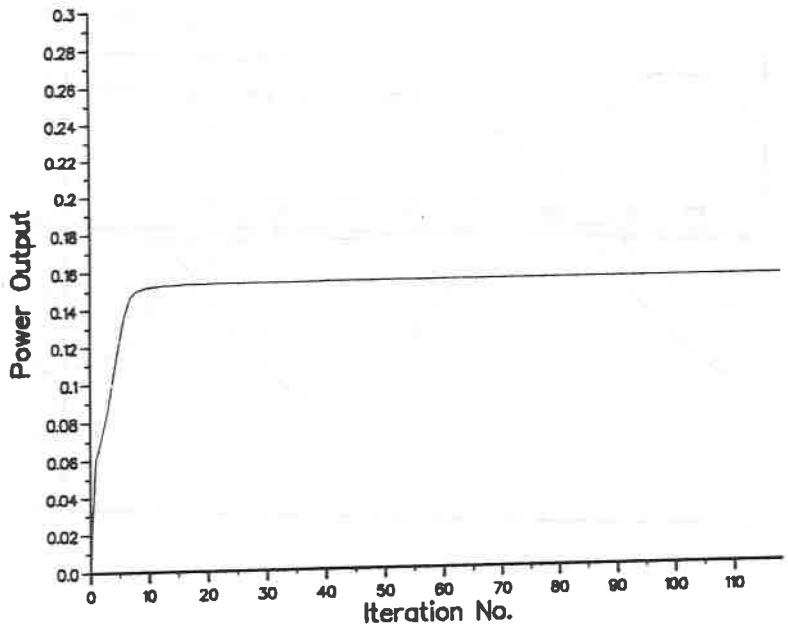

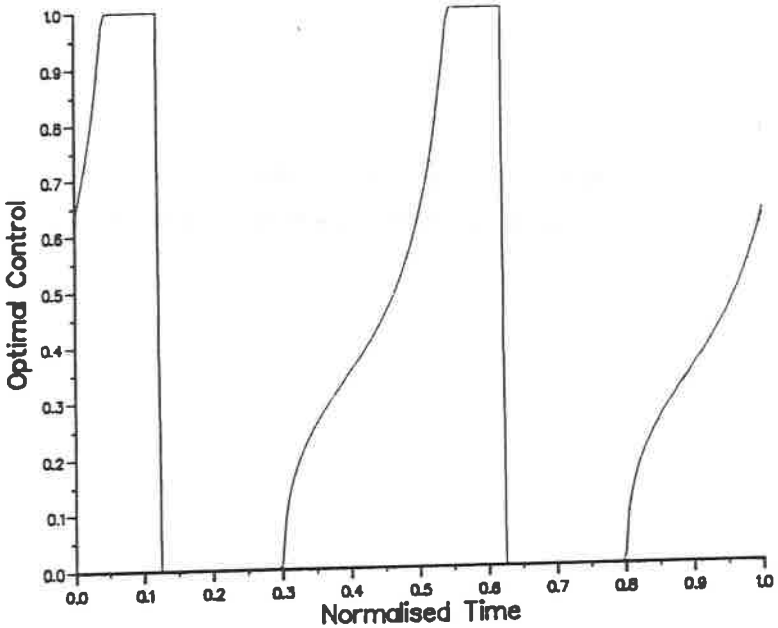

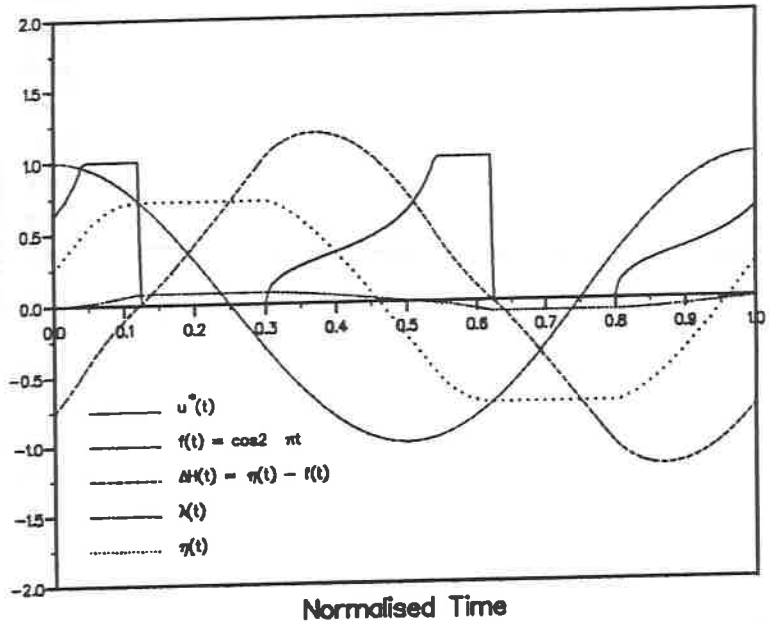

FIG. 23 Non-linear - PGA c = 1
Tol = 0.1%, N = 200

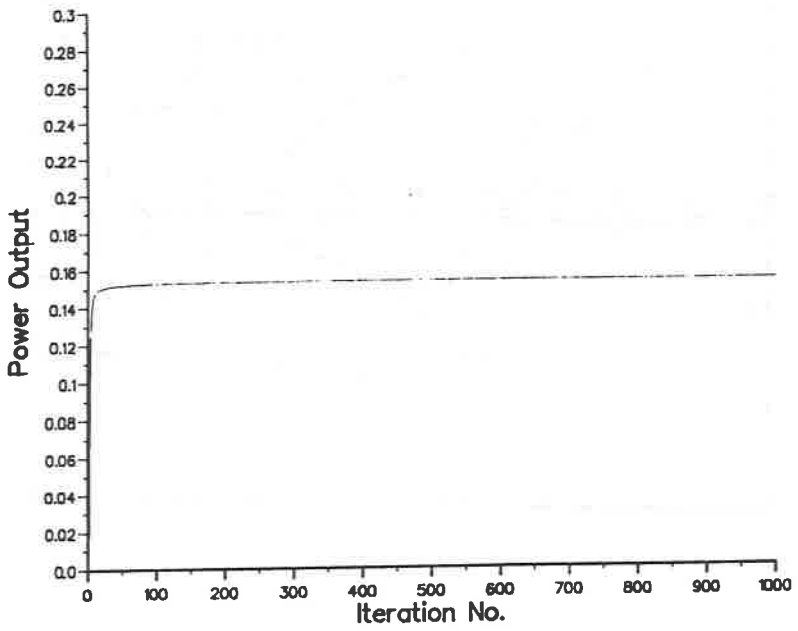

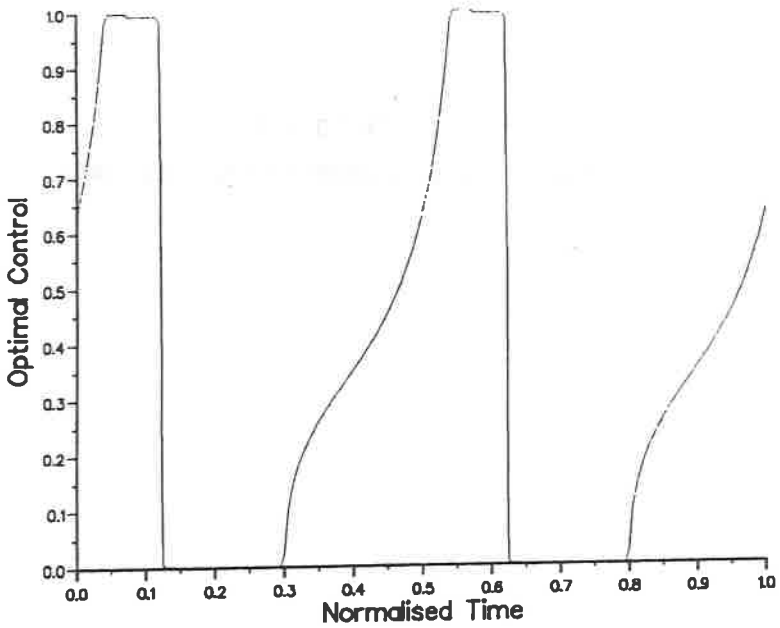

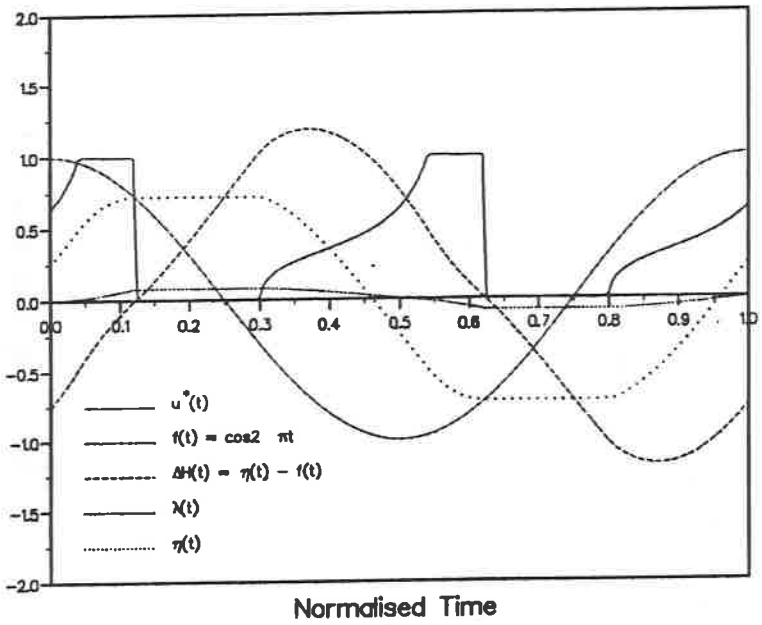

FIG. 24 Non-linear - NCGA c = 1
Tol = 0.1%, N = 200

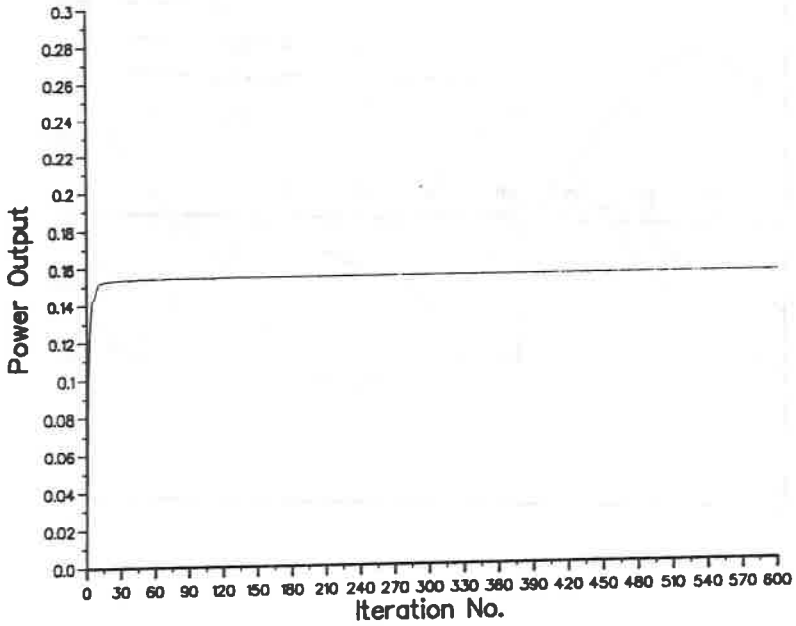

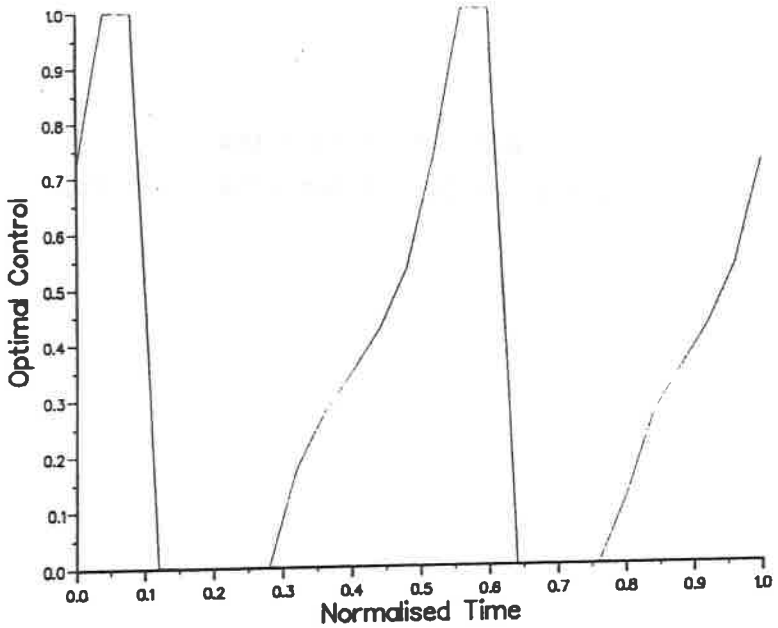

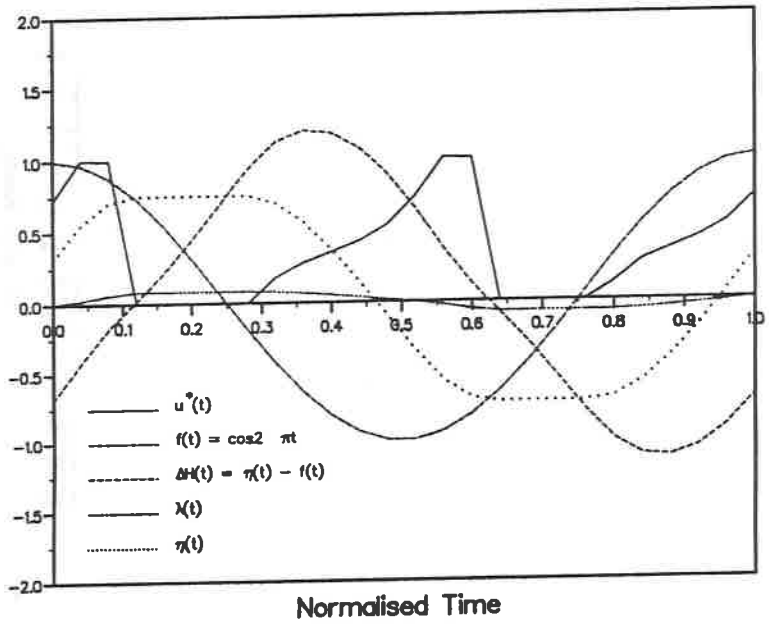

FIG. 25 Non-linear - CGA c = 1

Tol = 0.1%, N = 25

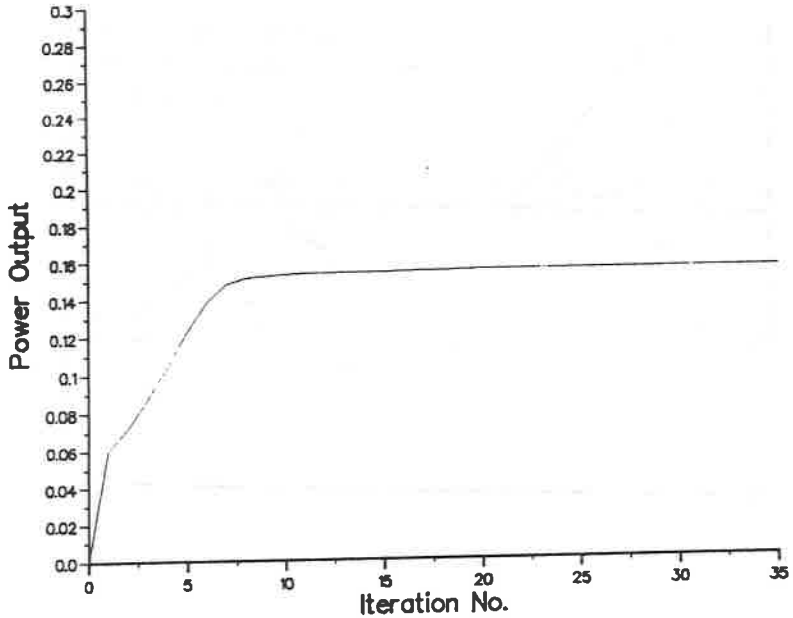

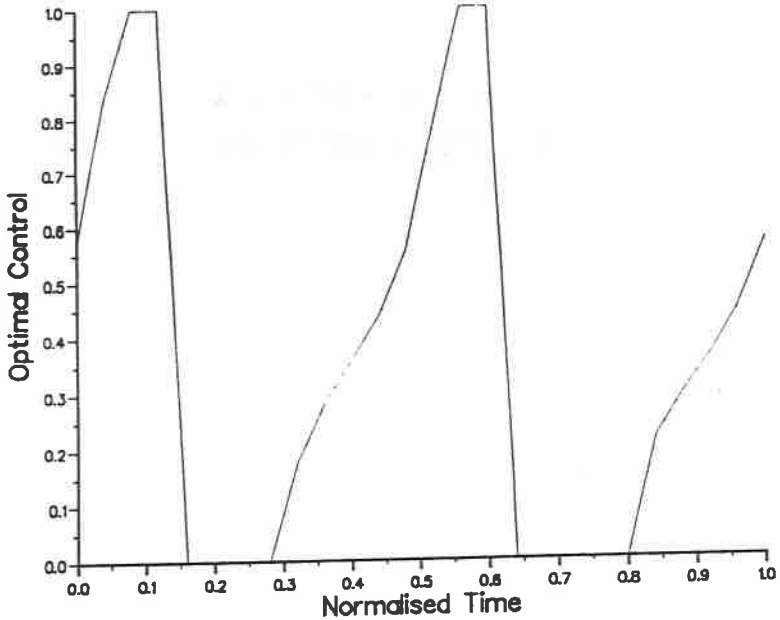

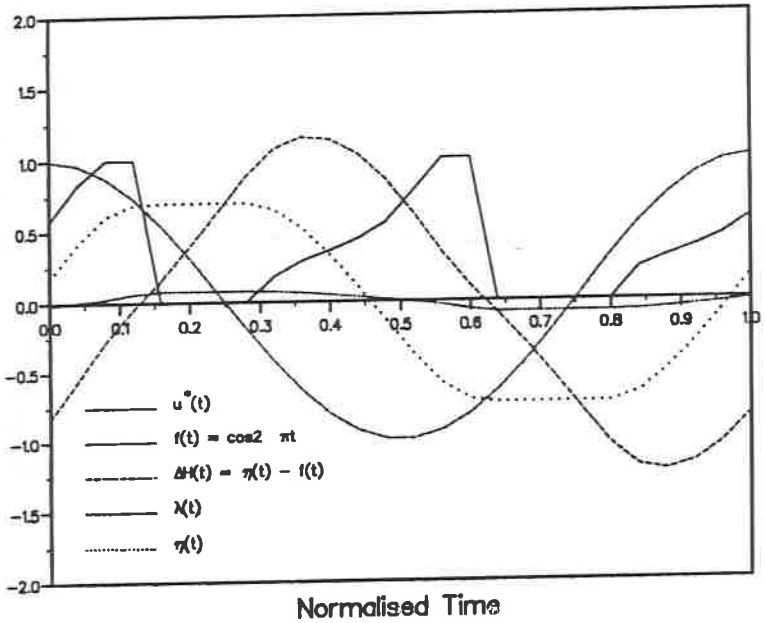

FIG. 26 Non-linear - PGA c = 1

Tol = 0.1%, N = 25

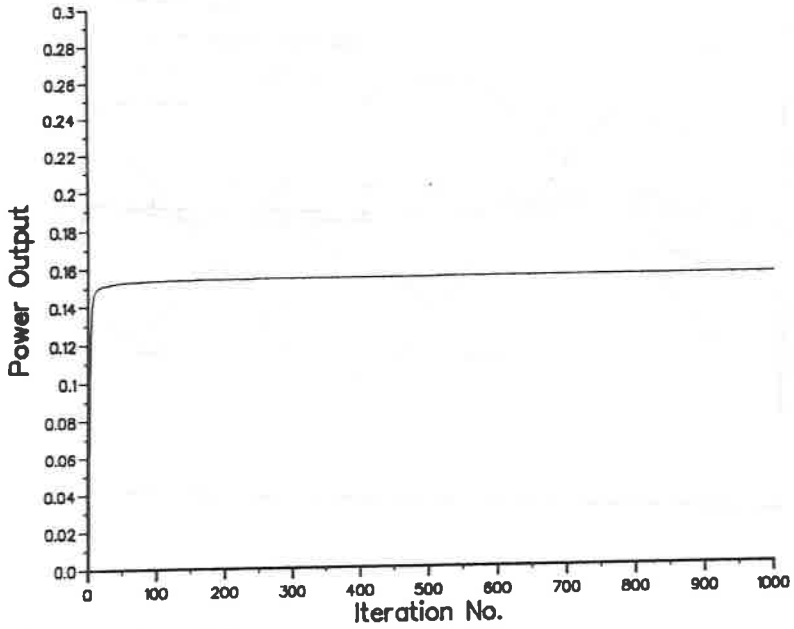

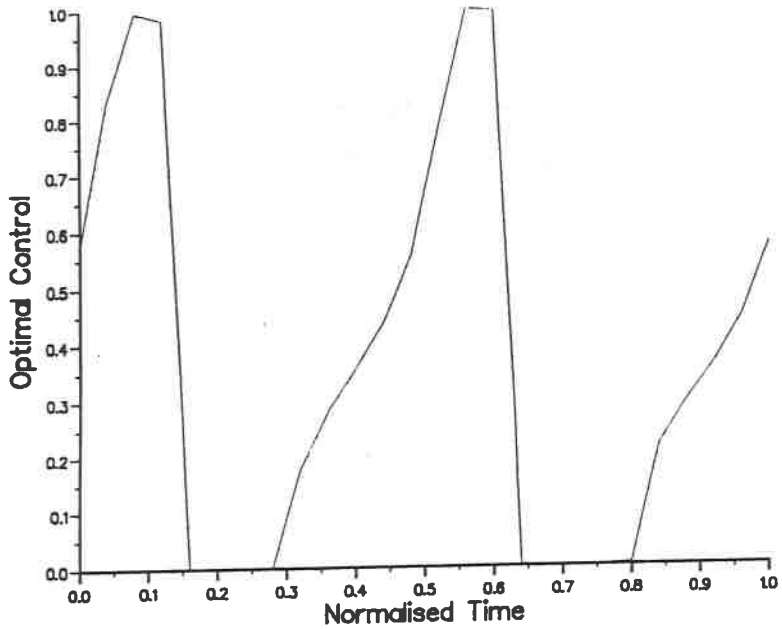

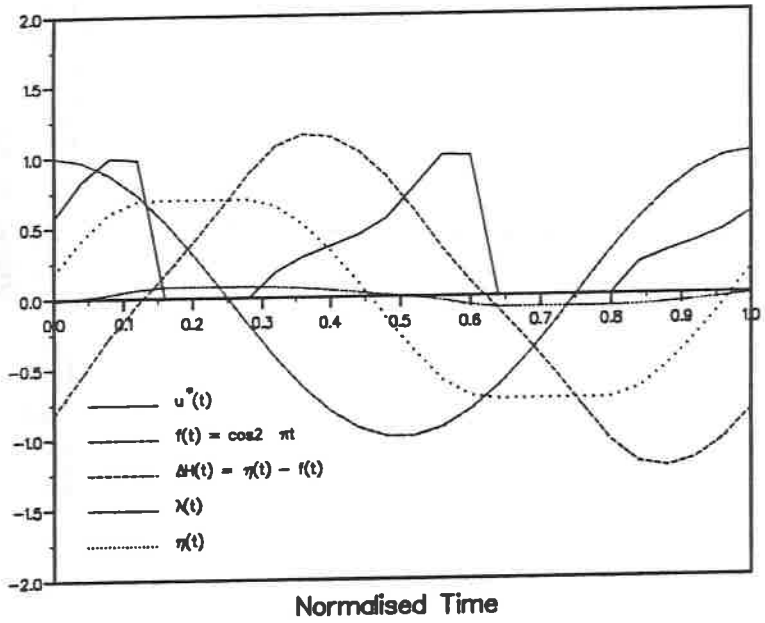

FIG. 27 Non-linear - NCGA c = 1
Tol = 0.1%, N = 25

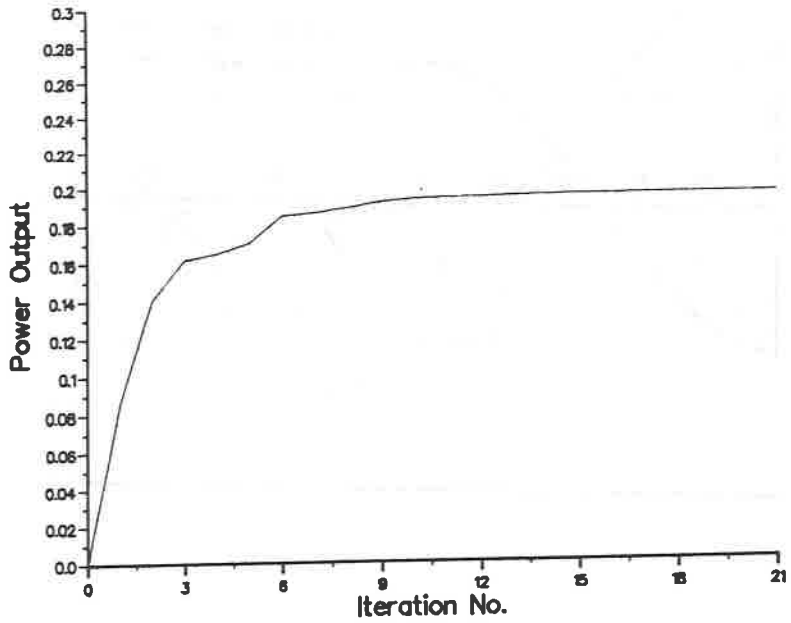

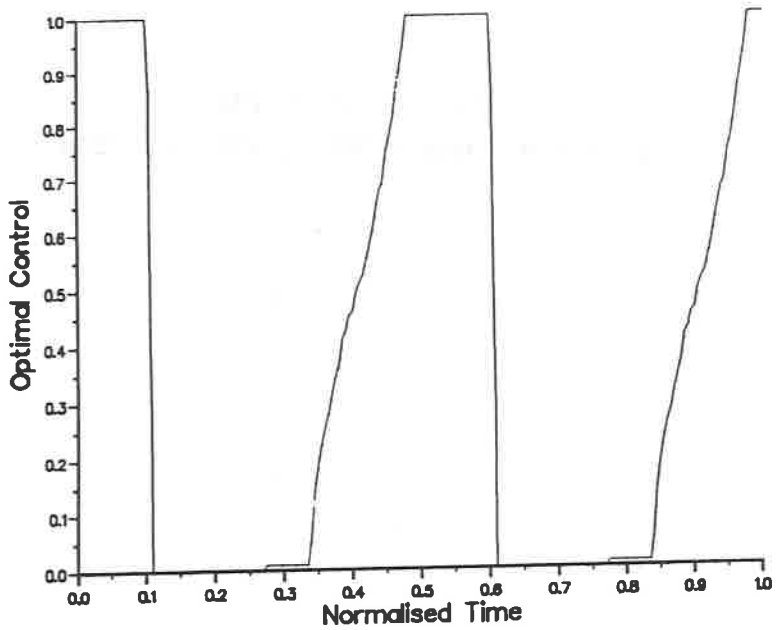

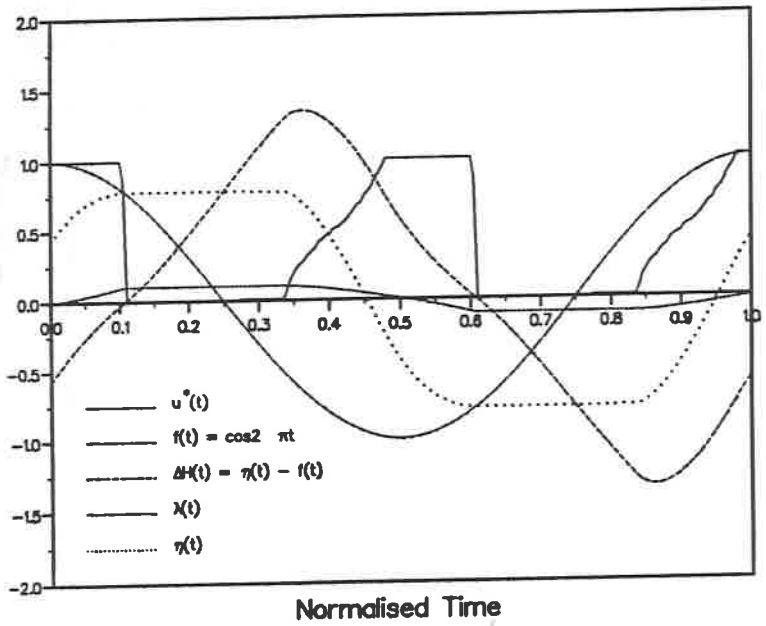

FIG. 28 Non-linear - CGA c = 0.25
Tol = 1%, N = 200

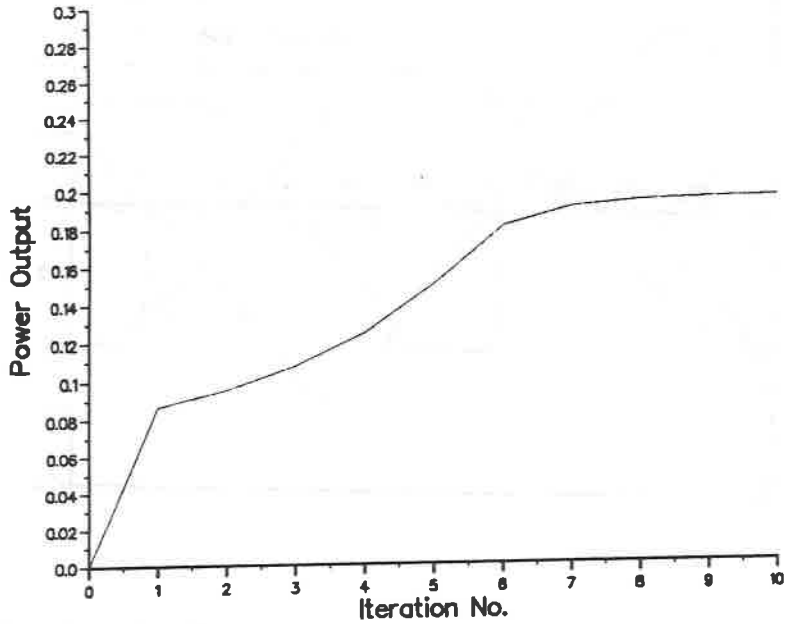

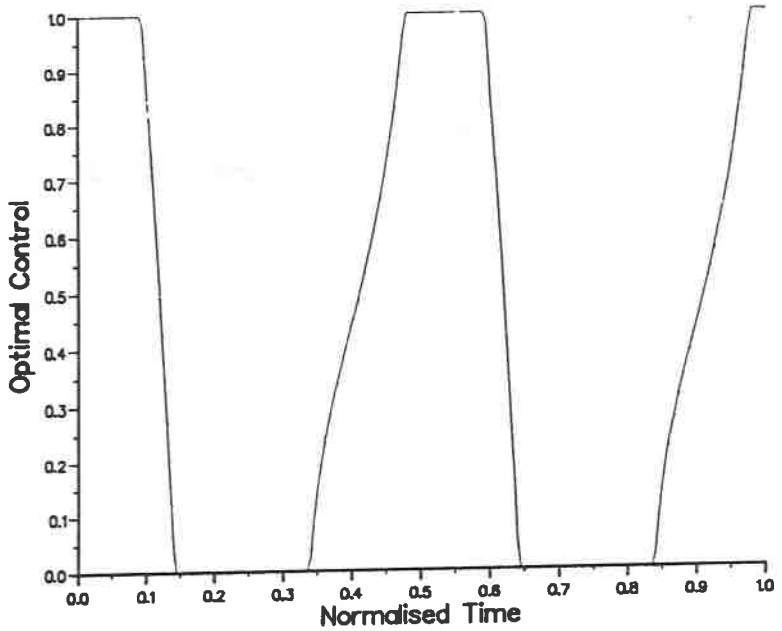

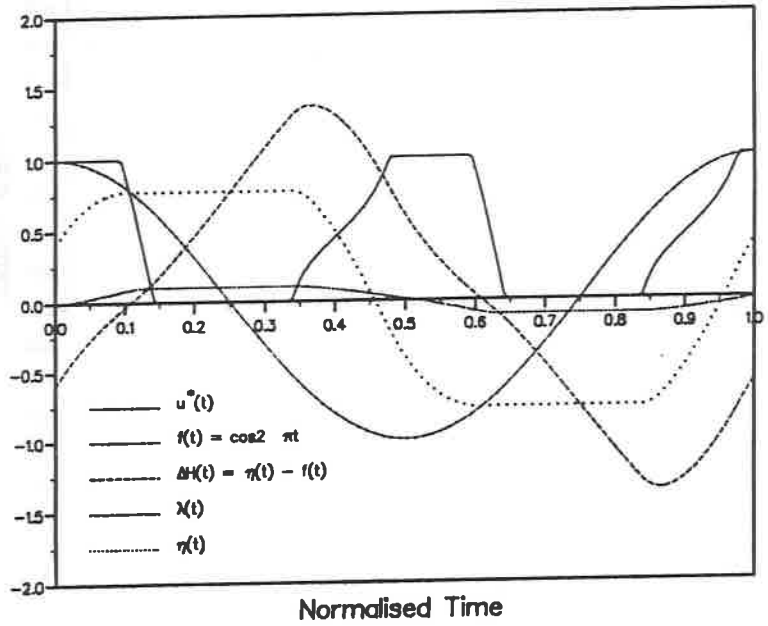

FIG. 29 Non-linear - PGA c = 0.25
Tol = 1%, N = 200

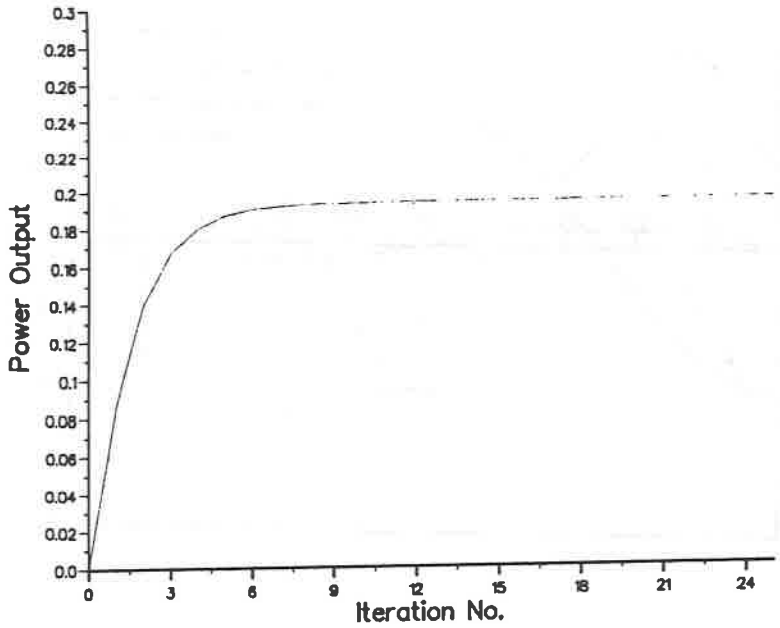

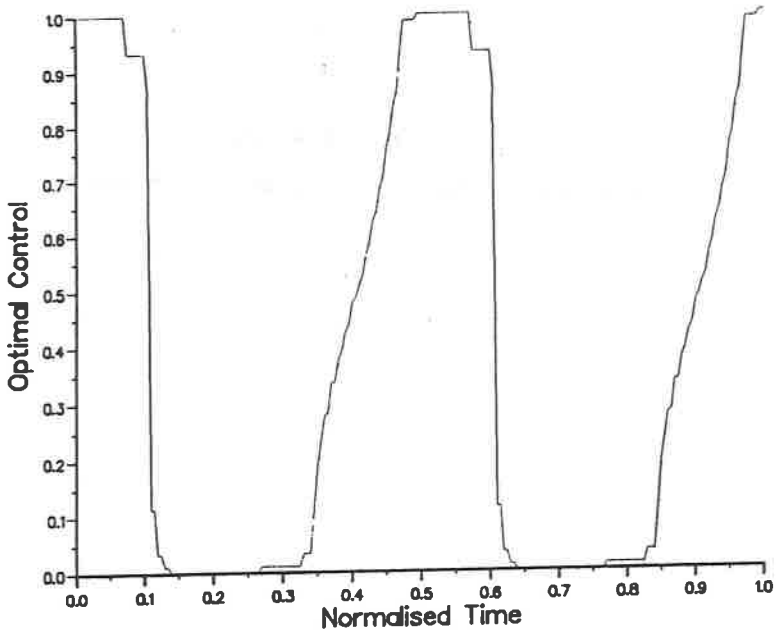

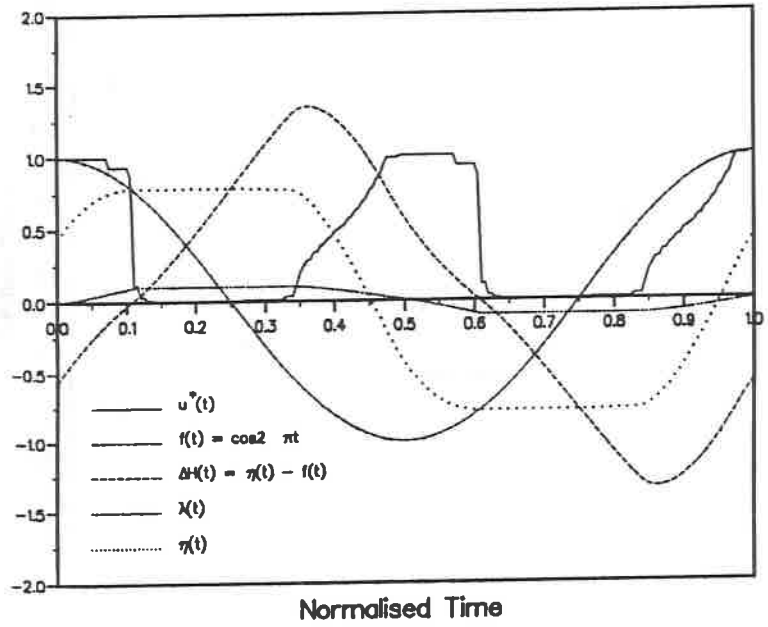

FIG. 30 Non-linear - NCGA c = 0.25
Tol = 1%, N = 200

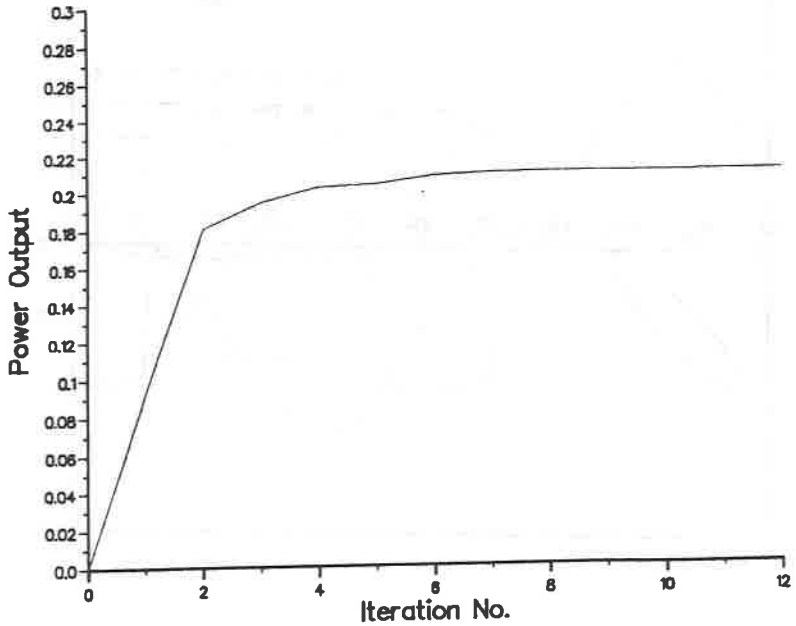

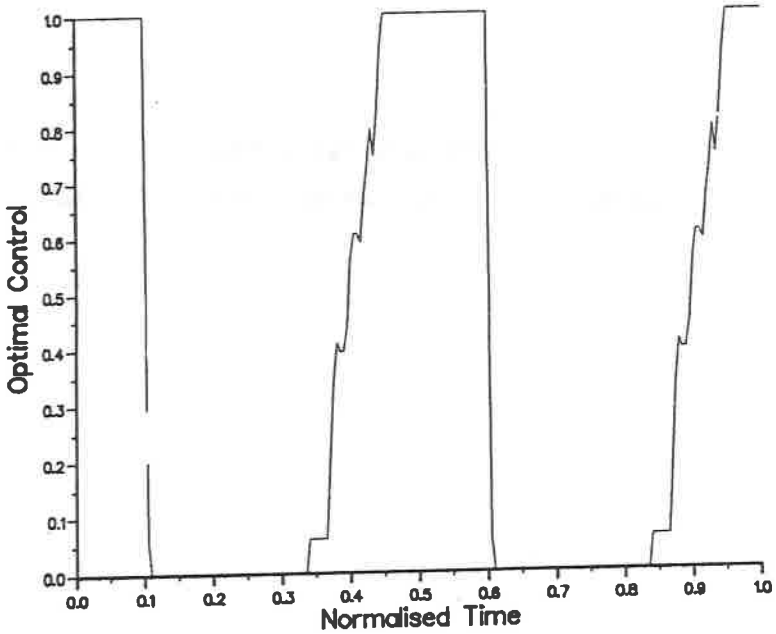

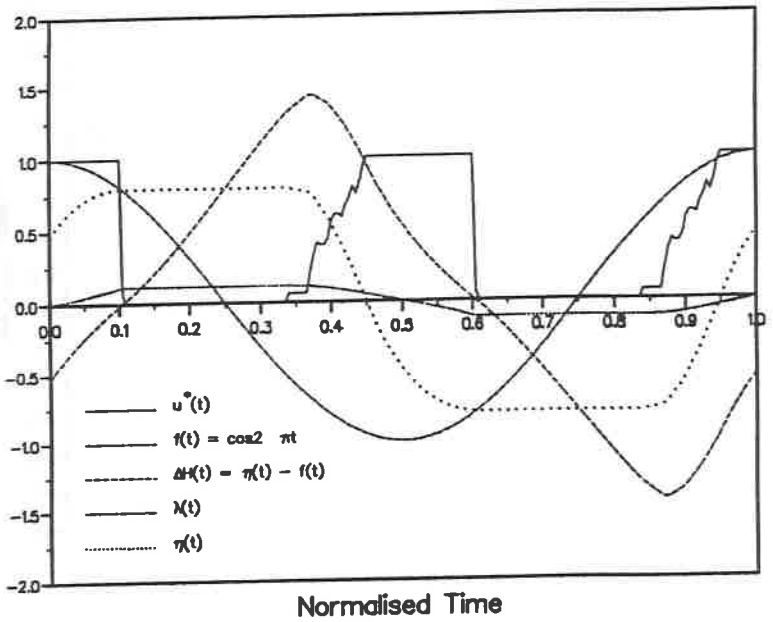

FIG. 31 Non-linear - CGA c = 0.1
Tol = 1%, N = 200

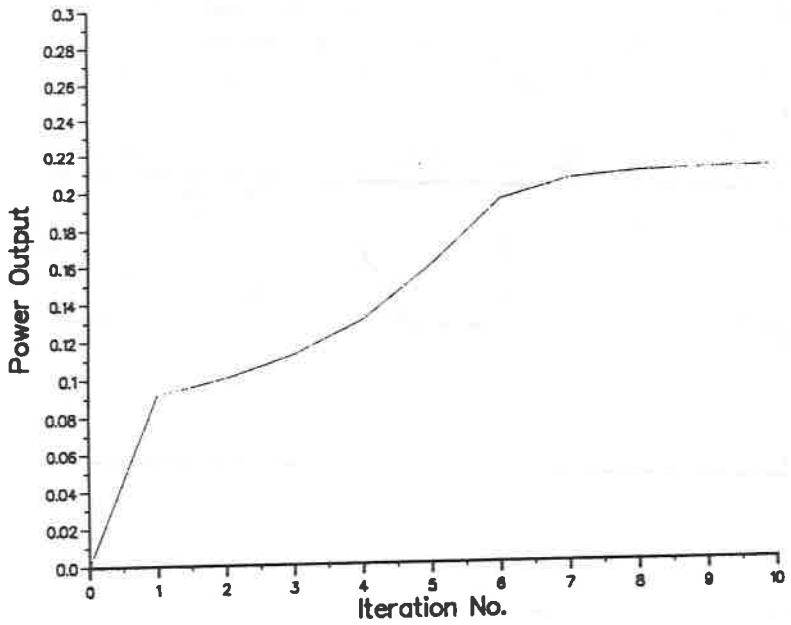

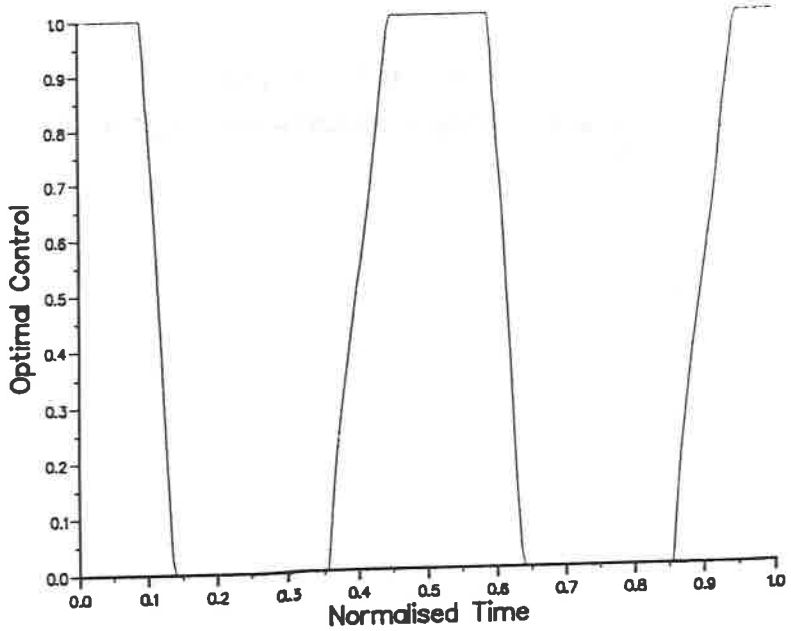

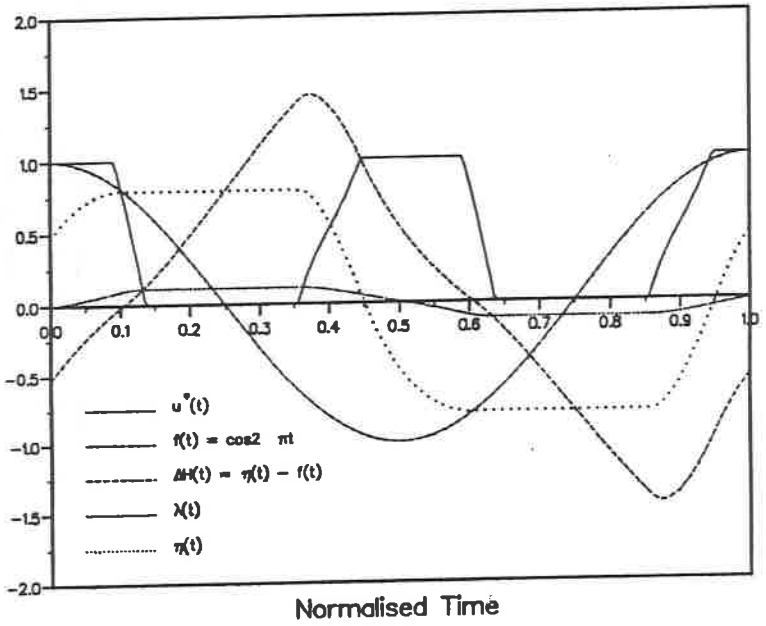

FIG. 32 Non-Linear - PGA c = 0.1
Tol = 1%, N = 200

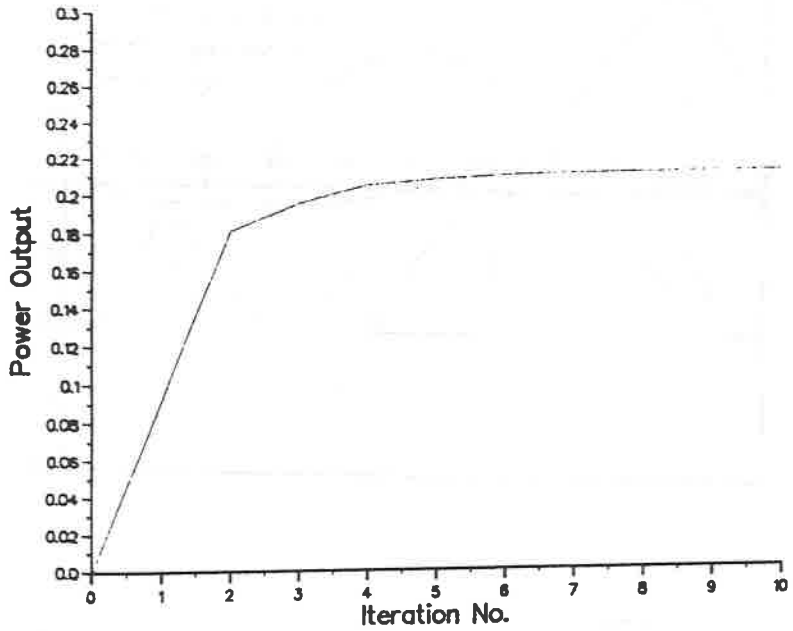

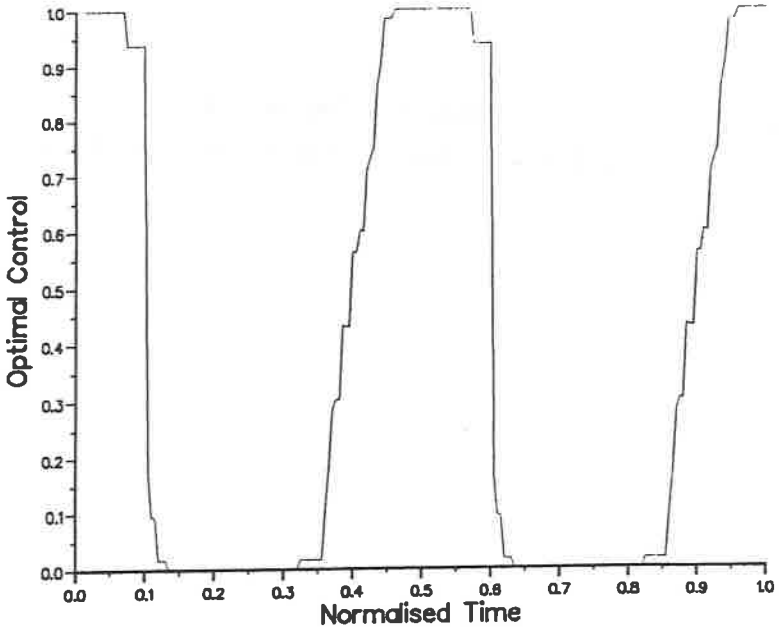

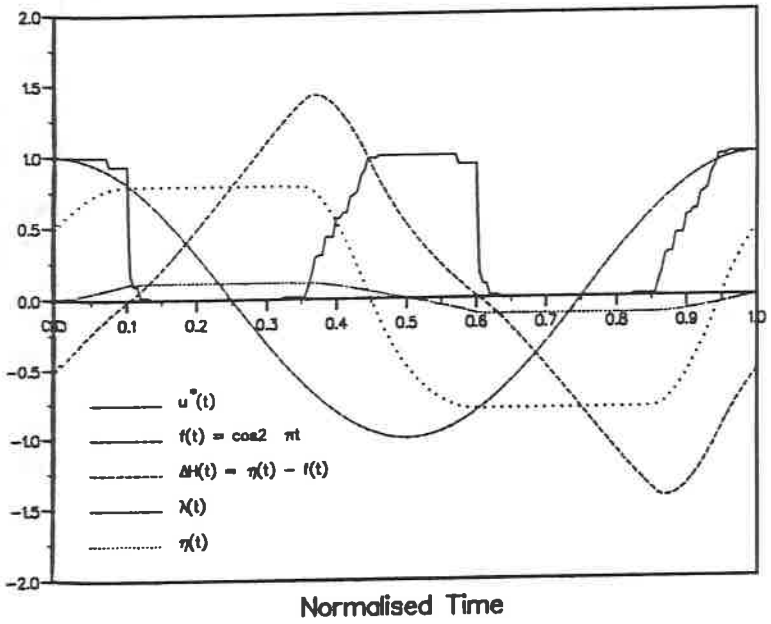

FIG. 33 Non-linear - NCGA c = 0.1
Tol = 1%, N = 200

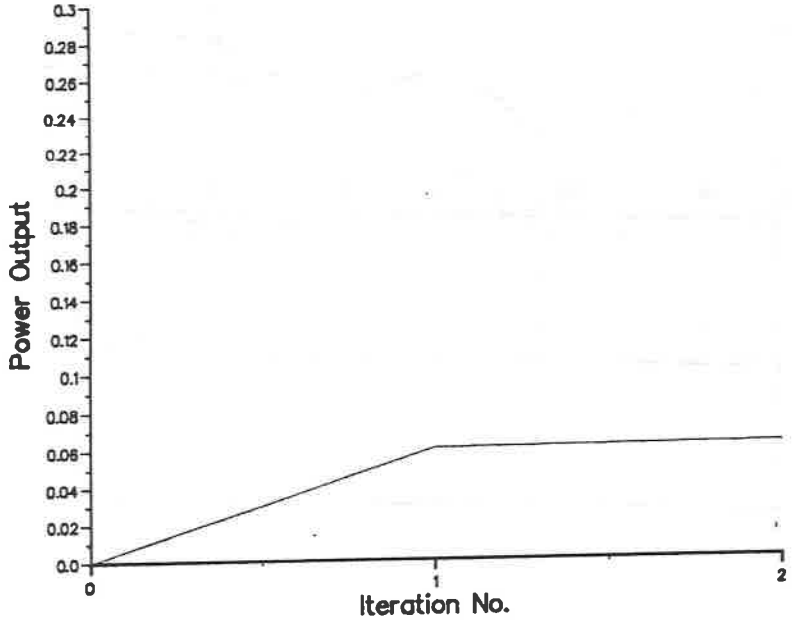

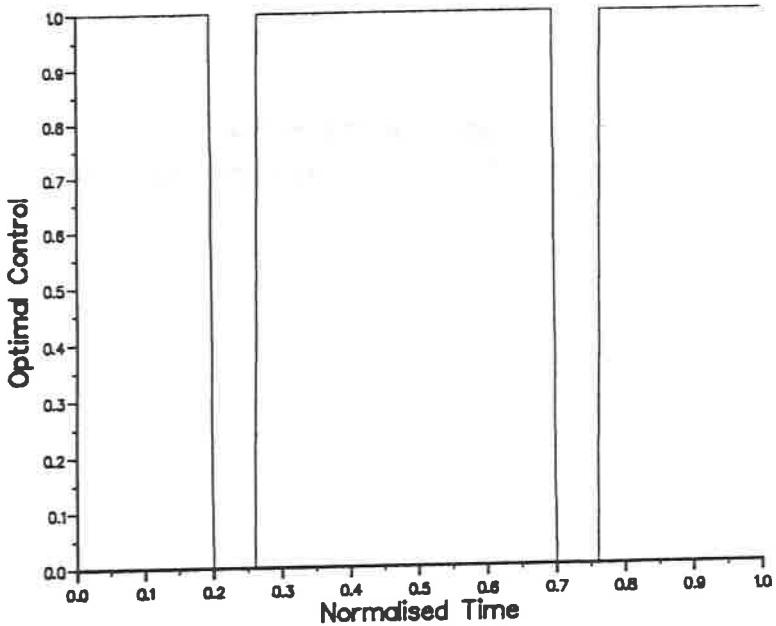

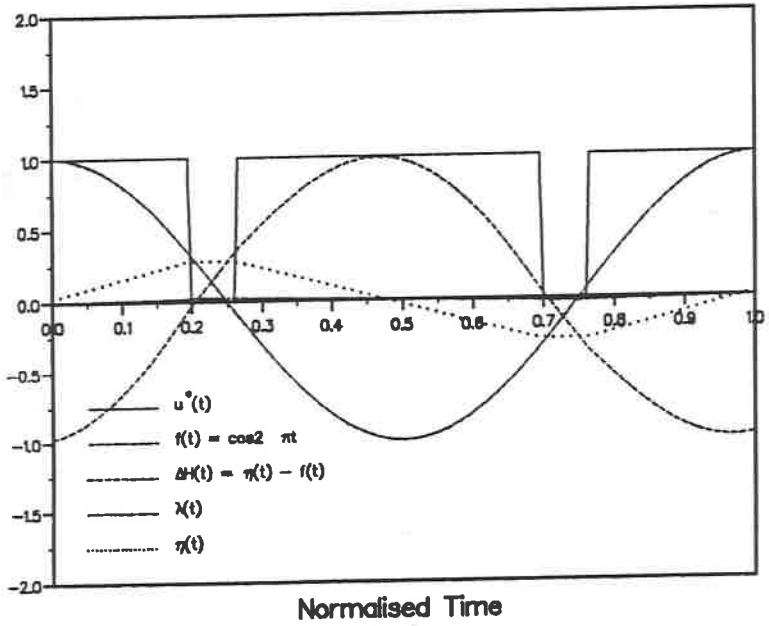

FIG. 34 Linear - CGA $h_o = 0.1$
Tol = 1%, N = 200

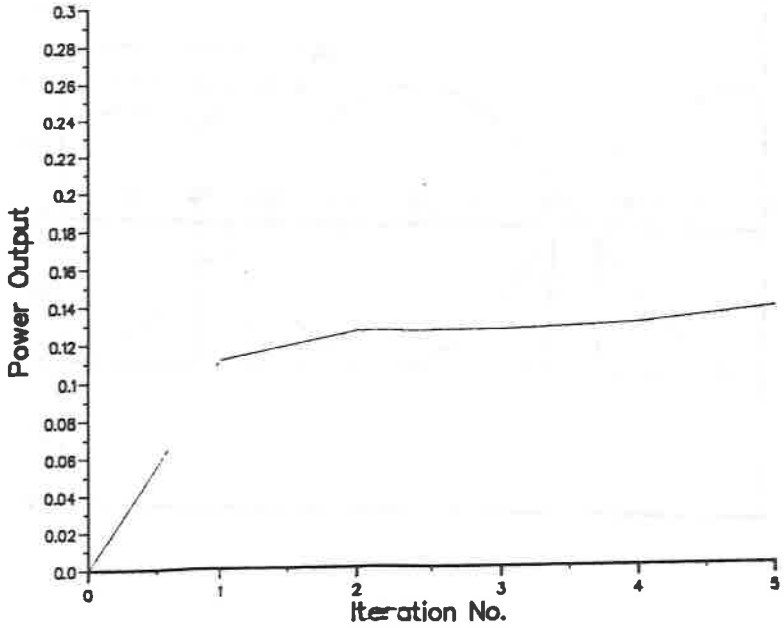

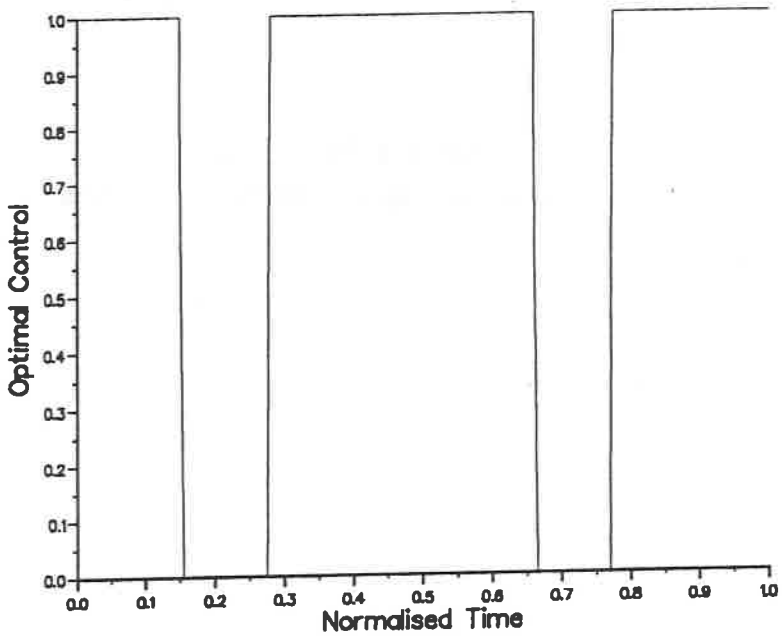

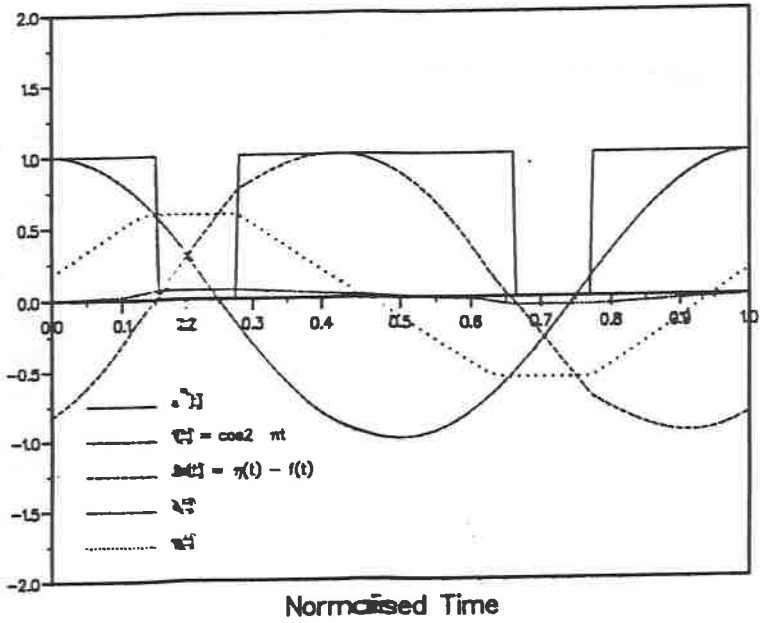

FIG. 35 Linear - CGA $h_o = 0.25$
Tol = 1%, N = 200

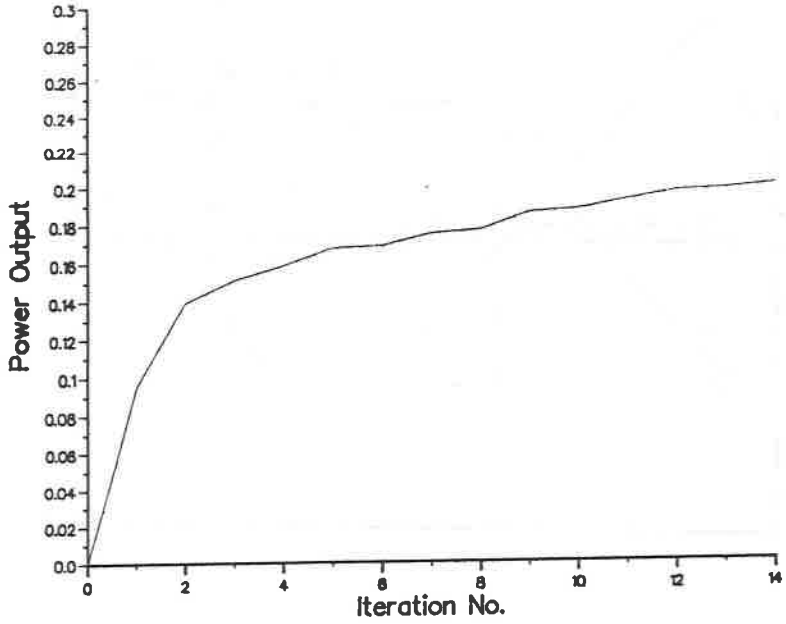

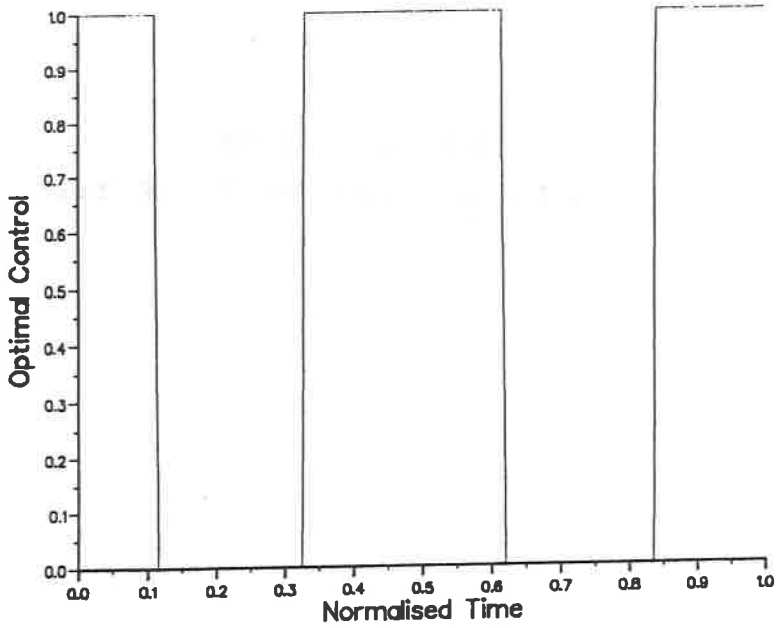

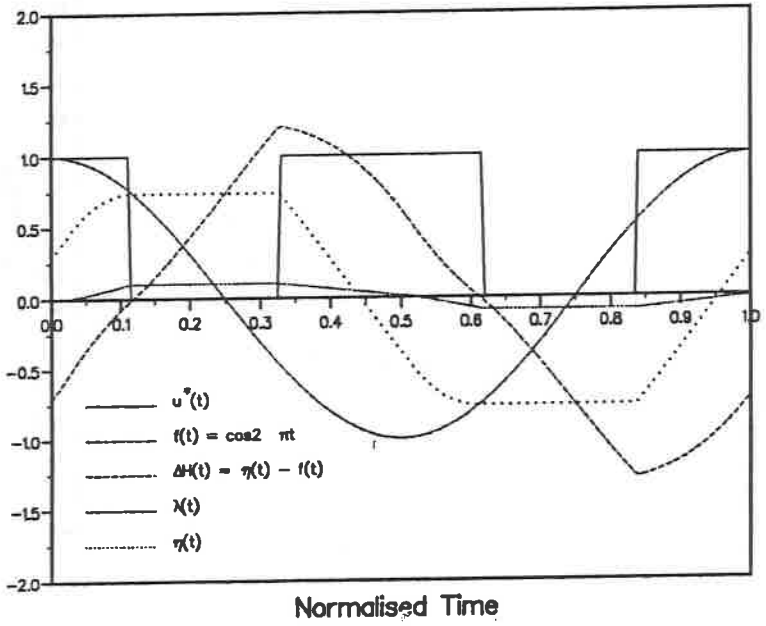

FIG. 36 Linear - CGA $h_o = 0.5$
Tol = 1%, N = 200

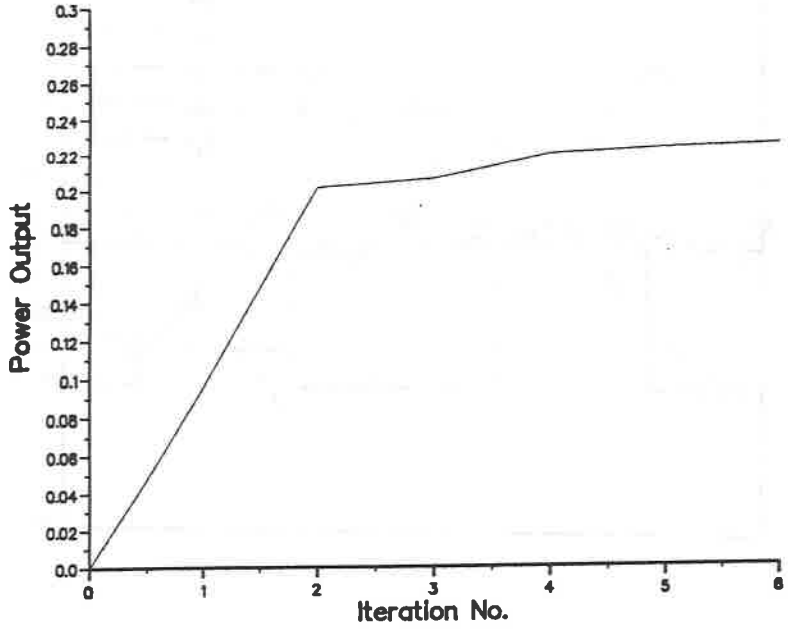

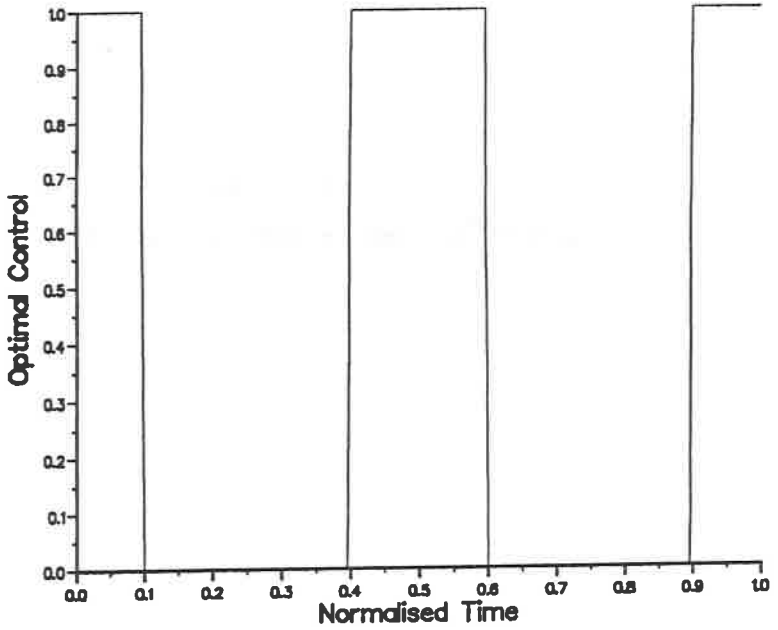

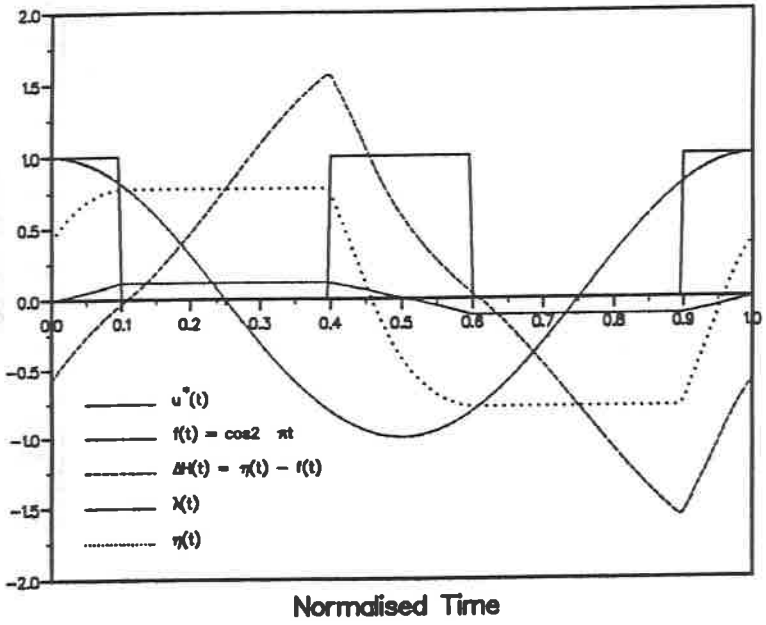

FIG. 37 Linear - CGA $h_o = 1.0$
Tol = 1%, N = 200

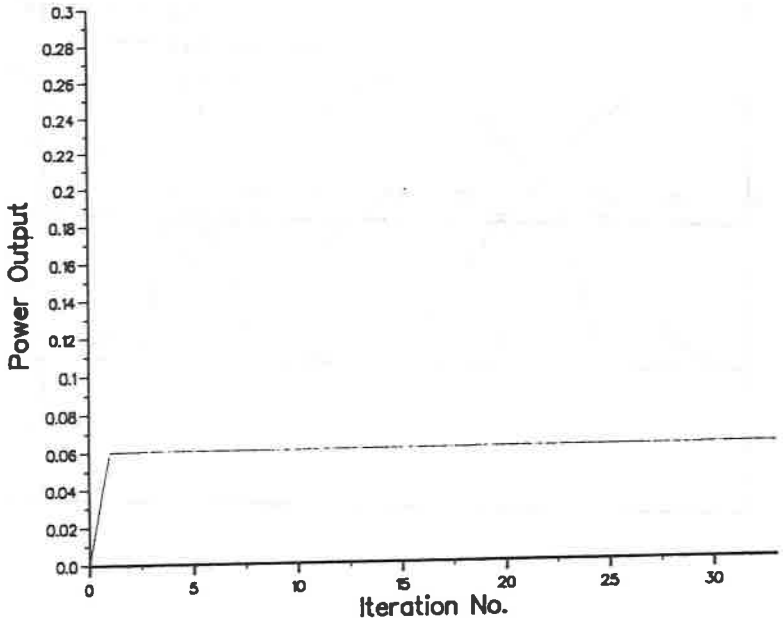

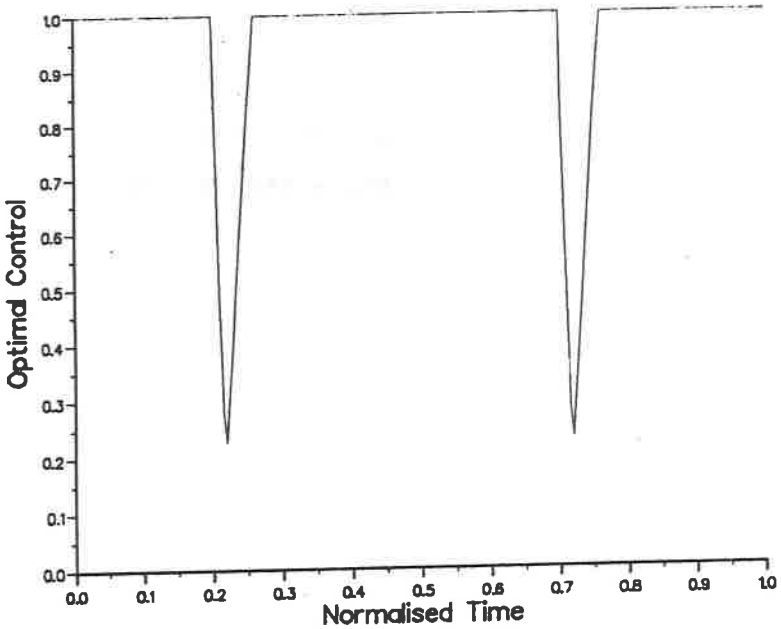

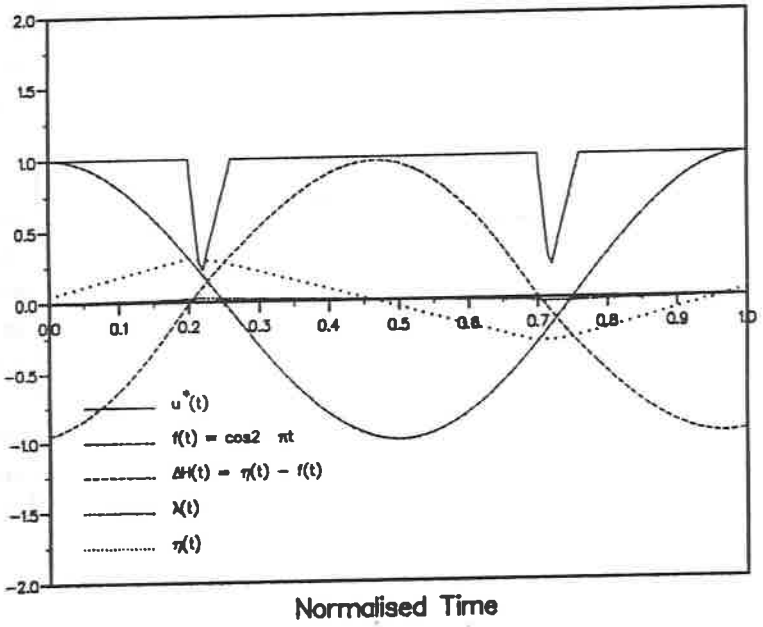

FIG. 38 Linear - PGA h_o = 0.1
Tol = 1% N = 200

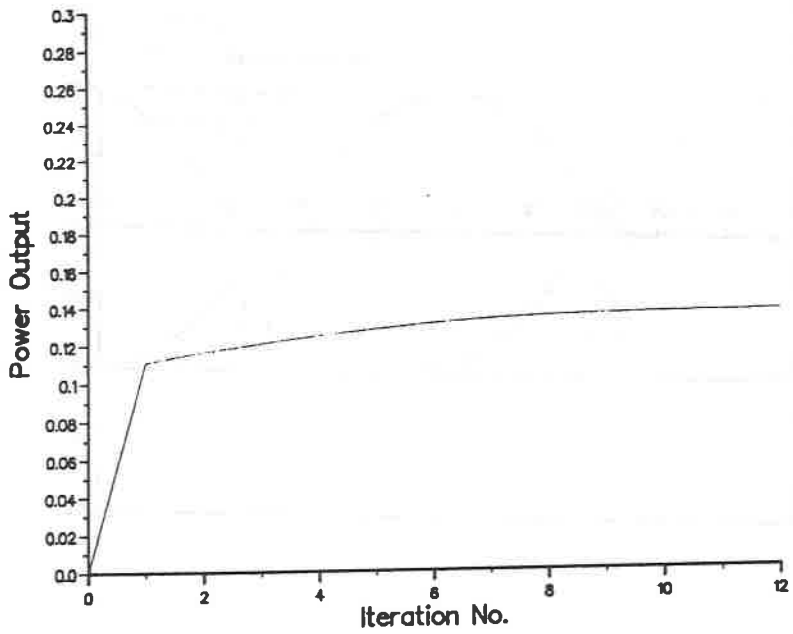

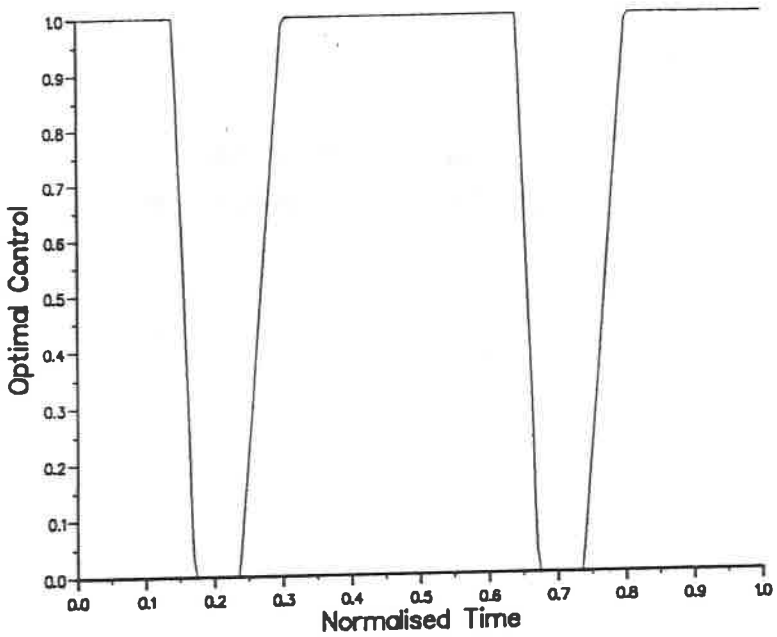

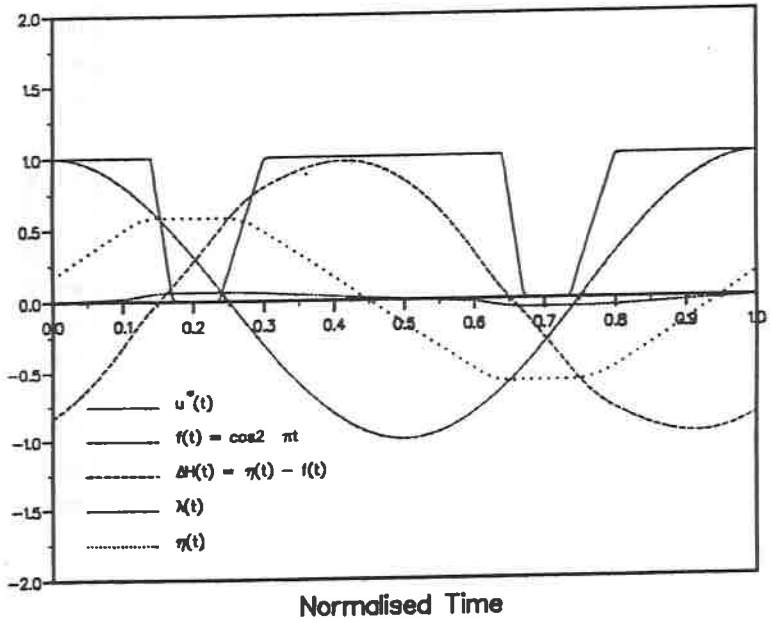

FIG. 39 Linear - PGA $h_o = 0.25$
Tol = 1% N = 200

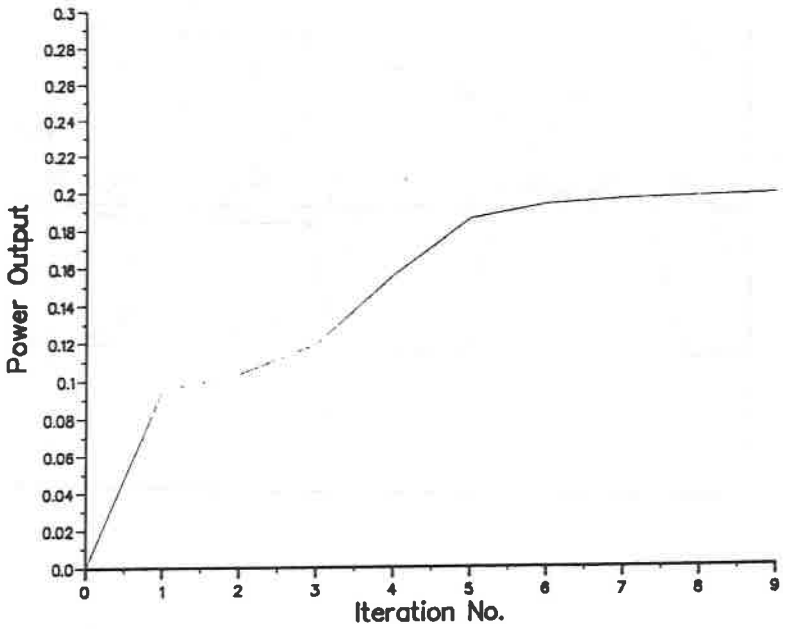

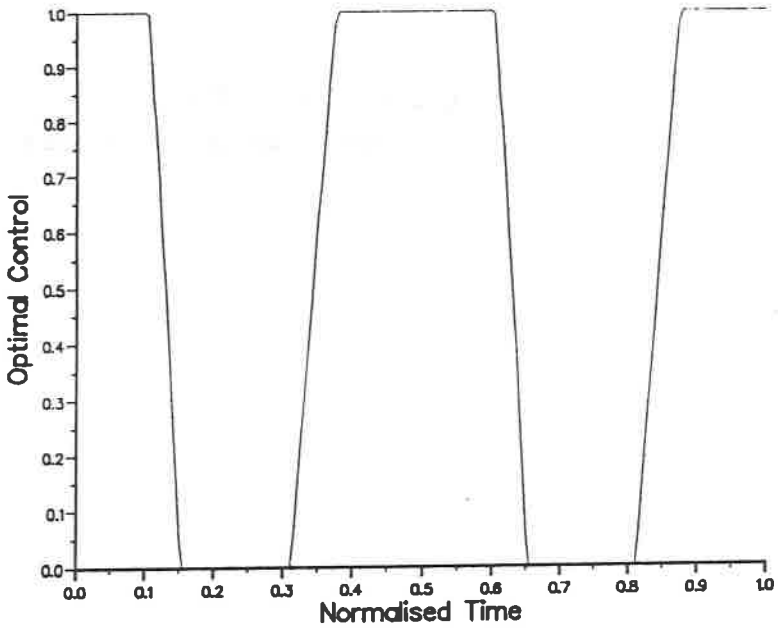

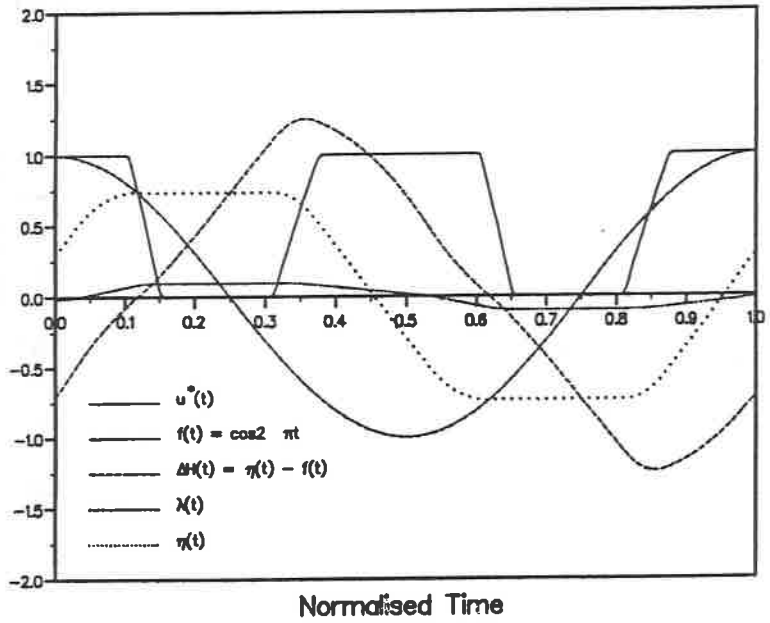

FIG. 40 Linear - PGA $h_o = 0.5$
Tol = 1%, N = 200

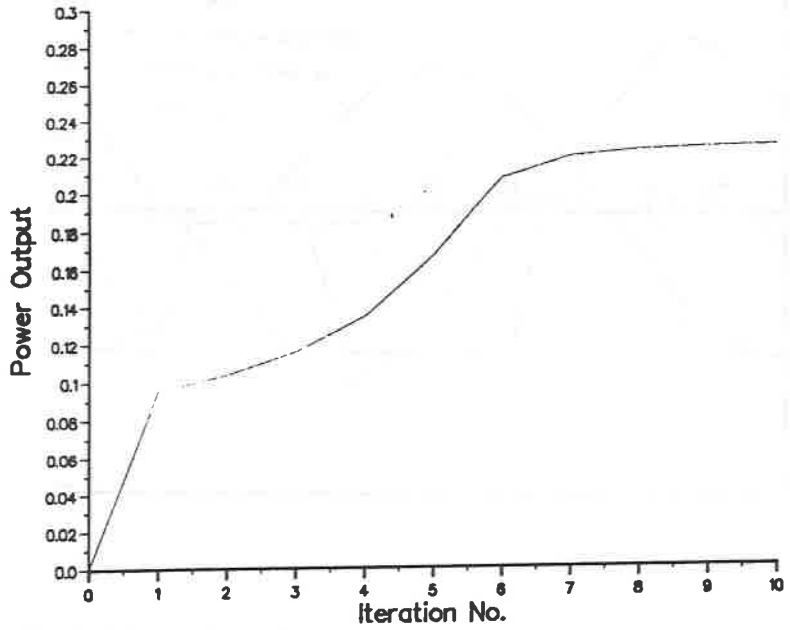

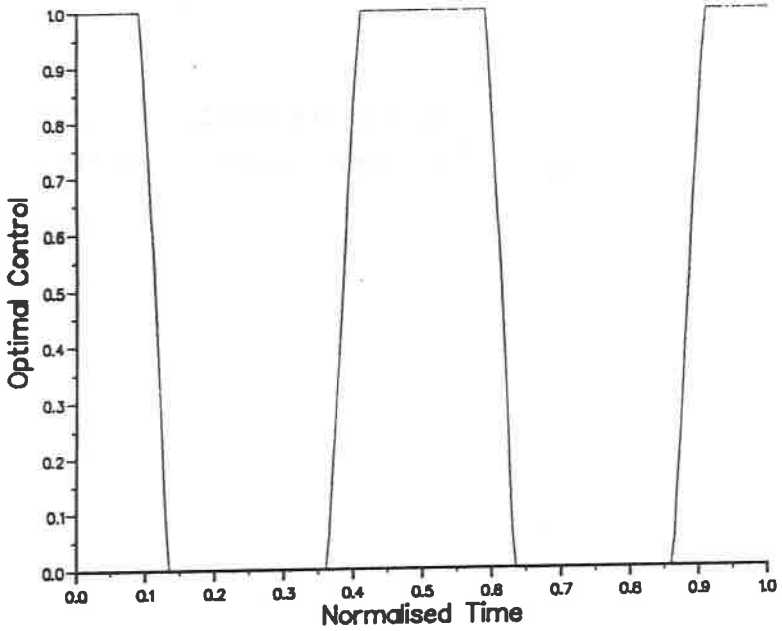

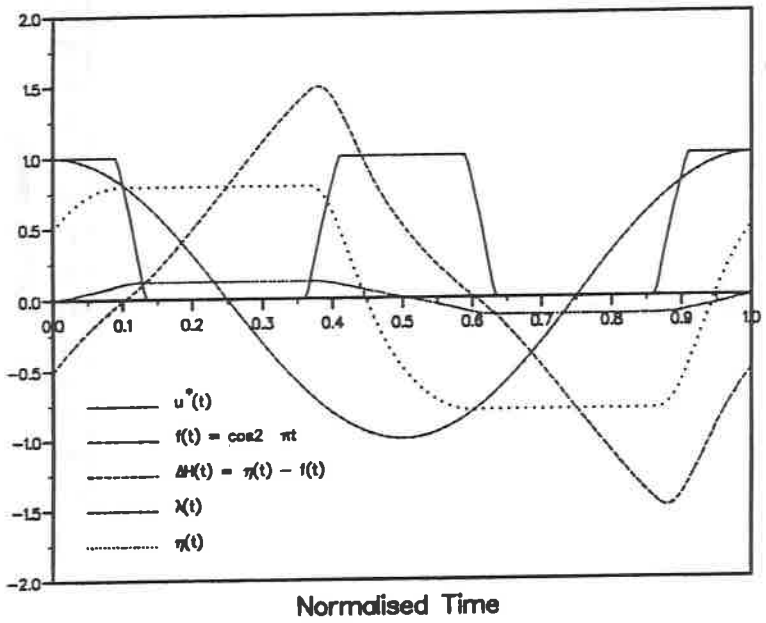

FIG. 41 Linear - PGA h_o = 1.0
Tol = 1%, N = 200

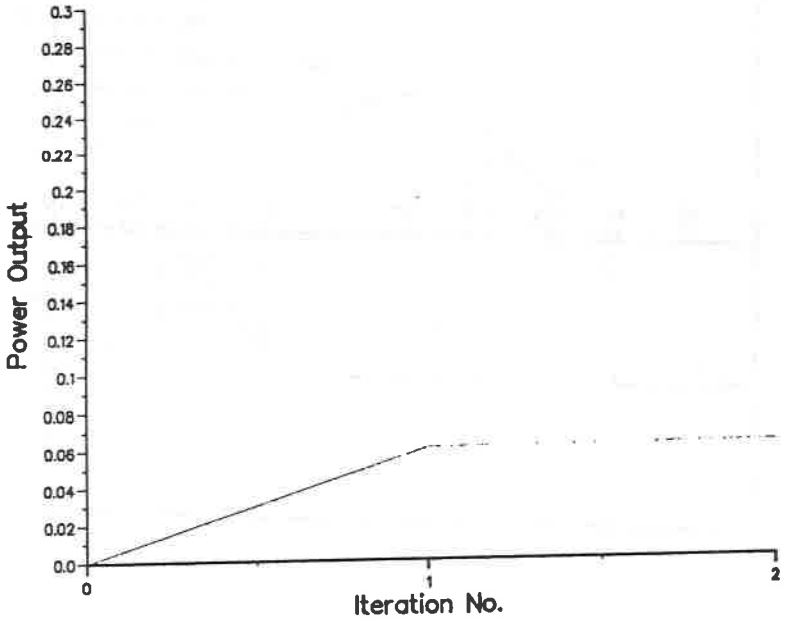

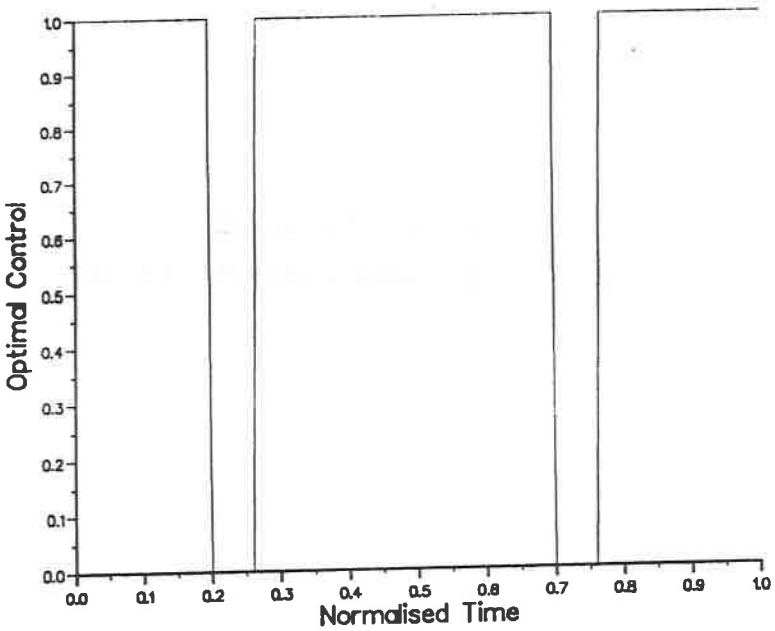

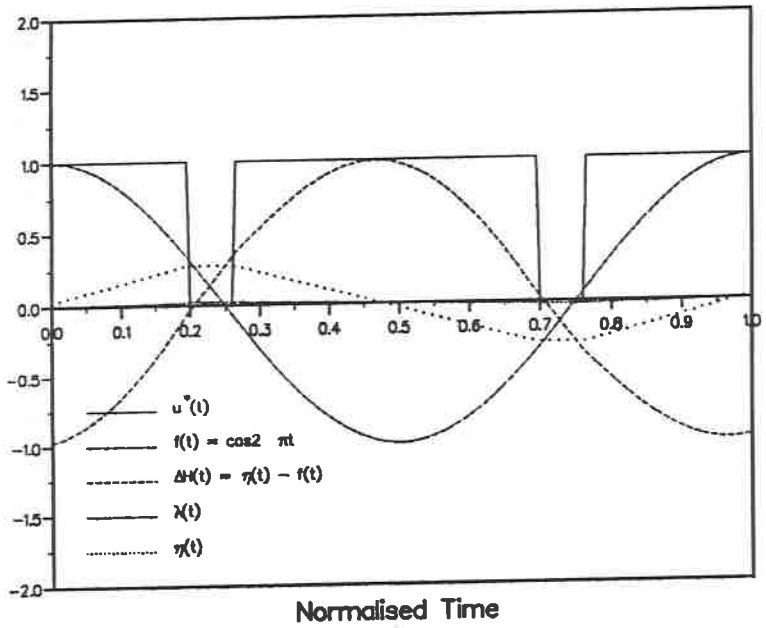

FIG. 42 Linear - NCGA $h_o = 0.1$
Tol = 1%, N = 200

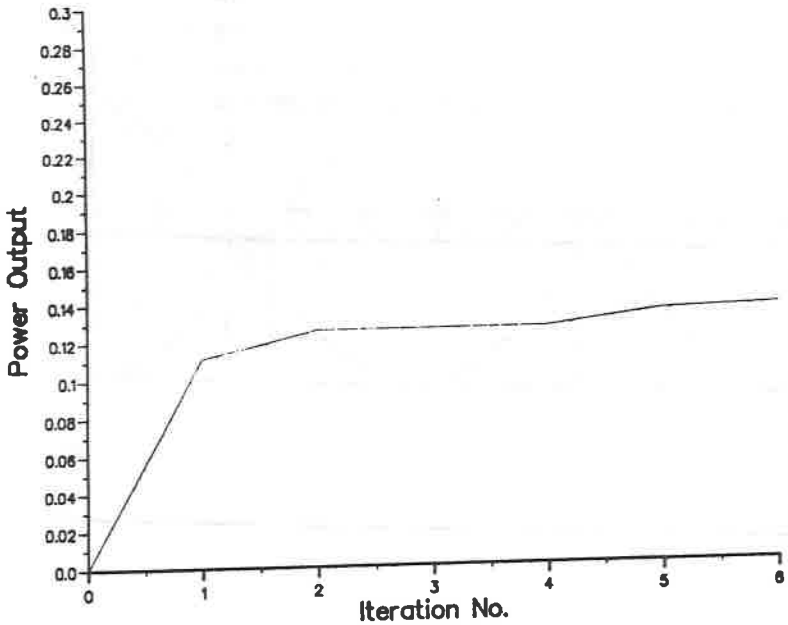

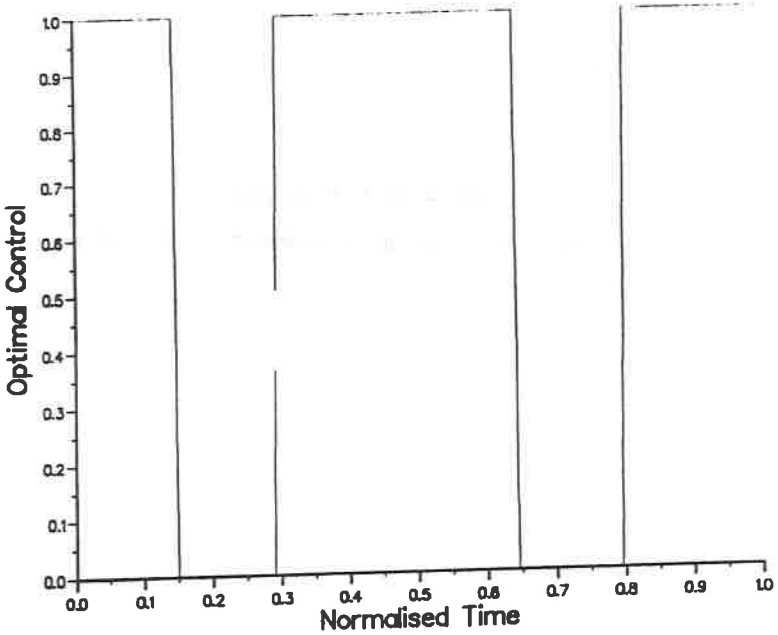

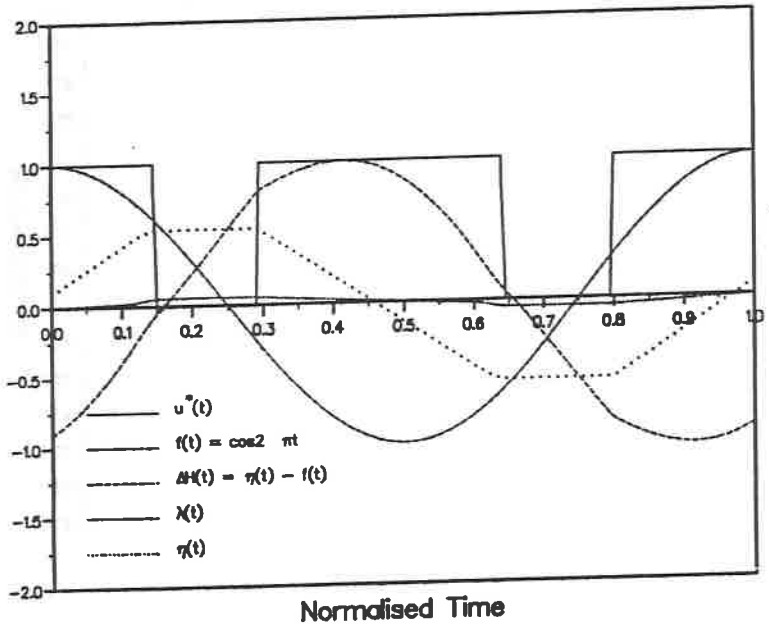

FIG. 43 Linear - NCGA $h_o = 0.25$
Tol = 1%, N = 200

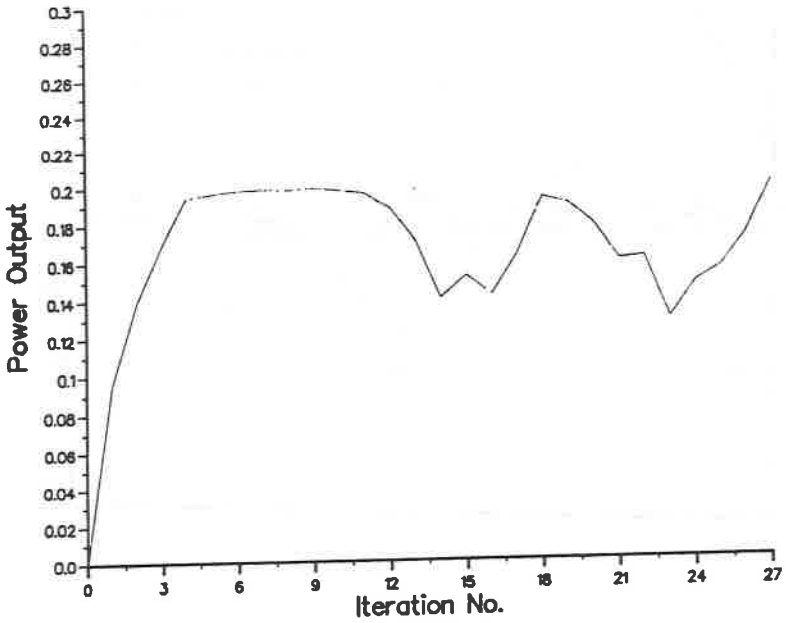

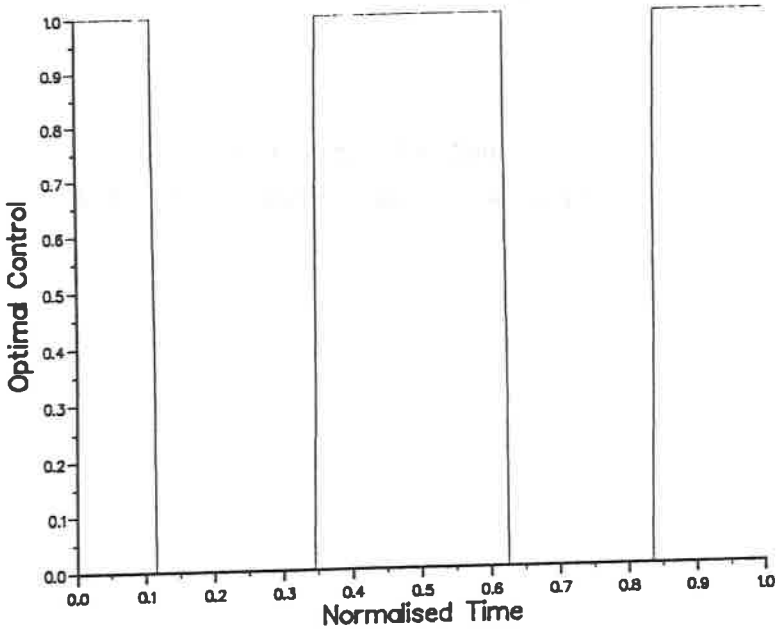

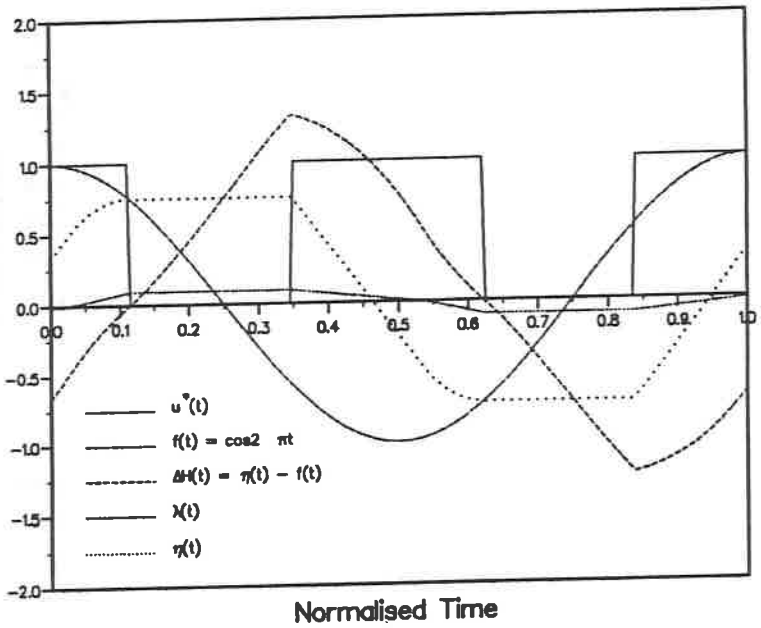

FIG. 44 Linear - NCGA $h_o = 0.5$
Tol = 1%, N = 200

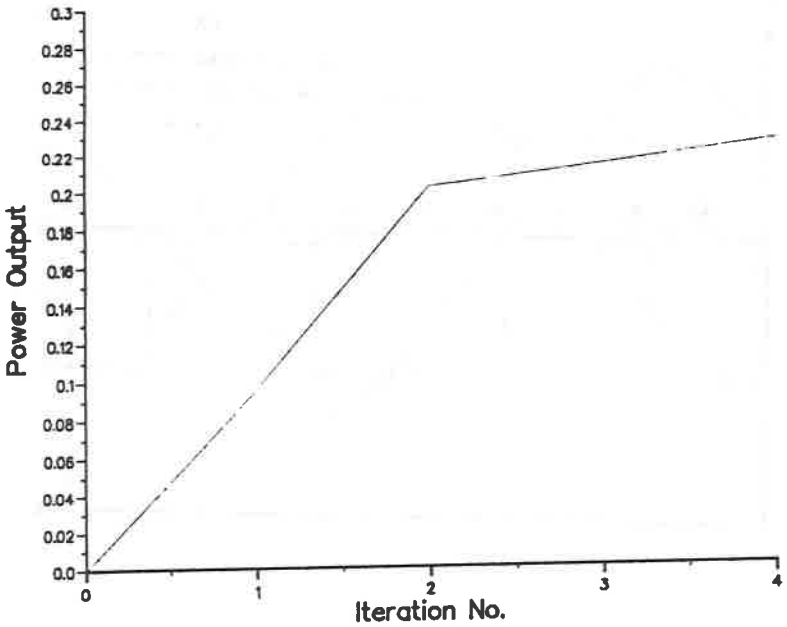

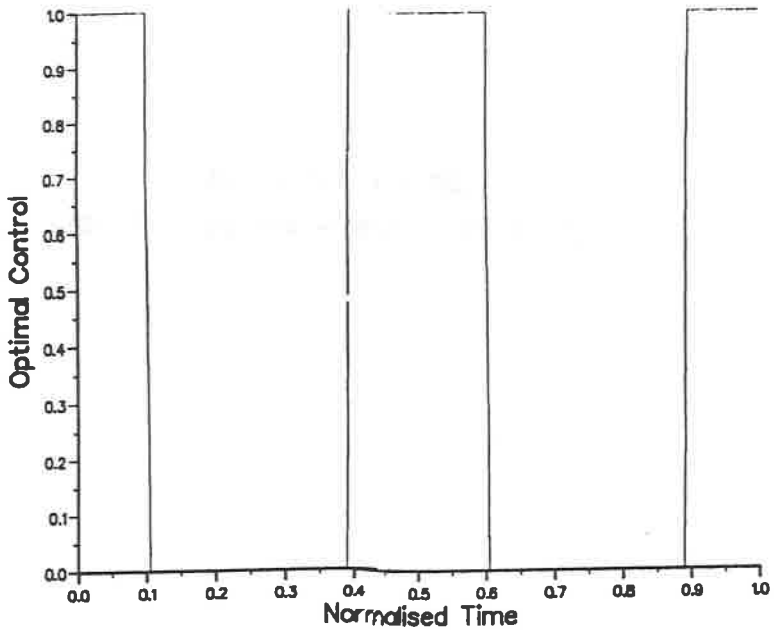

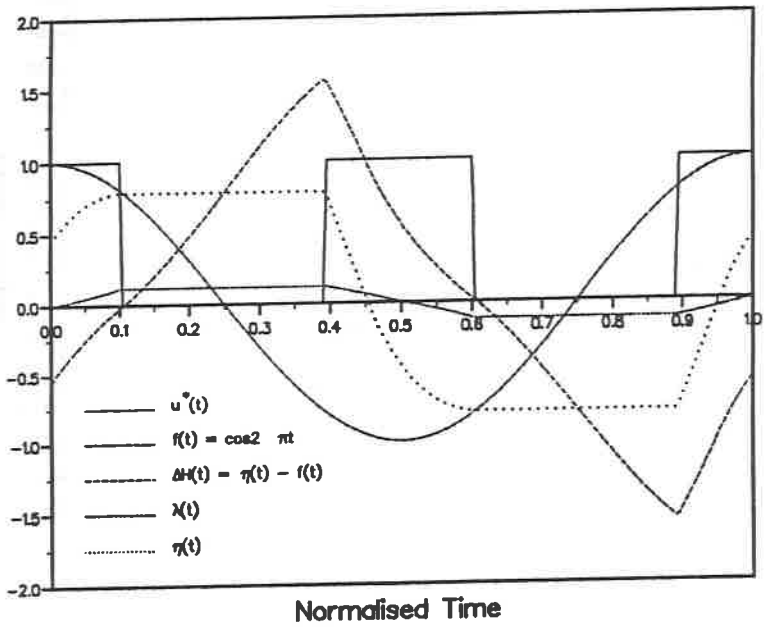

FIG. 45 Linear - NCGA h_o = 1.0
Tol = 1%, N = 200

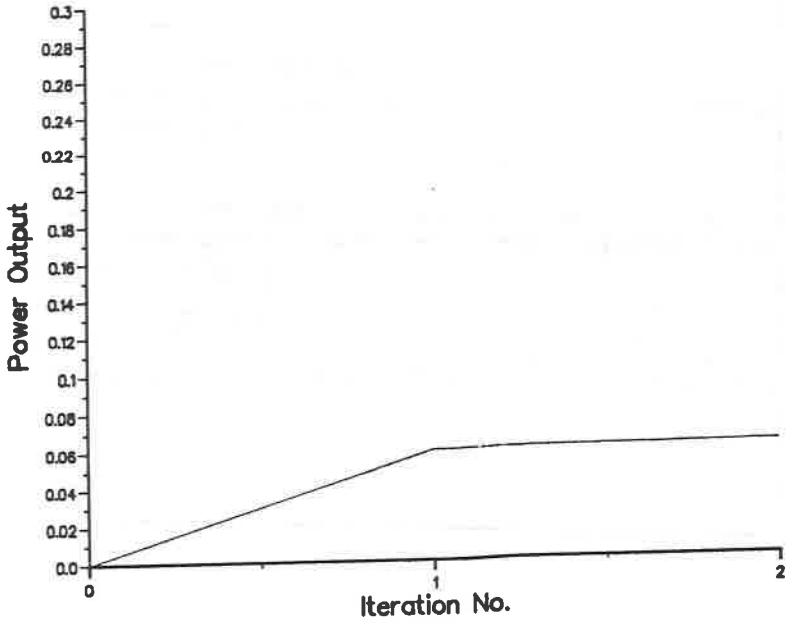

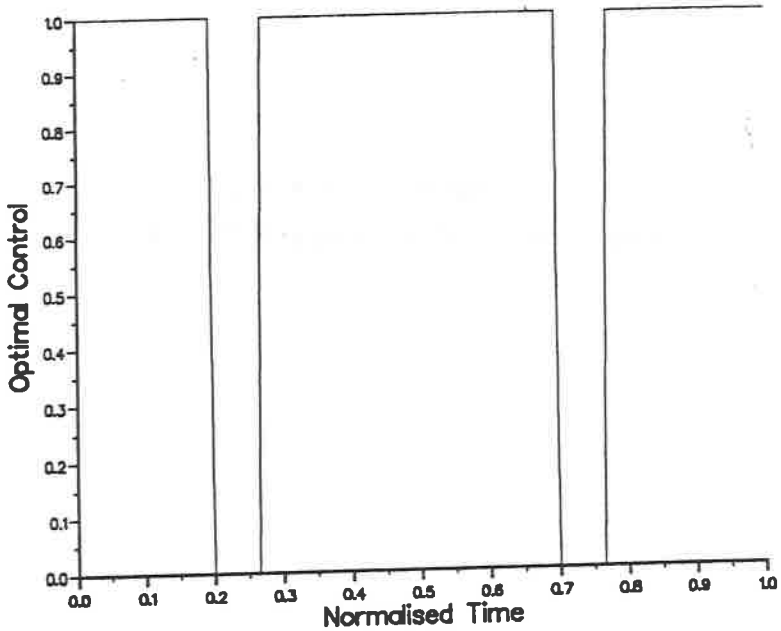

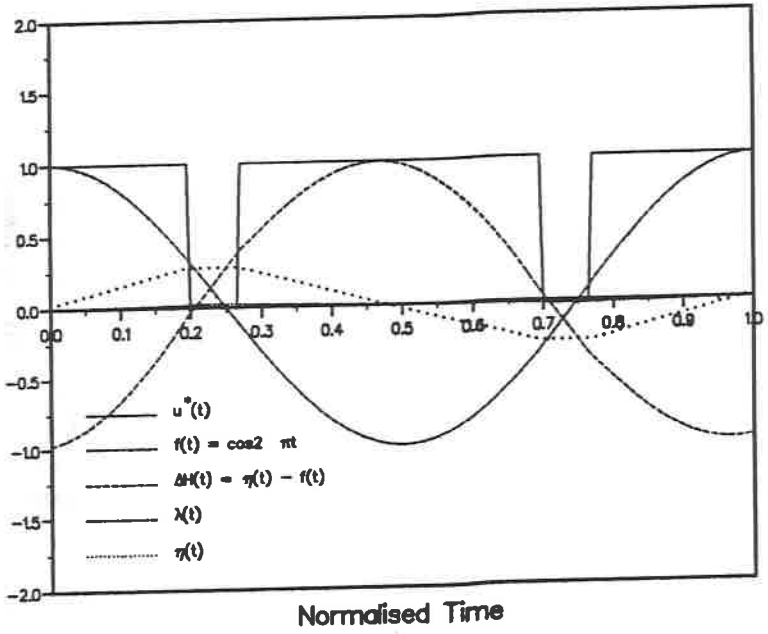

FIG. 46 Non-linear - CGA $h_o = 0.1$

Tol = 1%, N = 200

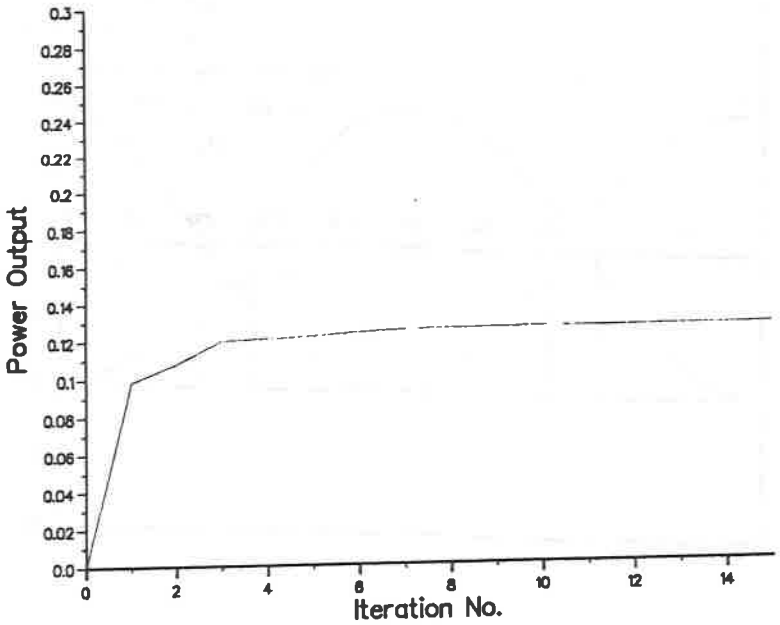

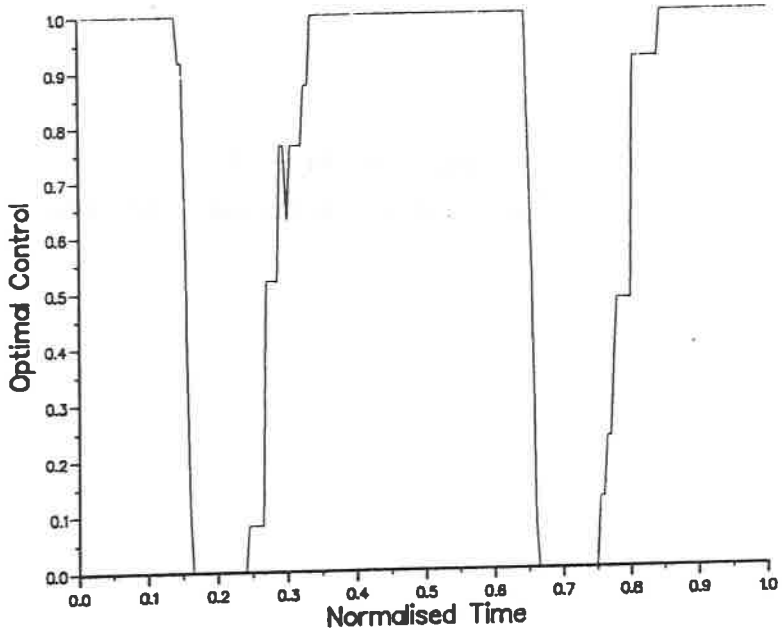

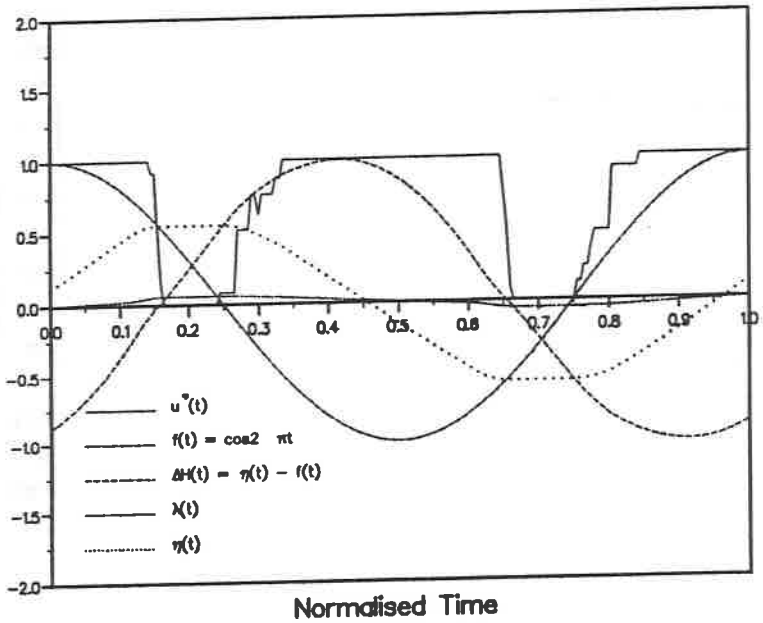

FIG. 47 Non-linear - CGA $h_o = 0.25$
Tol = 1%, N = 200

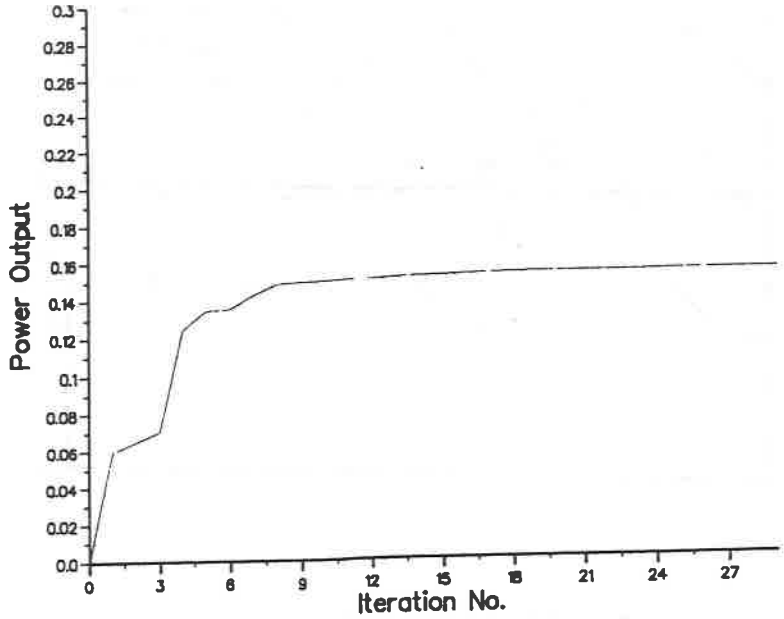

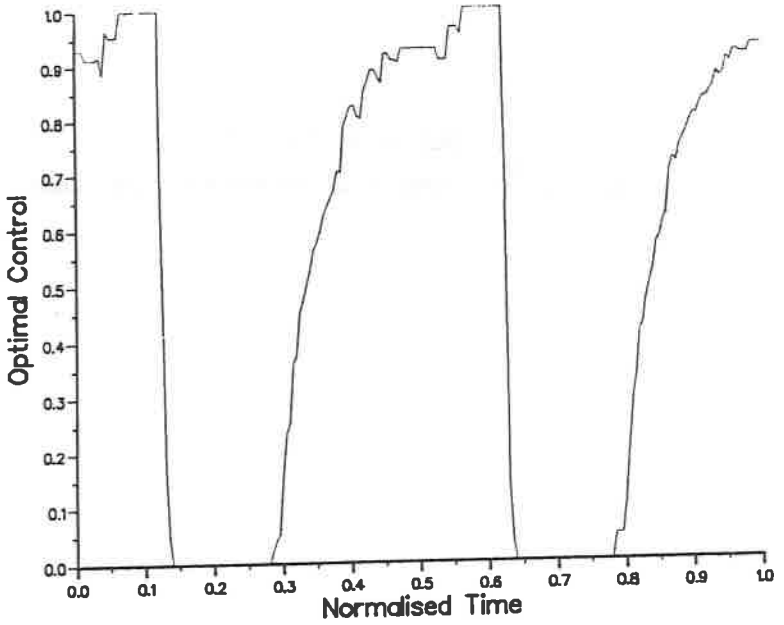

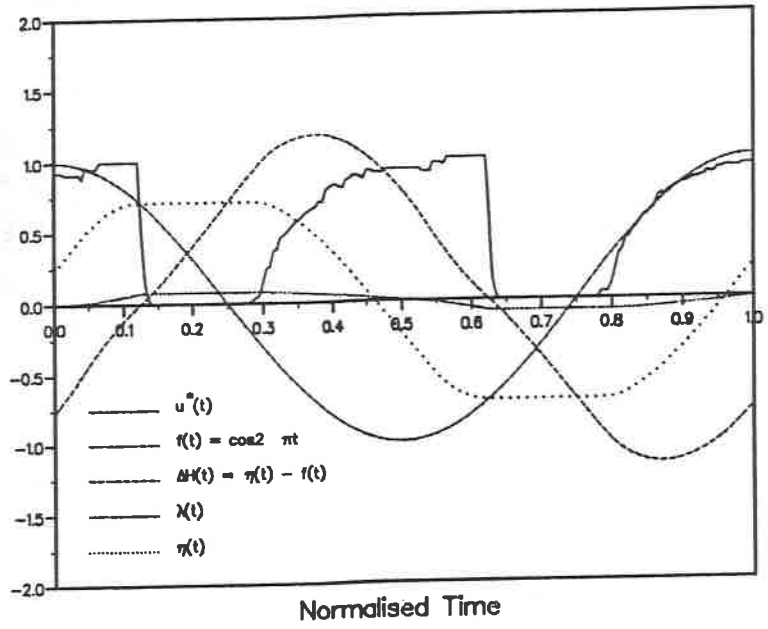

FIG. 48 Non-linear - CGA $h_o = 0.5$
Tol = 1%, N = 200

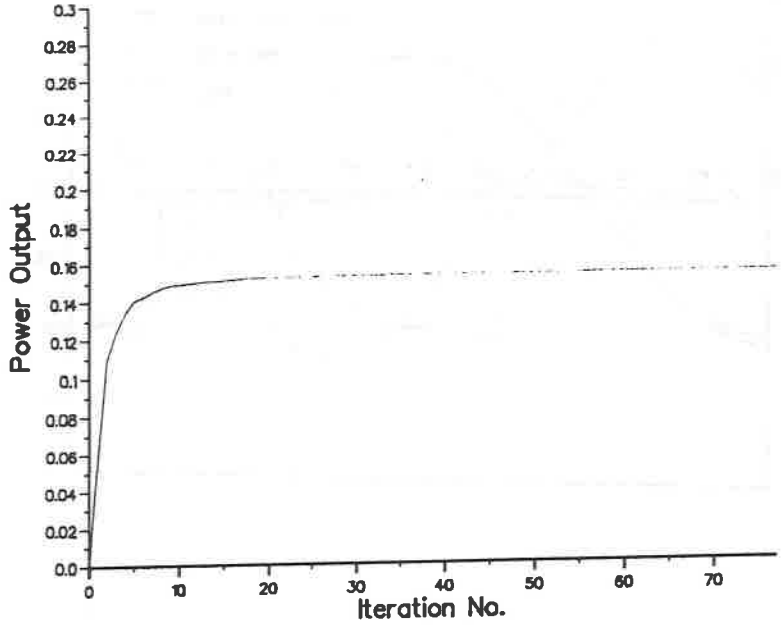

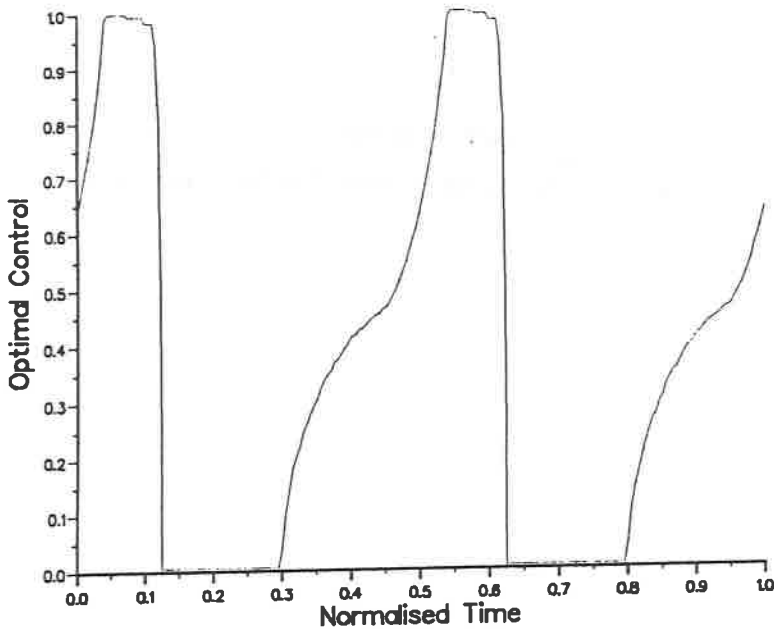

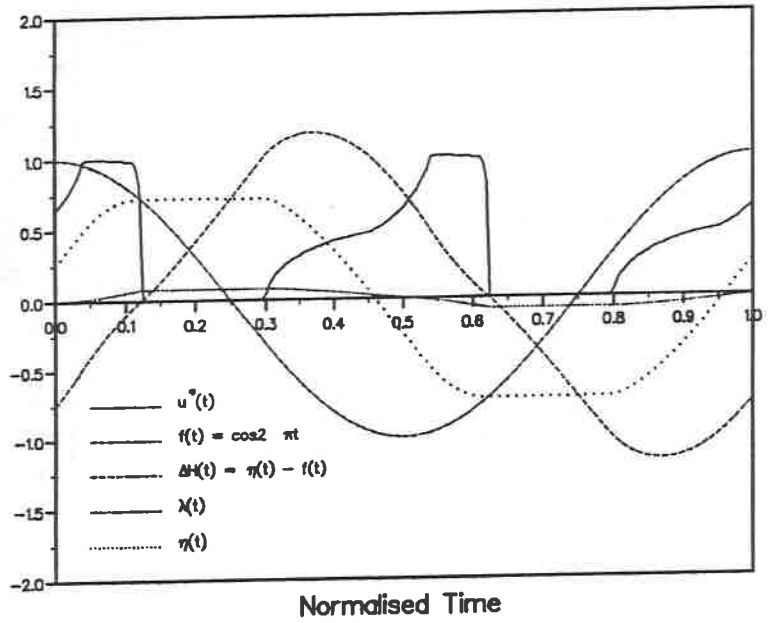

FIG. 49 Non-linear - CGA $h_o = 1.0$
Tol = 1%, N = 200

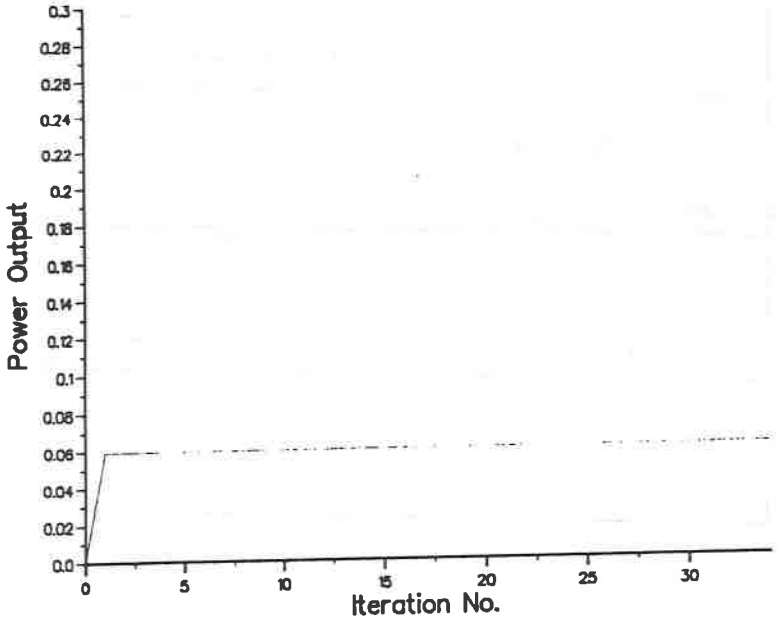

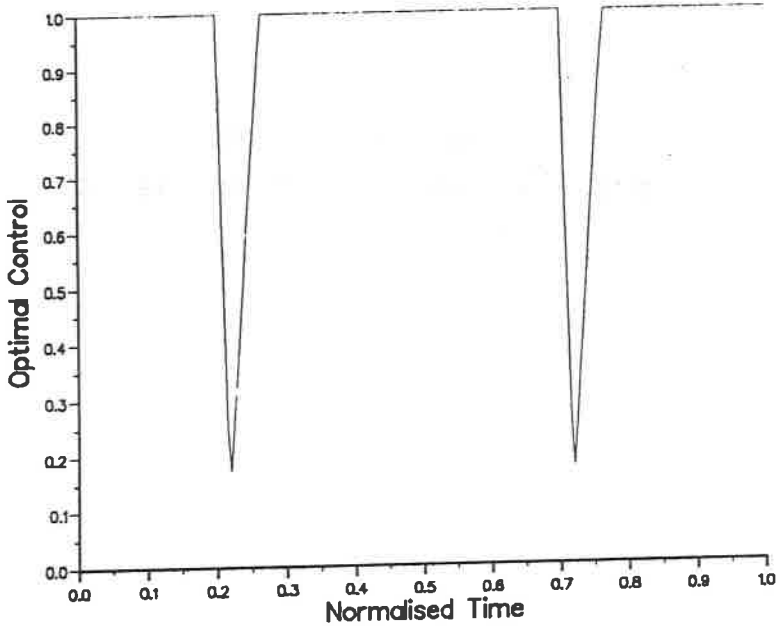

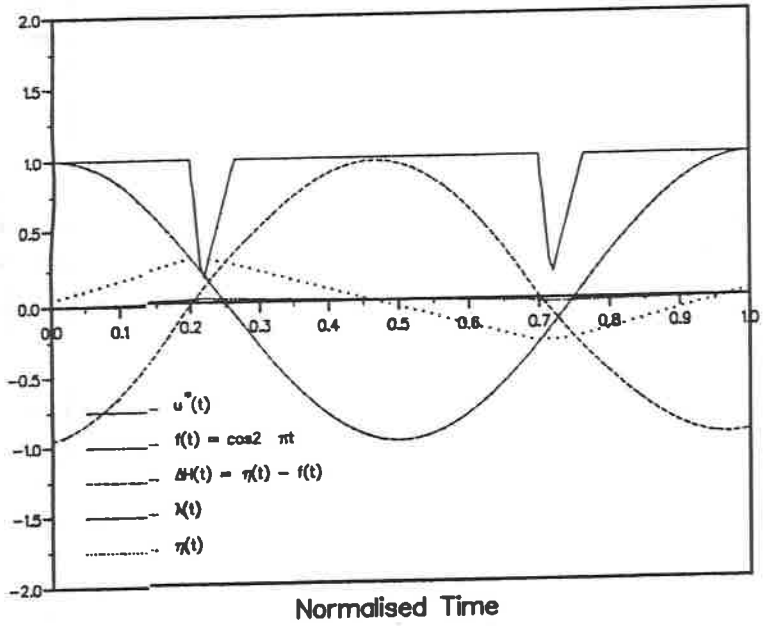

FIG. 50 Non-linear - PGA $h_o = 0.1$

Tol = 1%, N = 200

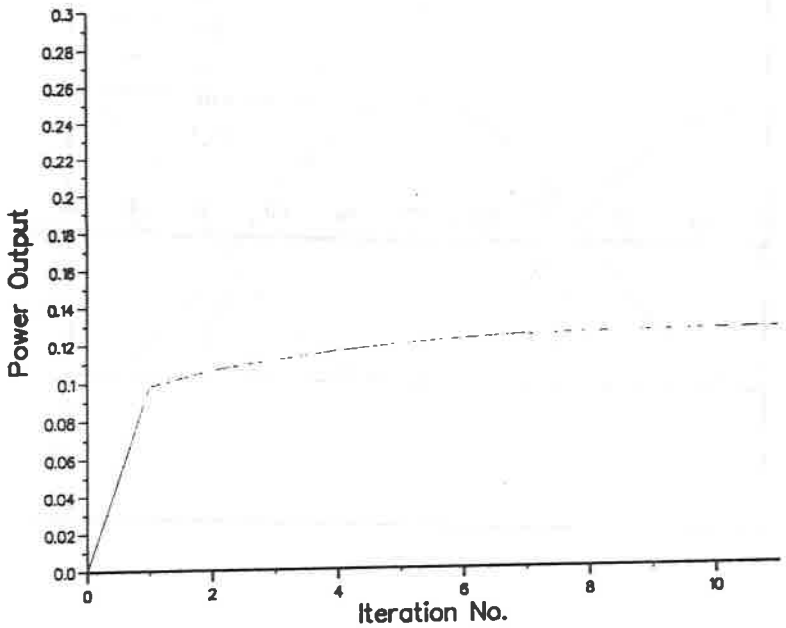

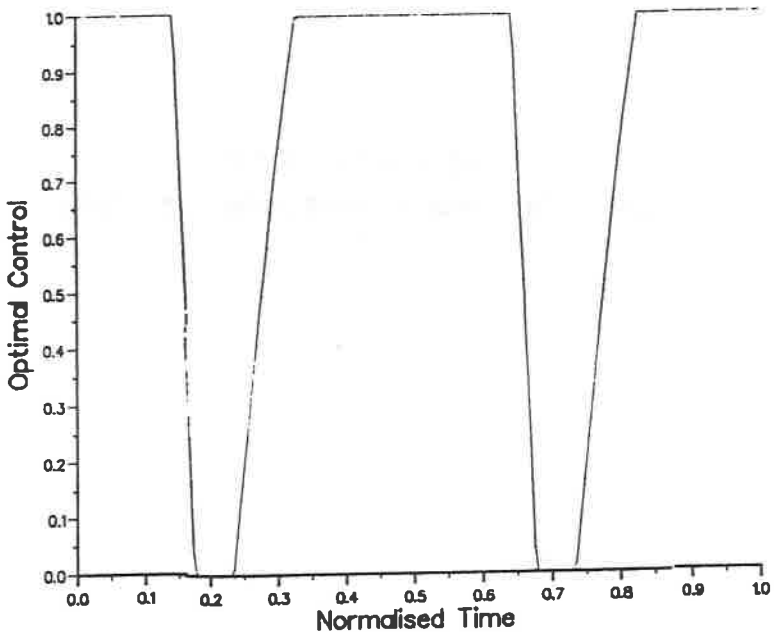

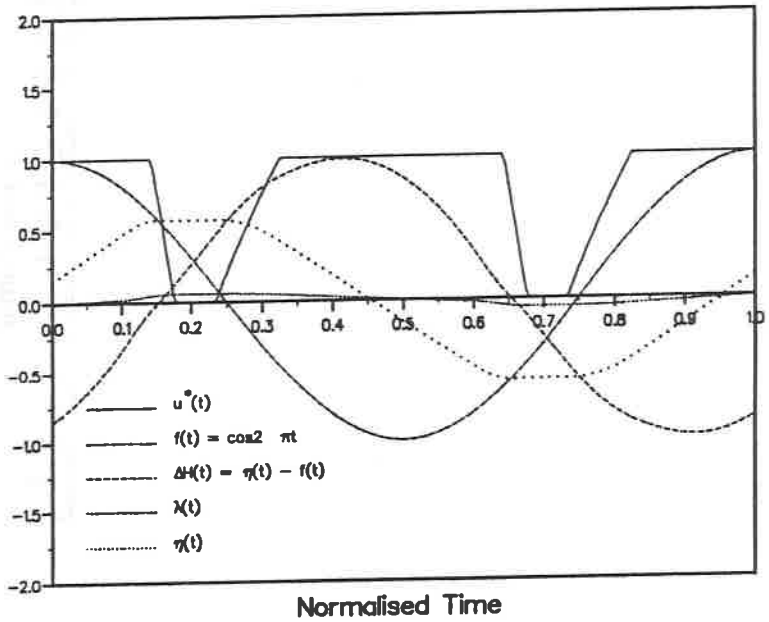

FIG. 51 Non-linear - PGA $h_o = 0.25$
Tol = 1%, N = 200

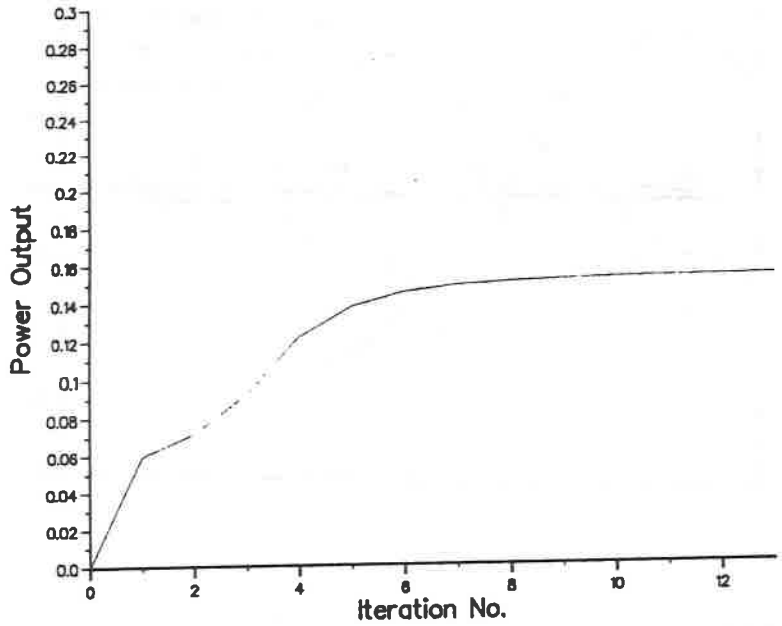

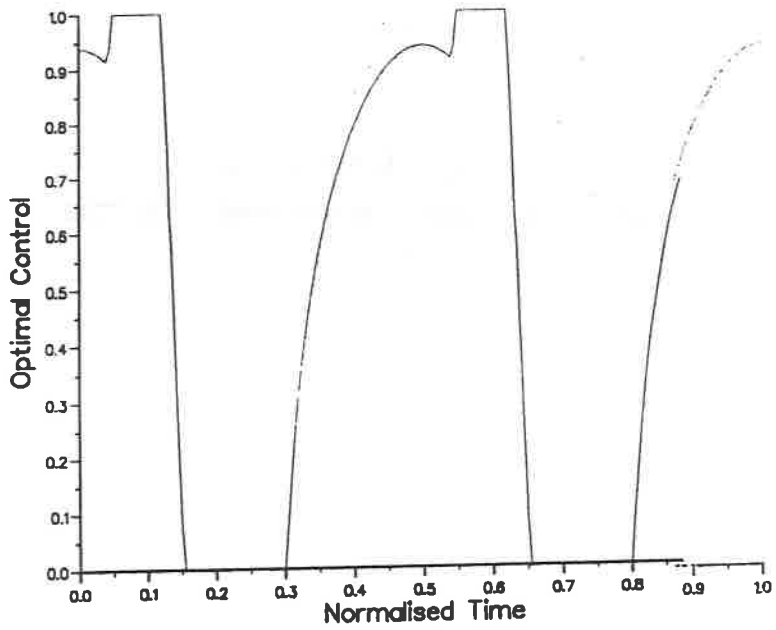

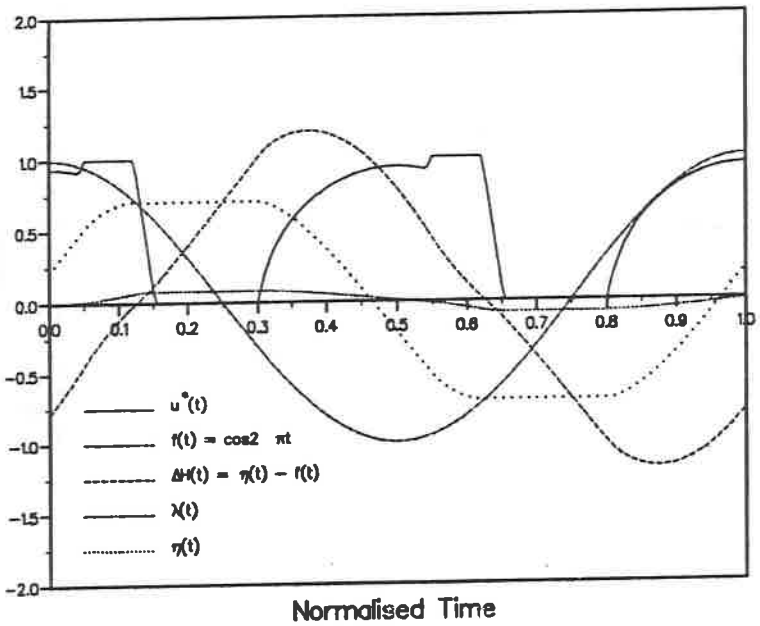

FIG. 52 Non-linear - PGA $h_o = 0.5$

Tol = 1%, N = 200

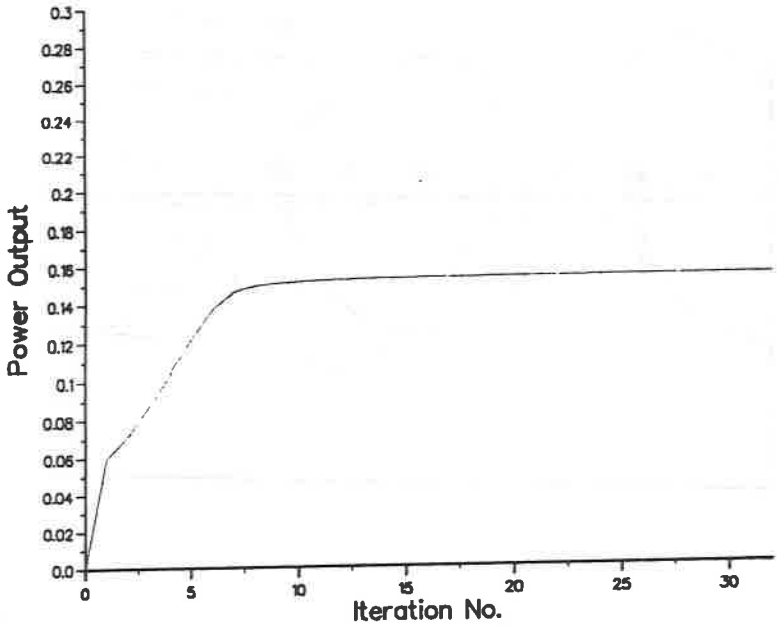

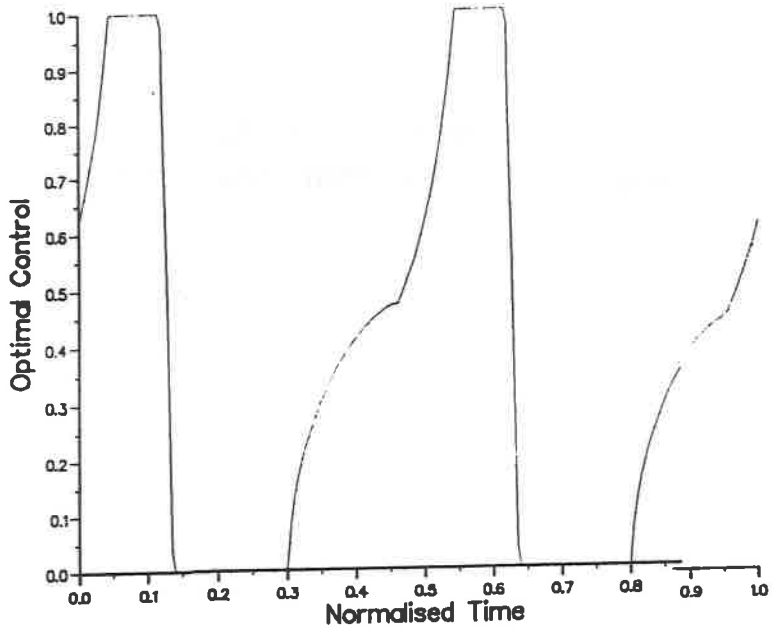

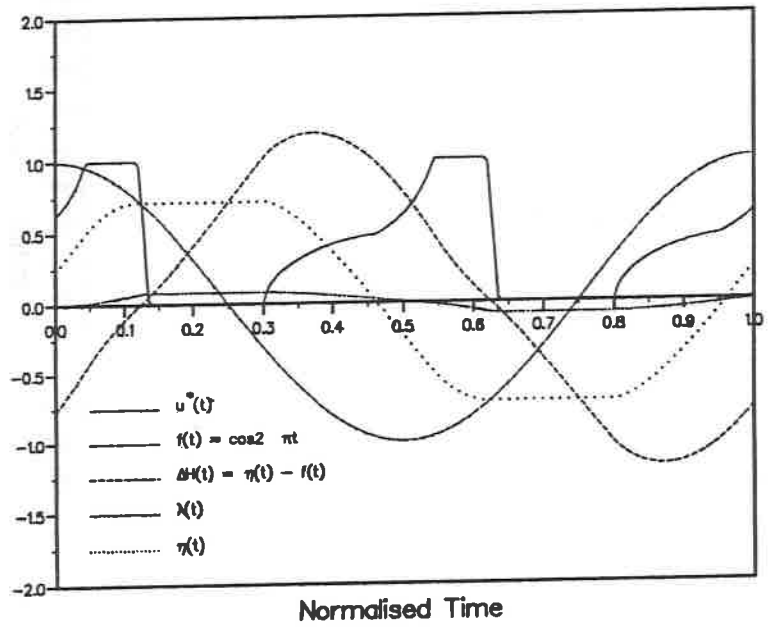

FIG. 53 Non-linear - PGA $h_o = 1.0$

Tol = 1%, N = 200

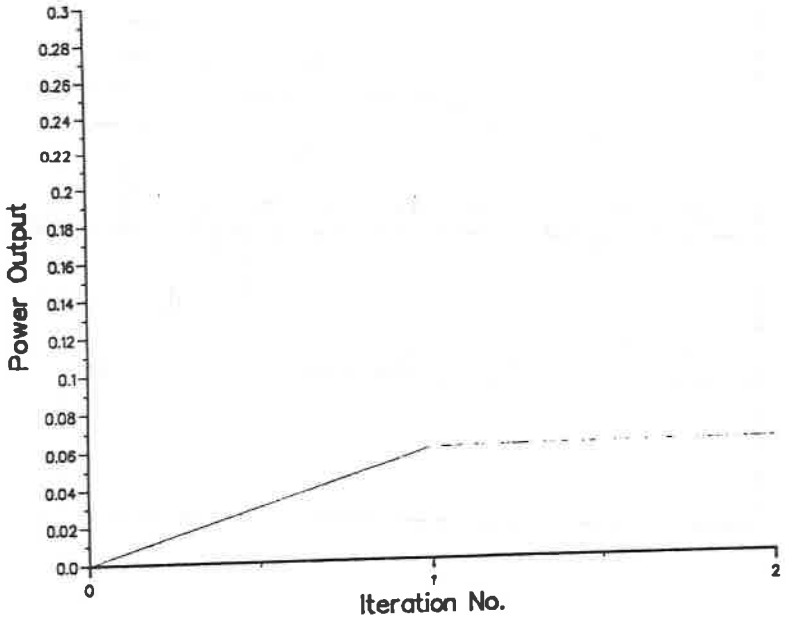

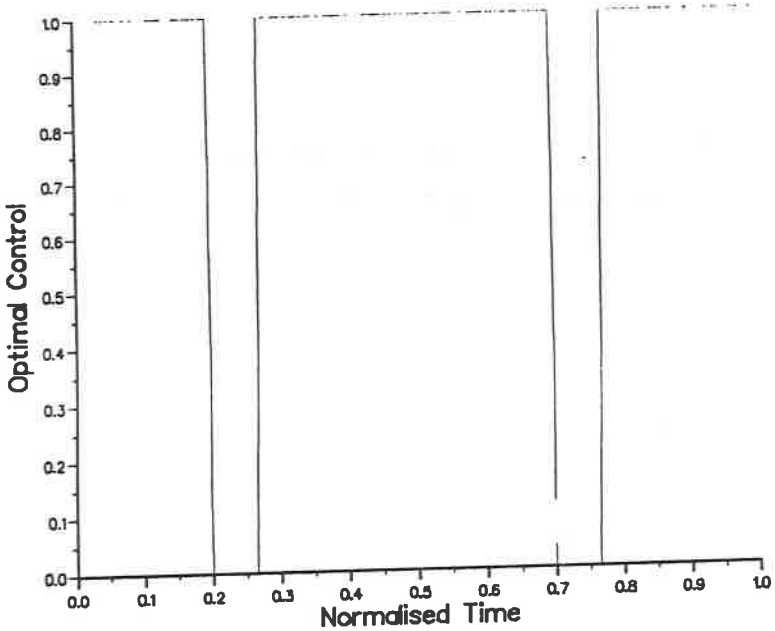

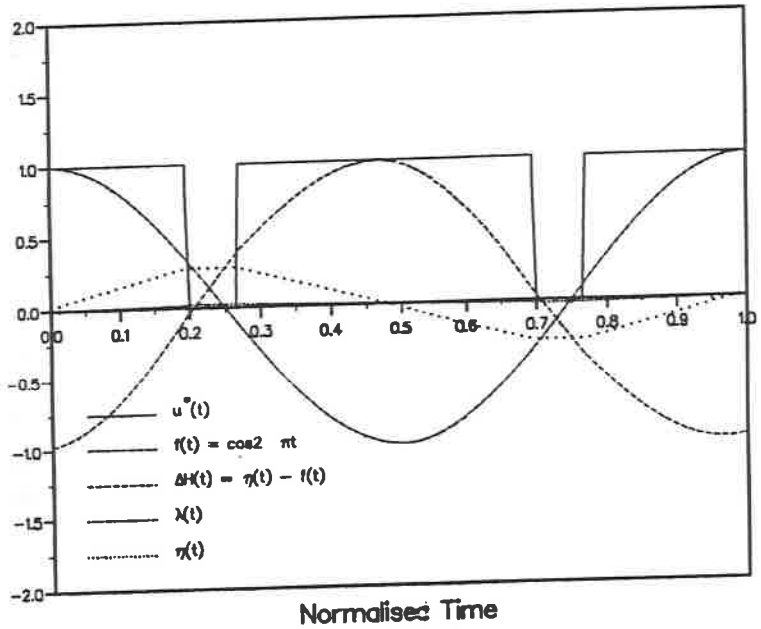

FIG. 54 Non-linear - NCGA $h_o = 0.1$

Tol = 1%, N = 200

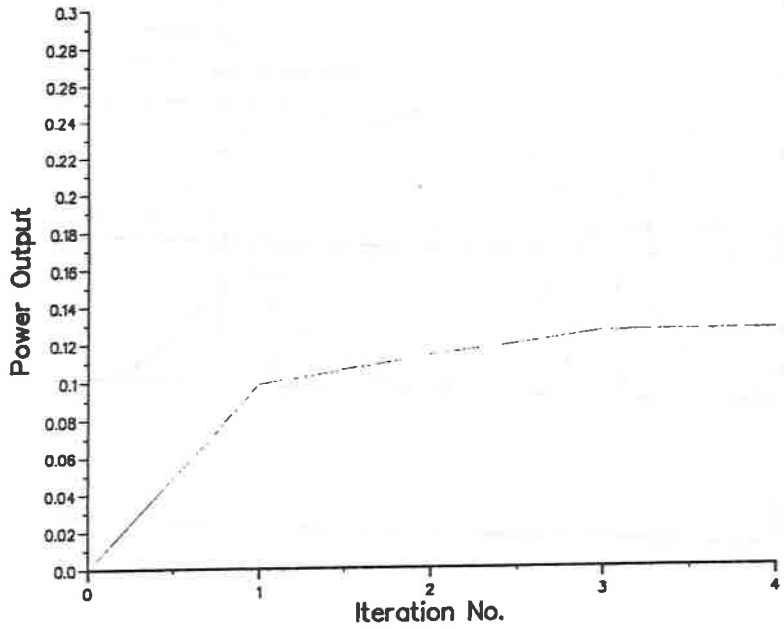

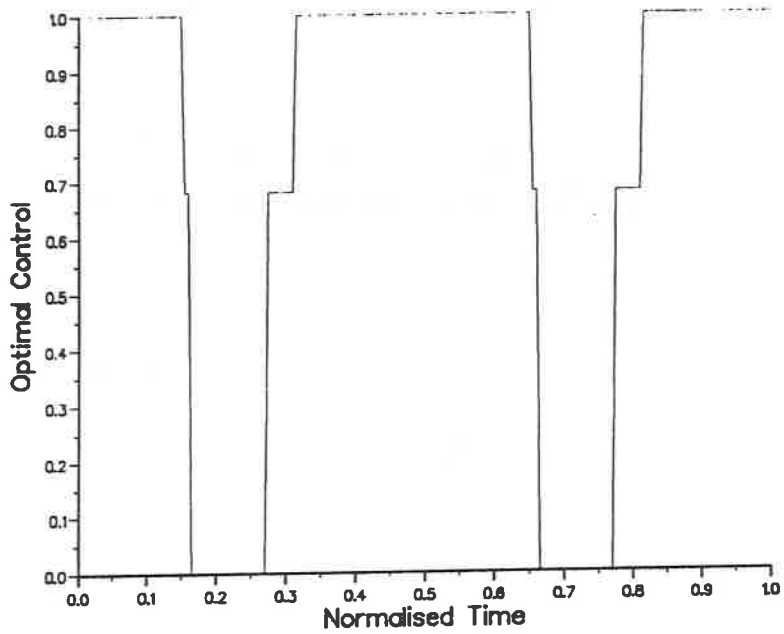

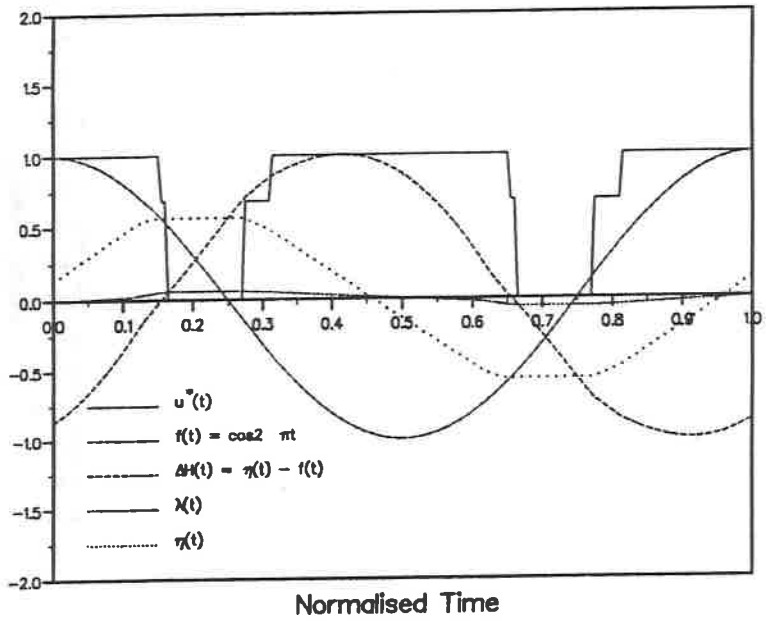

FIG. 55 Non-linear - NCGA $h_o = 0.25$
Tol = 1%, N = 200

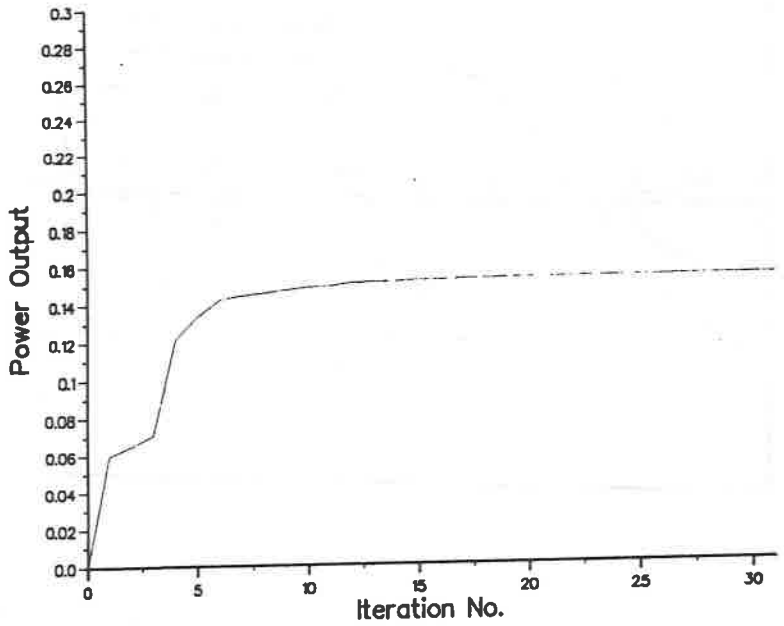

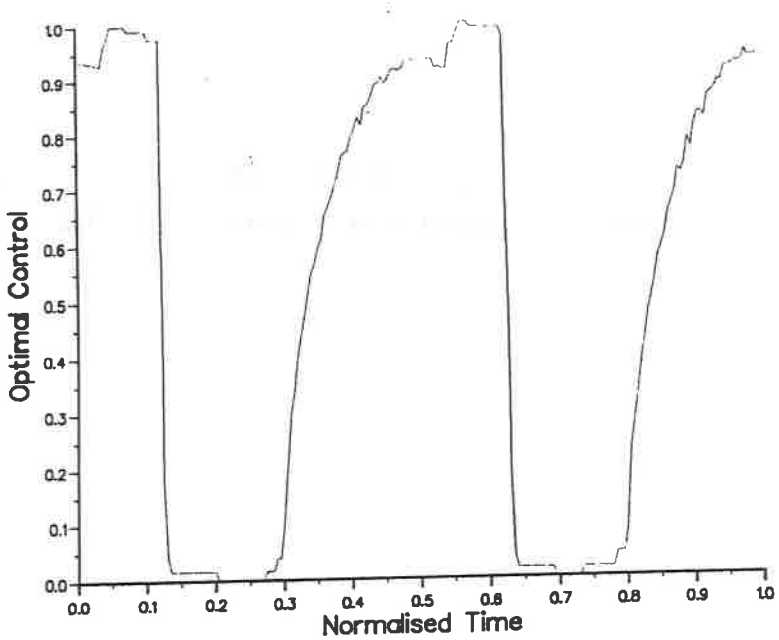

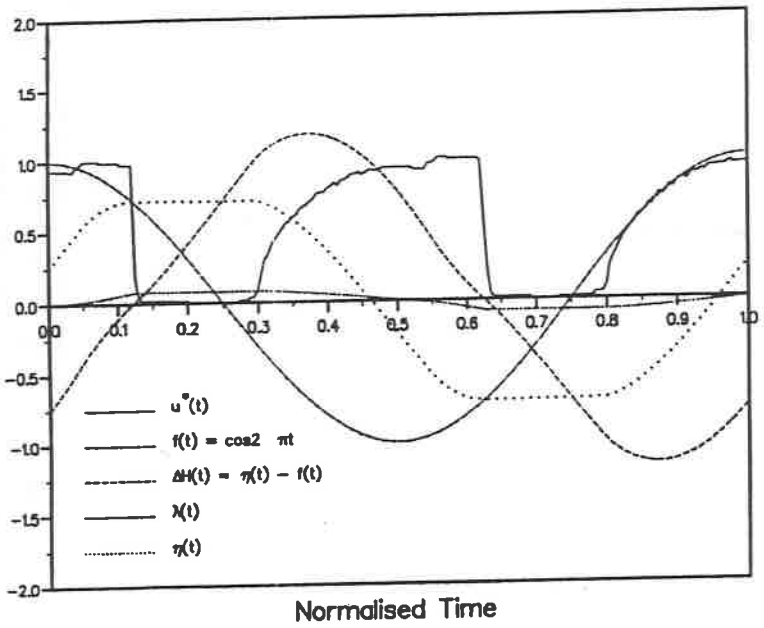

FIG. 56 Non-linear - NCGA $h_o = 0.5$
Tol = 1%, N = 200

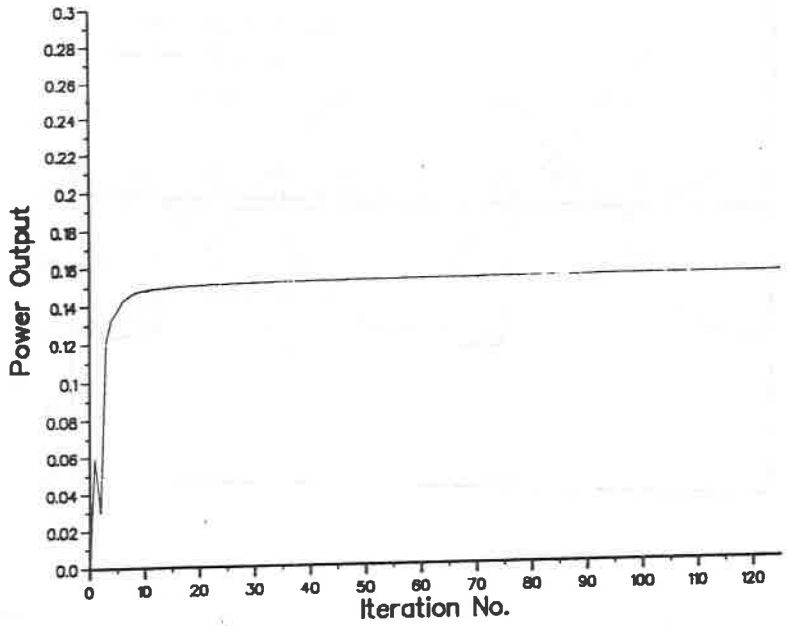

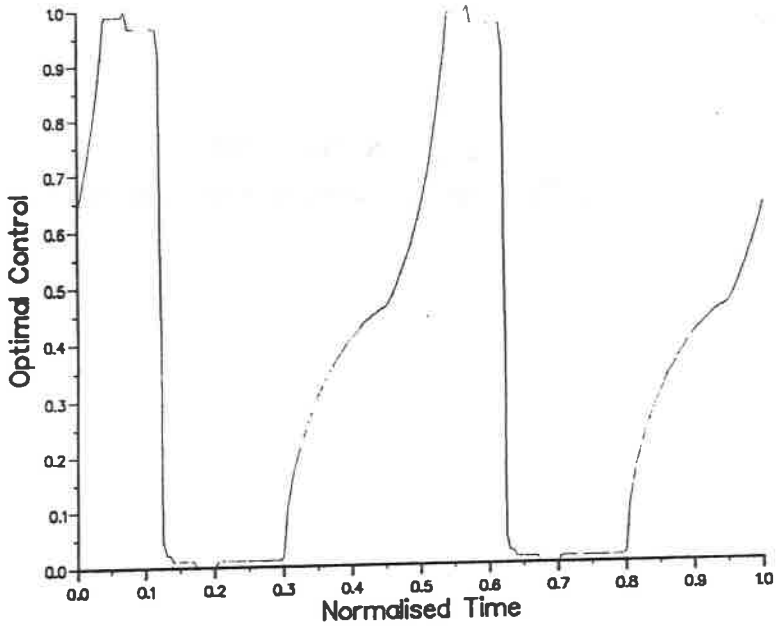

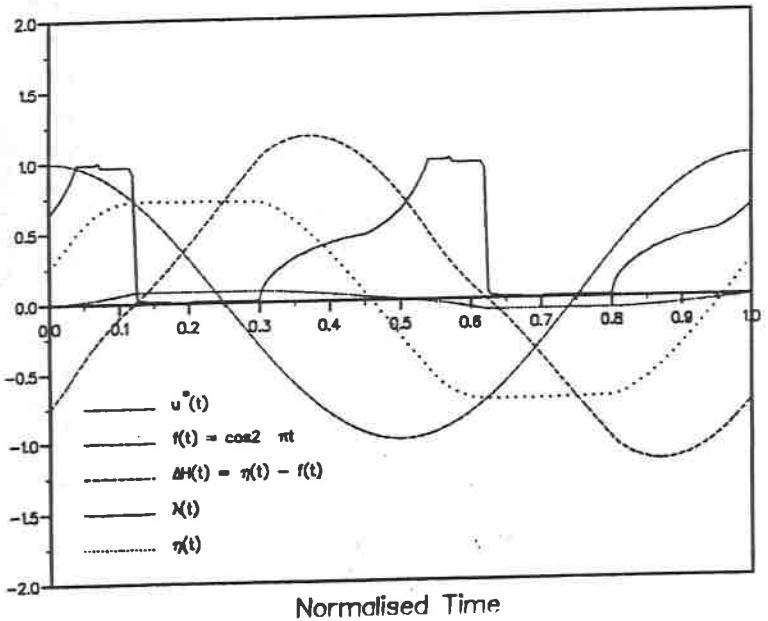

FIG. 57 Non-linear - NCGA $h_o = 1.0$
Tol = 1%, N = 200

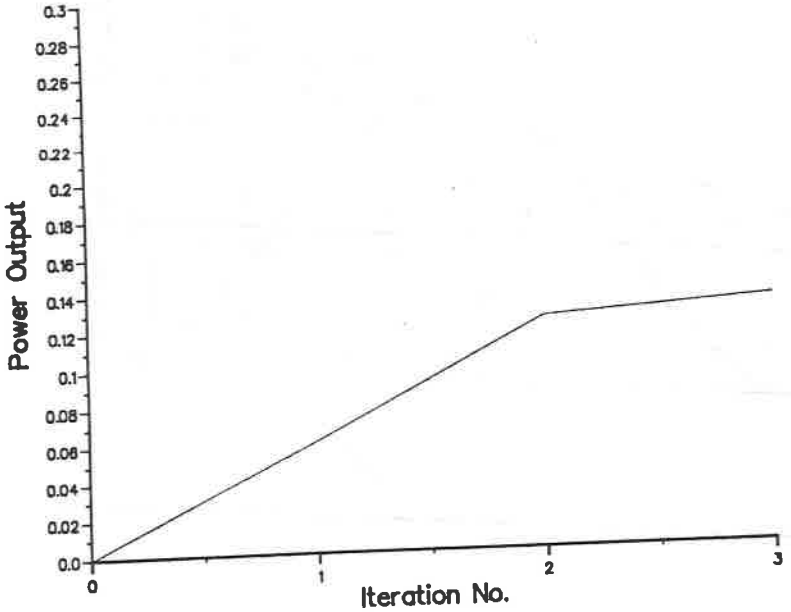

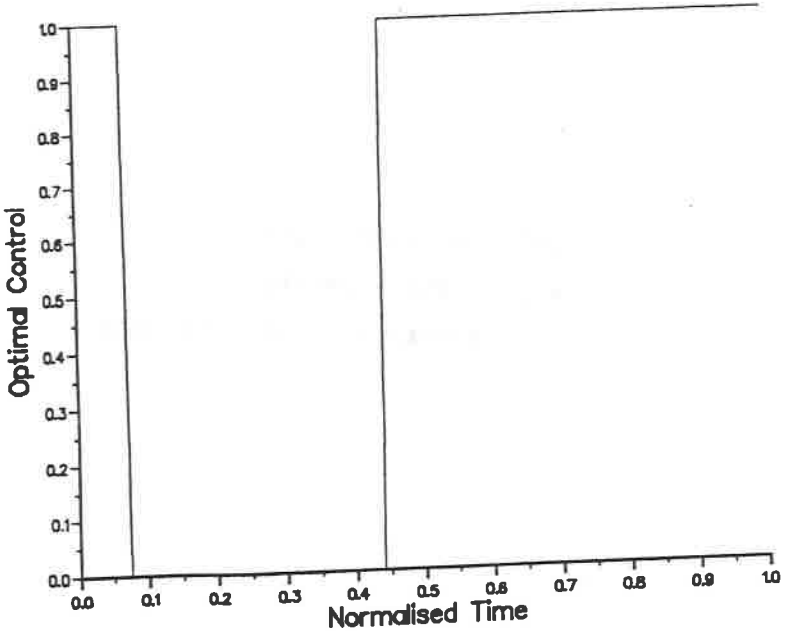

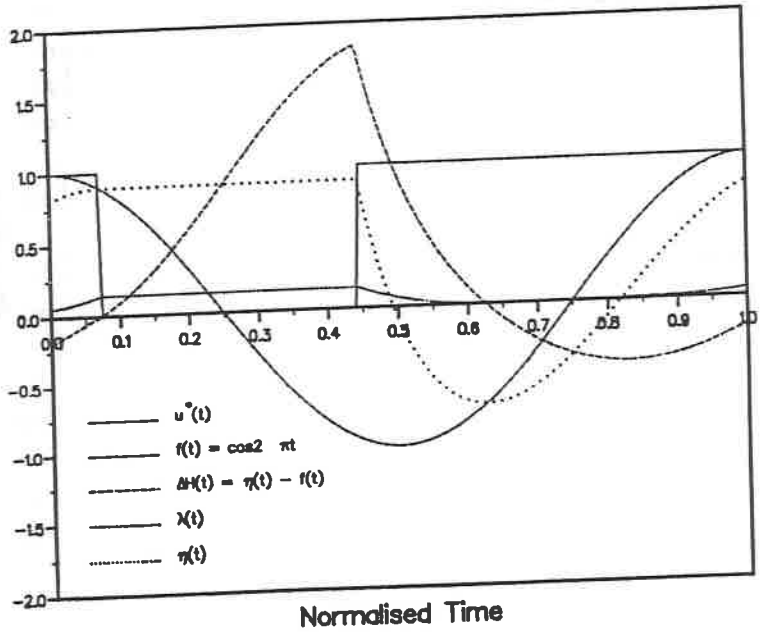

FIG. 58 Ebb Generation
Linear - CGA
Tol = 0.1%, N = 200

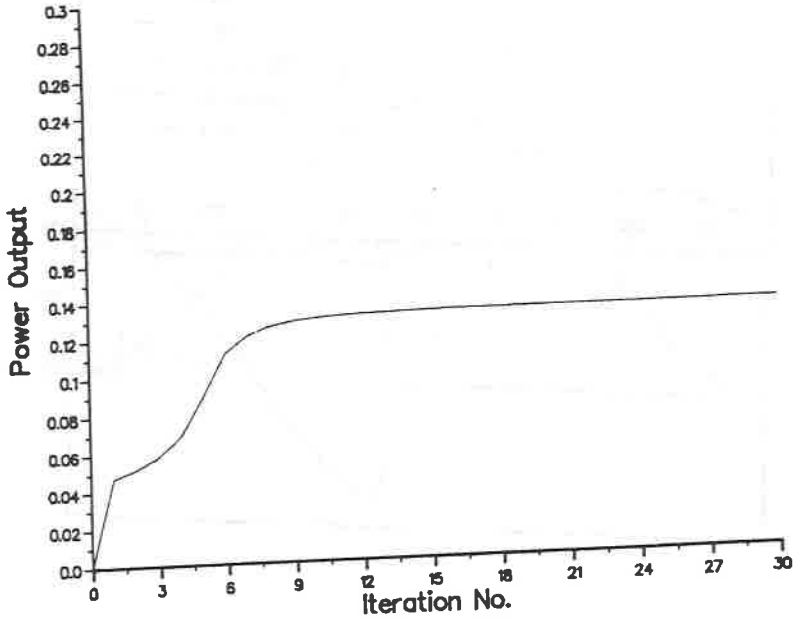

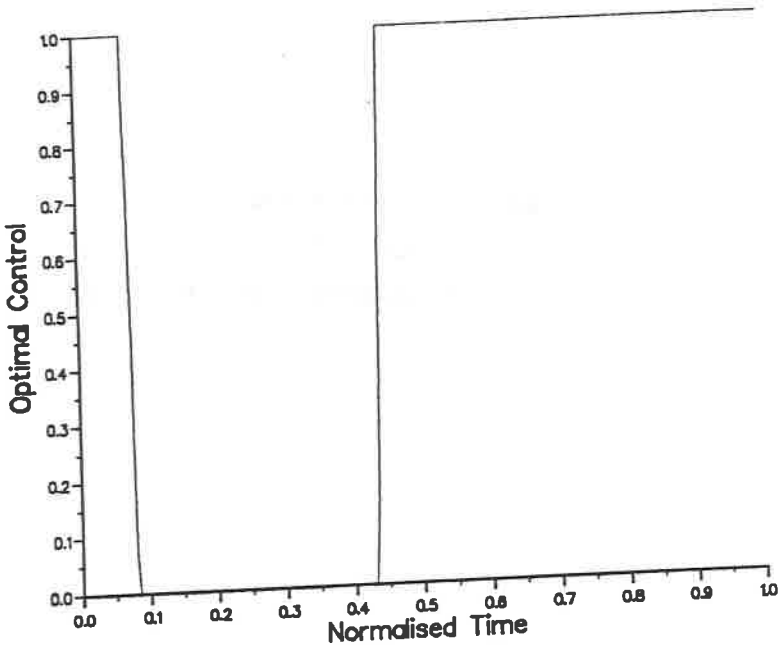

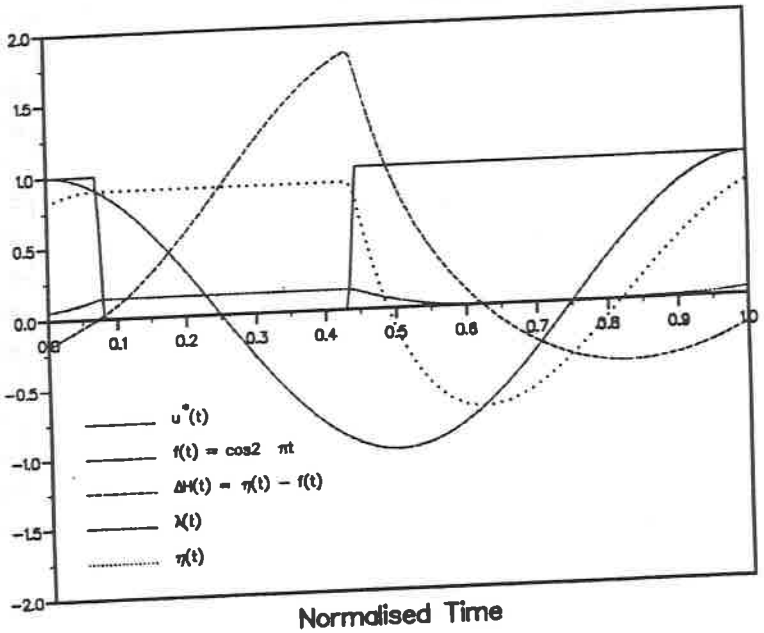

FIG. 59 Ebb Generation

Linear - PGA $u^{O} = 1$

Tol = 0.1%, N = 200

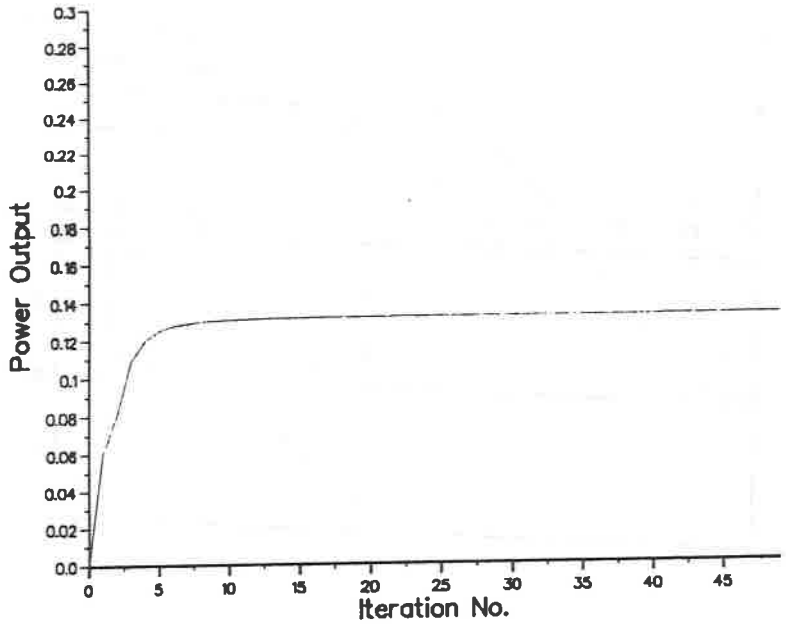

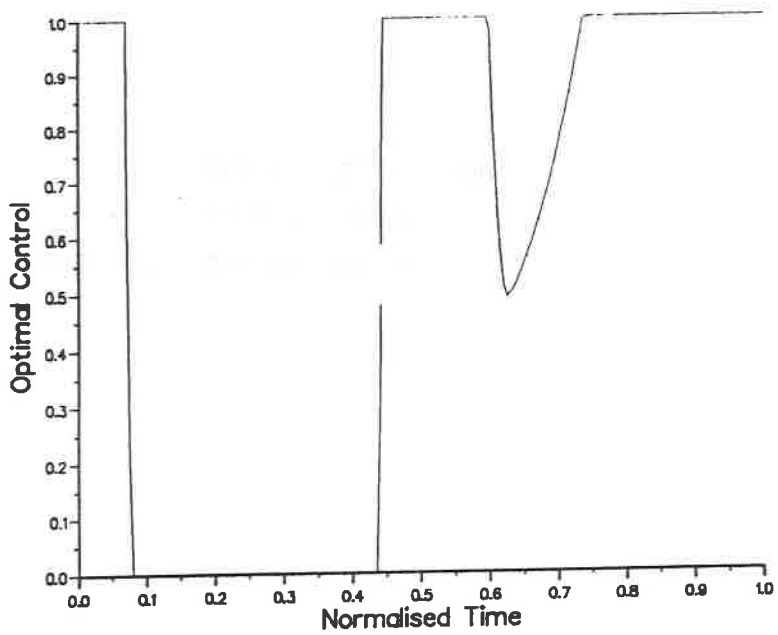

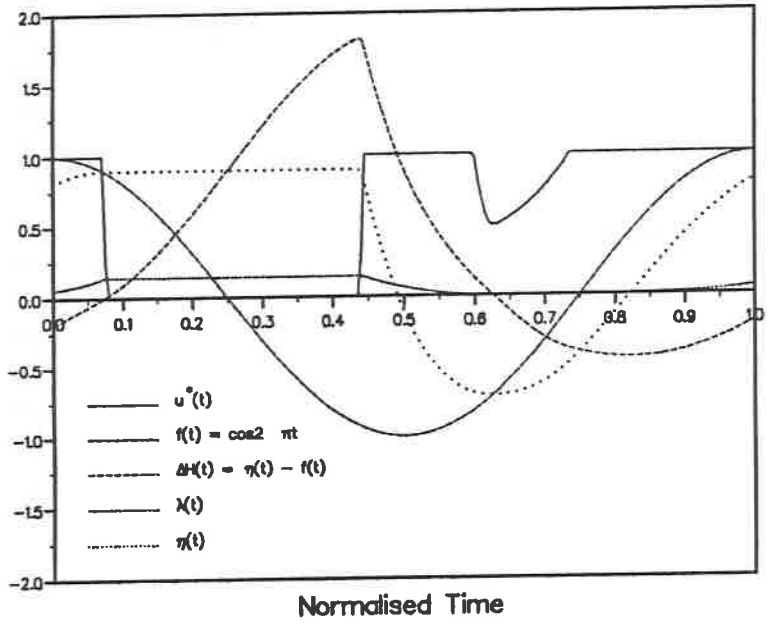

FIG. 60 Ebb Generation

Linear - PGA $u^{o} \neq 1$

Tol = 0.1%, N = 200

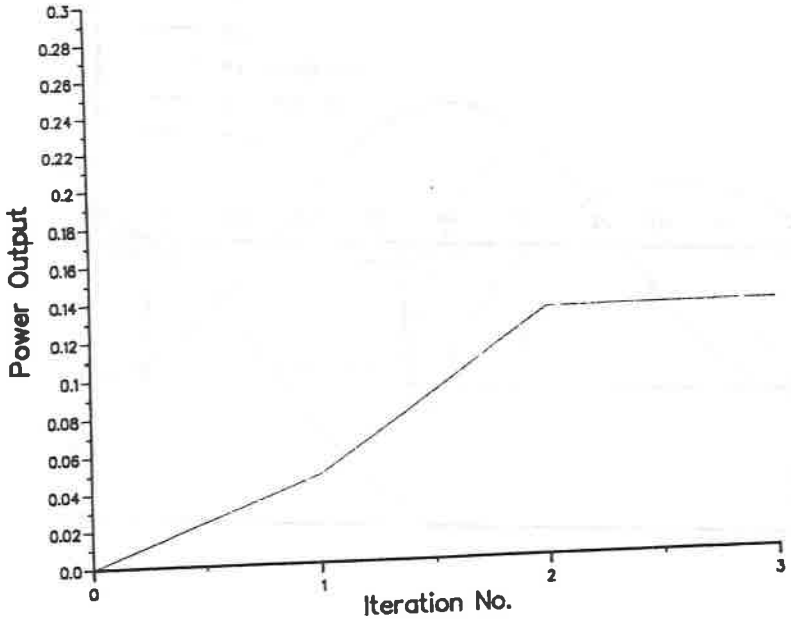

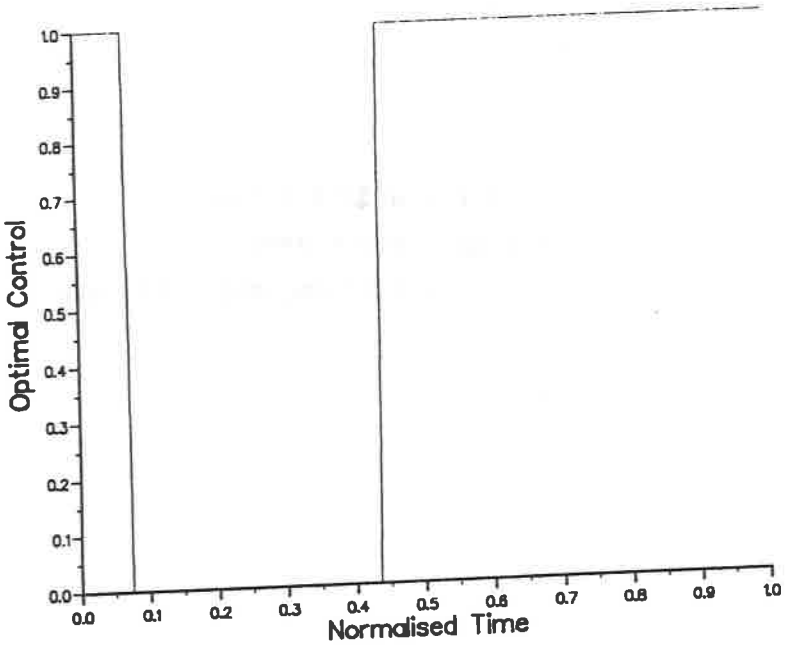

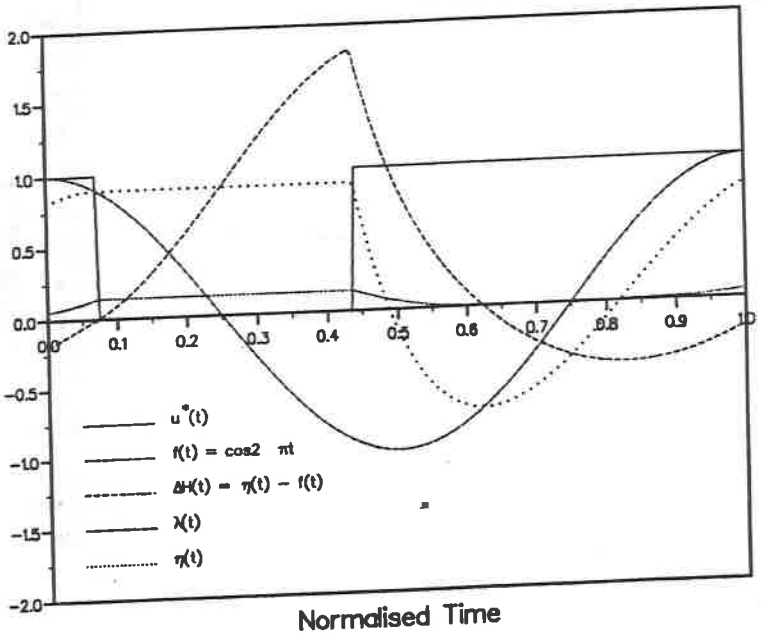

FIG. 61 Ebb Generation
Linear - NCGA
Tol = 0.1% N = 200

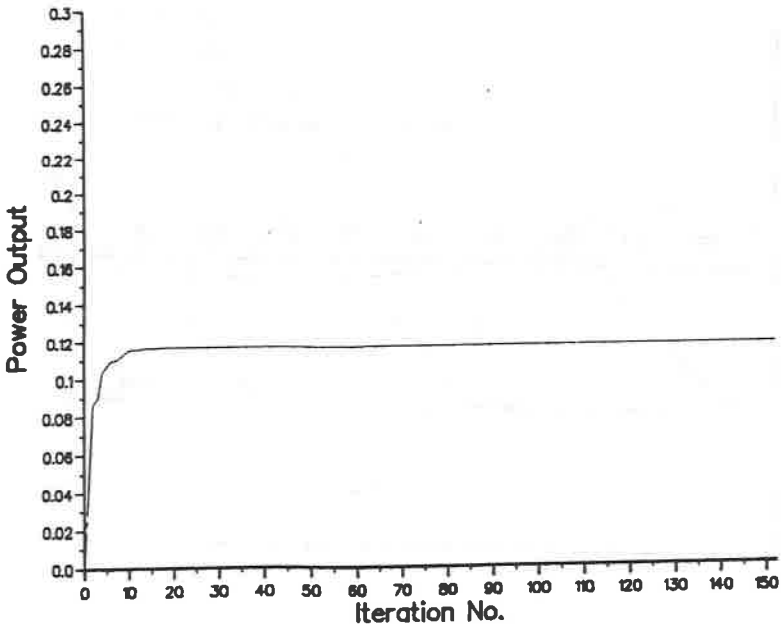

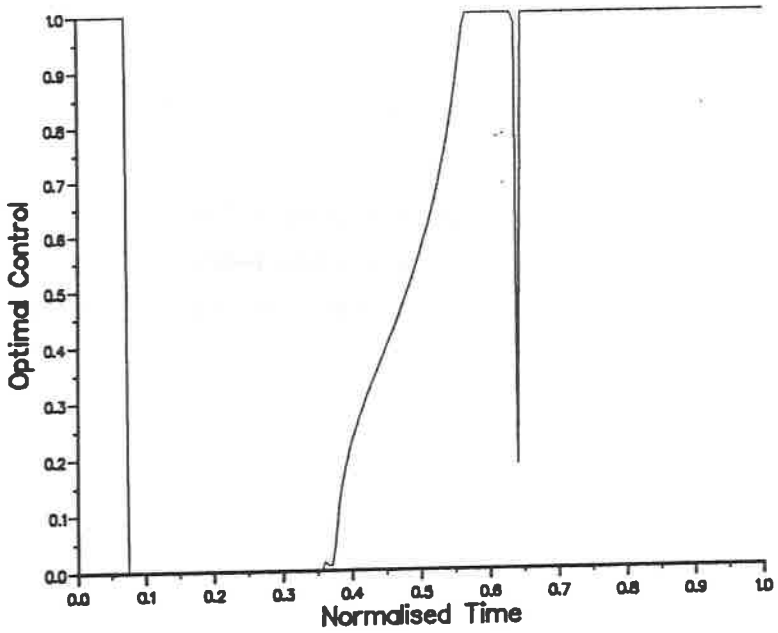

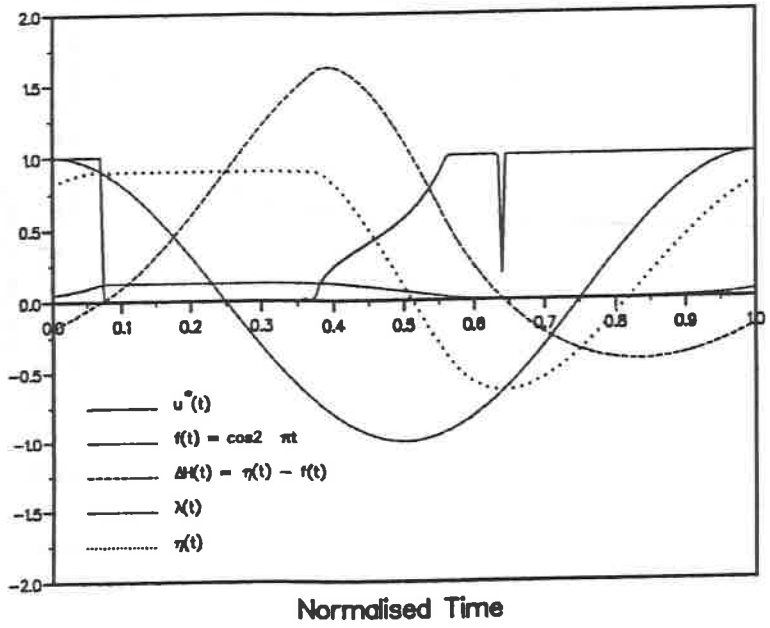

FIG. 62 Ebb Generation
Non-linear - CGA
Tol = 0.1% N = 200

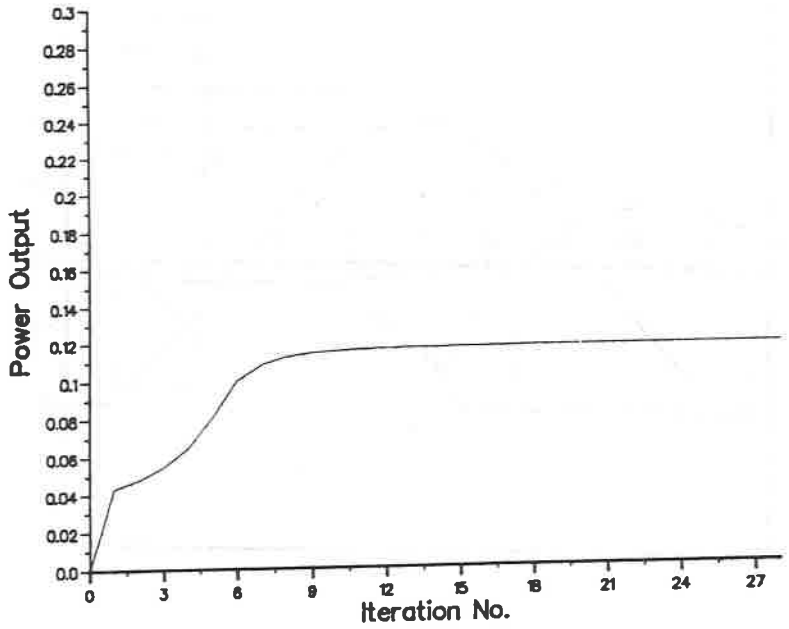

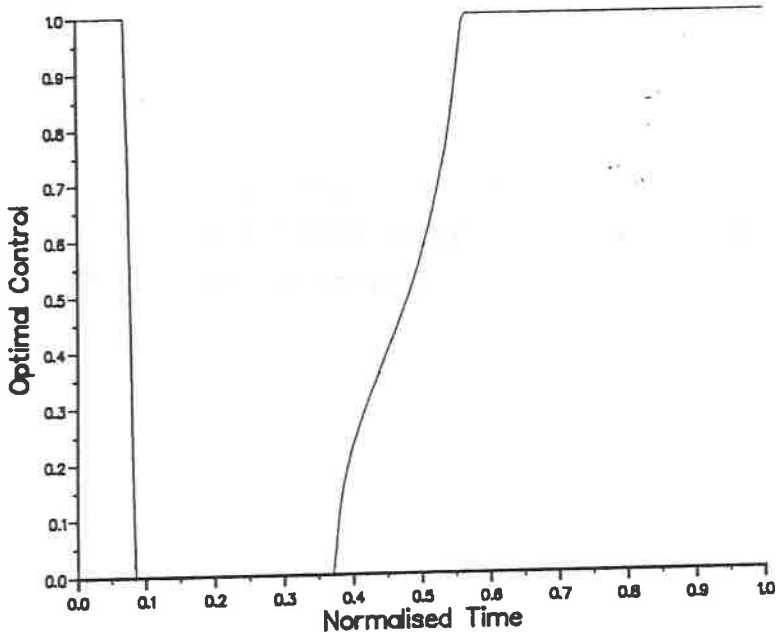

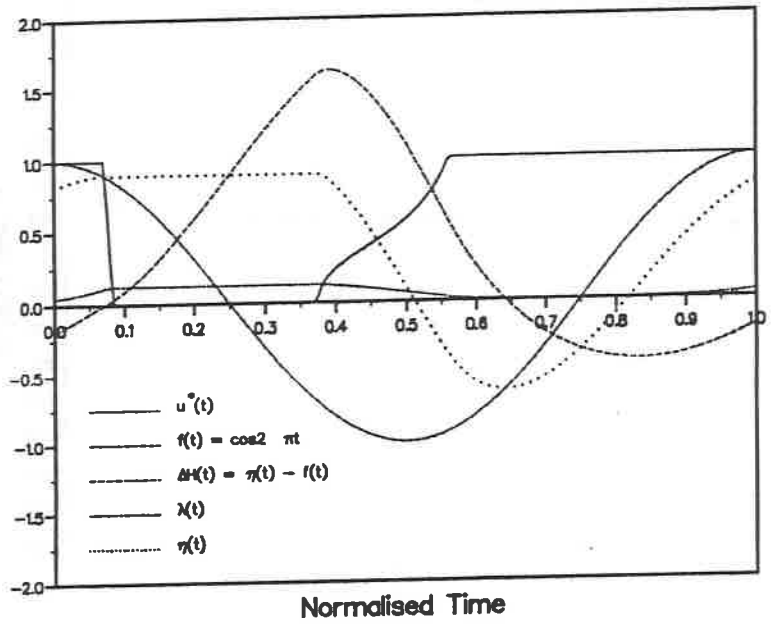

FIG. 63 Ebb Generation
Non-linear - PGA
Tol = 0.1% N = 200

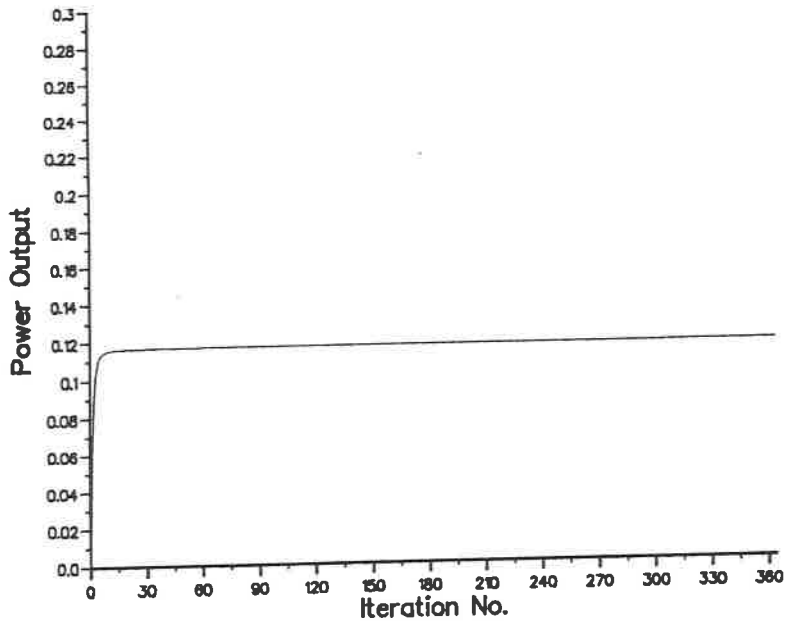

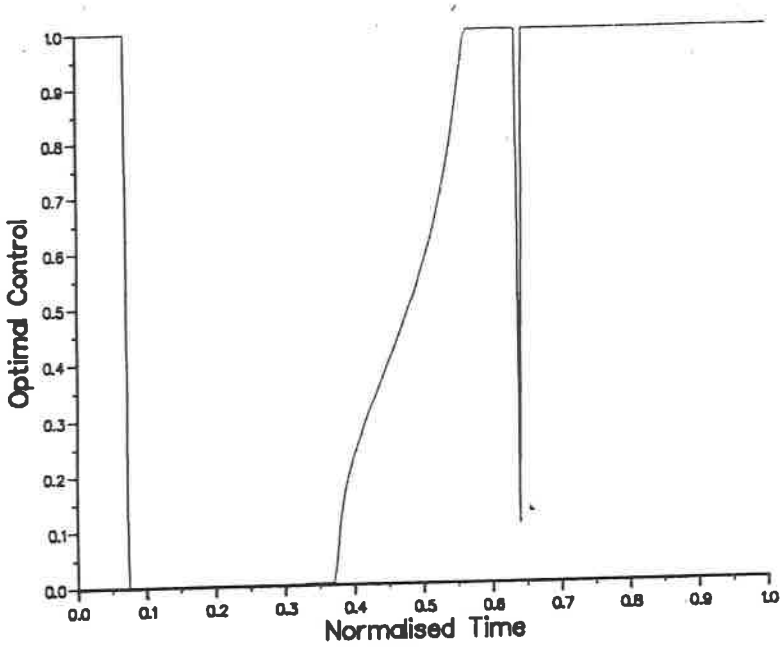

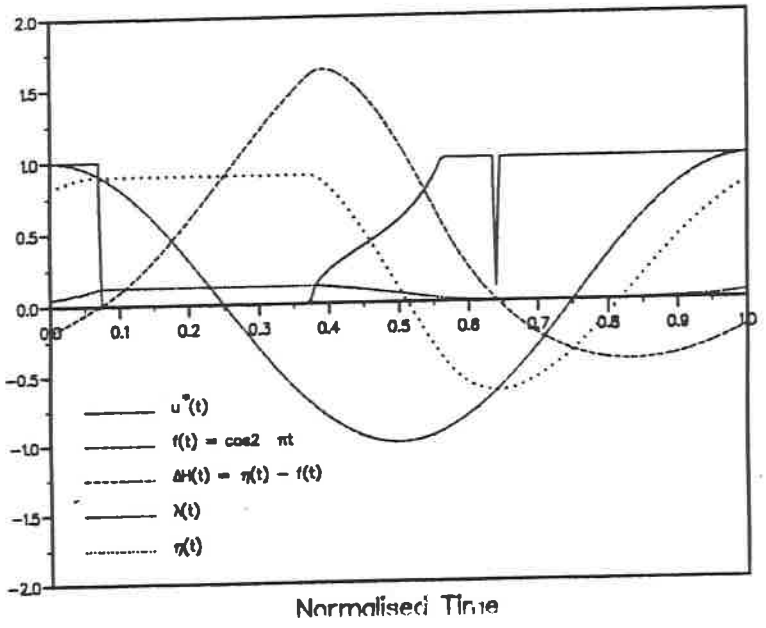

FIG. 64 Ebb Generation
Non-linear - NCGA
Tol = 0.1%, N = 200